ASSESSMENT OF BIOENHANCED BACK DIFFUSION AND REDUCTIVE DEHALOGENASE GENE ABUNDANCE IN AN AQUIFER CELL PACKED WITH HETEROGENEOUS SOILS

By

Spencer Cothran

A thesis submitted to the Graduate Faculty of

Auburn University

in partial fulfillment of the

requirements for the Degree of Master of Science

Auburn, Alabama

May 6, 2023

Approved by

Natalie Cápiro, Chair, PhD, Assistant Professor, Department of Civil and Environmental Engineering

Ann Ojeda, PhD, Assistant Professor, Department of Geosciences

Shiqiang Zou, PhD, Assistant Professor, Department of Civil and Environmental Engineering

Abstract

Remediation of chlorinated ethenes can be challenging at complex contaminated sites with low permeability soils acting as secondary source zones due to back diffusion of adsorbed contaminant mass. To better understand how bioremediation impacts back diffusion, a biotic aquifer cell packed with heterogenous porous media was established to monitor chlorinated ethene concentrations and *Dehalococcoides mccartyi* (*Dhc*) abundance during engineered remediation and after simulated source zone removal. Soils with high organic carbon content (greater than 0.27%) and low hydraulic conductivities (less than 0.05 m/day) measured the greatest increase in *Dhc* and reductive dehalogenase (RDase) gene abundances, greater bioenhanced back diffusion of stored contaminant mass (up to 72% near clay soil), and increased ethene production with *Dhc* abundance greater than 10^3 gene copies/mL. These findings assist in understanding the relationship between bioremediation and the removal of adsorbed contaminant mass and provide supporting information to help practitioners better implement remediation at complex sites.

Acknowledgements

I would like to thank Dr. Natalie Cápiro for the advice and guidance at all hours of the day, and for providing an environment that allowed me to make mistakes, learn, and grow from them. You taught me how to be a better engineer and I will always be thankful for that. Thank you to my committee members, Dr. Ann Ojeda and Shiqiang (Nick) Zou, for your feedback and insightful questions that allowed me to think about things from a different perspective.

Thank you to Pengfei Yan and Sheng Dong for teaching me everything I know in the lab. You both were such great mentors and always provided help when needed. Thank you, Harry Vaslo, for being by my side during class, in the lab, and for a lot of late-night sampling. Thank you, Savannah Cummins and Temitope Popoola for maintaining the aquifer cell like it was your own while I was gone. I would also like to thank Dr. Hamed Torkzadeh for answering the many questions I had, and Dr. Gerald John for making the lab run smoothly and helping with analytical methods.

Thank you to the Strategic Environmental Research and Development Program (project ER20-1079, Development of Predictive Tools for Assessment of Natural Attenuation Capacity and Treatment Transition at Chlorinated Solvent Sites) and the Auburn University Civil and Environmental Engineering department for funding this research.

To my wife, Hallie. Thank you for being very patient with me, supporting my goals, and for loving me so well along the way.

Table of Contents

List of Tables

List of Figures

List of Abbreviations

bvcA	*Vinyl chloride reductase b*
COC	Contaminant of concern
DCE	Dichloroethene
Dhc	*Dehalococcoides myccartyi*
Dhgm	*Dehalogenimonas*
DNAPL	Dense non-aqueous phase liquid
DOC	Dissolved organic carbon
GC-ECD	Gas chromatograph – electron capture device
GC-FID	Gas chromatograph - flame ionization detector
Geo	*Geobacter* species
HPLC	High performance liquid chromatography
IS	Ionic strength
EISB	Enhanced in-situ bioremediation
K_d	Soil-water distribution coefficient
MNA	Monitored natural attenuation
MRD	Microbial reductive dechlorination
NAC	Natural attenuation capacity
OC	Organic carbon

PCE	Tetrachloroethene
ppm	Parts per million (mg/L)
PV	Pore volume
qPCR	Quantitative polymerase chain reaction
RDase	Reductive dehalogenase
SERDP	Strategic Environmental Research and Development Program
TCE	Trichloroethene
tceA	*Trichloroethene reductase*
TOC	Total organic carbon
VC	Vinyl chloride
vcrA	*Vinyl chloride reductase a*
VOCs	Volatile organic compounds

Chapter 1 – Introduction and Objectives

Chlorinated ethenes are volatile organic compounds (VOCs) that are listed on the Comprehensive Environmental Response, Compensation, and Liability Act (CERCLA) Priority List and are the most common contaminant found at Superfund sites (Huang, Lei et al. 2014, EPA 2017). Common chlorinated ethenes, such as tetrachloroethene (PCE) and trichloroethene (TCE), were frequently used as degreasers and cleaning agents in industries such as dry-cleaning and military operations (Moran, Zogorski et al. 2007, EPA 2020).

Chlorinated ethenes are released into aquifers from improper disposal techniques and failure of historical storage vessels. Once released, they tend to permeate through porous media to the lower sections in an aquifer since they are denser than the surrounding groundwater (Mercer and Cohen 1990, Guard 1999). As shown in Figure 1.1, TCE contaminated sites with heterogeneous soils often include a source zone at depth while low-permeability soils act as secondary source zones throughout the aquifer (Mackay and Cherry 1989, Yang, Annable et al. 2015, Russell, Matthews et al. 2019). Due to their persistence and hydrophobic nature, chlorinated ethenes can adsorb to low-permeability media with high organic carbon content and remain there for years (NRC 2013). Chlorinated ethenes from the initial source zone, or back diffusion from adsorbed contaminant mass, creates a plume in the bulk of the aquifer. This plume can travel downgradient to other sections of the aquifer making it difficult to keep record of, and remediate, contaminate mass. Examining the complex behavior (adsorption,

degradation, back diffusion) of chlorinated ethenes in low permeability zones is key to understanding where to focus remediation efforts and how to best remove stored contaminant mass.

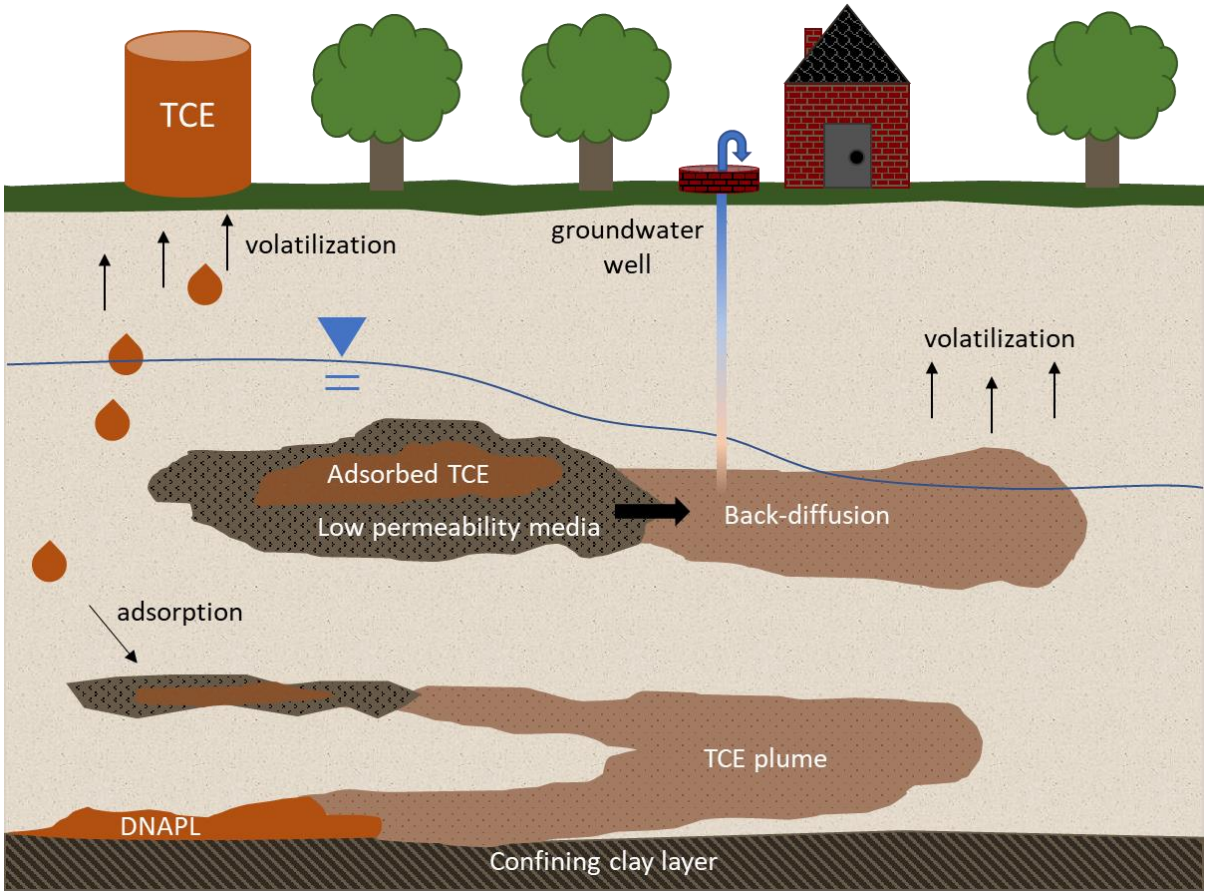

Figure 1.1 Chlorinated ethene contaminated site source zone and plume development

Complex sites are characterized by heterogeneous hydrogeology, the presence of recalcitrant contaminants, and persistent contamination above remediation goals (NRC 2013). Complex sites contaminated with chlorinated ethenes bring about several challenges to remediation. First, it is challenging to remove the source zone since it can be deep within an aquifer and unavailable for physical removal (Abriola, Christ et al. 2012). Second, low solubility of chlorinated ethenes make it challenging for remediation techniques, such as pump and treat,

that rely on downgradient transport of the contaminant of concern (COC) and amendment substrates (Mackay and Cherry 1989). Third, sorption to low-permeability media can create secondary source zones that persist for long periods of time – even after source zone removal (Grisak and Pickens 1980). Lastly, due to the complex biogeochemical processes, it can be very challenging to estimate and achieve remediation goals within reasonable budgets and time frames (NRC 2014).

Bioremediation has become an increasing popular remediation technique and is the primary treatment remedy selected at 25% of Superfund sites with contaminated groundwater (EPA 2023). Bioremediation of chlorinated ethenes uses dechlorinating microorganisms to transform harmful parent compounds (PCE and TCE) to the non-toxic end-product ethene. *Dehalococcoides mccartyi* (*Dhc*) is a well-studied microbial species that is commonly used in microbial consortiums for bioaugmentation at field sites (Hendrickson, Payne et al. 2002). *Dhc* is capable of transforming PCE all the way to ethene (Löffler, Yan et al. (2013)), and specific reductive dehalogenase (RDase) genes (*tceA, bvcA, vcrA*) participate in catalyzing different steps of the dechlorination process (Ritalahti, Amos et al. 2006). The presence of these genes can help indicate the extents to which biological dechlorination is expected (Löffler, Yan et al. 2013).

Enhanced in-situ bioremediation (EISB) often includes the addition of microorganisms (bioaugmentation) and electron donor and/or other amendments (biostimulation) to introduce and enhance microbial populations to achieve complete detoxification, respectively within

reasonable time frames (< 30-50 years) (Lendvay, Löffler et al. 2003, NRC 2014). EISB success becomes especially challenging to predict at complex sites (Sale, Parker et al. 2013). Sites that are unable to reach remediation goals within their expected time frame, due to back diffusion and desorption from low-permeable zones, can lead to an increase in duration and cost for remediation projects (Chapman and Parker 2005, Kueper, Stroo et al. 2014). This observation, along with a better understanding of complex sites, has shifted the focus from a singular active engineered treatment (pump and treat, chemical oxidation, or thermal treatment) to a more holistic site approach that often requires a polishing step to remove residual contaminant mass.

Chlorinated ethene contaminated complex sites are great candidates for coupled treatments where EISB is paired with passive remediation technique. For this research, passive remediation was defined as decreasing amendments (electron donor and biomass) and/or relying on in-situ conditions (without further engineered manipulation) to finish remediation. An example of active remediation includes bioaugmentation and biostimulation (through continuous or pulsed electron donor addition) to remove the bulk of contaminant source zone. Following active treatment, passive remediation could be implemented to treat residual stored mass. An example of passive remediation includes transitioning to a slow release electron donor source. This transition is often marked by a shift in remediation that targets the source zone (active) and remediation that targets residual contaminant mass (passive) (Brooks, Yarney et al. 2021). This coupled strategy emphasizes how a transition from active to passive remediation might be beneficial as a wholistic remediation approach at complex sites. Passive remediation is feasible at chlorinated ethene contaminated sites since bioremediation is capable of PCE and TCE to

benign ethene to achieve remediation goals [< maximum contaminant level (MCL)] (NRC 2013) . Additionally, lasting effects of active remediation could prove beneficial during passive remediation when amendments are decreased or stopped entirely. Coupling of source zone treatment (physical and chemical treatments) with posttreatment bioremediation has been studied using DNAPL source zones in homogeneous aquifers and has proven to potentially reduce clean-up durations by an order of magnitude (Christ, Ramsburg et al. 2005, Rossi, Matturro et al. 2022). However, using microbial reductive dechlorination as a polishing step to remediate residual adsorbed TCE mass in a heterogeneous aquifer has not been well documented (Aulenta, Majone et al. 2006).

While most of the research on chlorinated ethene remediation has been performed using batch reactors or columns, few experiments have been done using an aquifer cell. An aquifer cell offers several advantages when compared to batch reactor and column studies including 2-D flow and the ability to represent the heterogeneous packing of soils. The present research supports previous studies that have analyzed bioenhanced back diffusion using well defined low-permeability zones using continuous addition of lactate as an electron donor (Hnatko, Yang et al. 2020). However, it differs when analyzing more complex and realistic heterogeneity, and an alternative electron donor source as a polishing step to support residual mass removal after EISB.

The goals for this research are to:

- Measure how bioremediation affects adsorption, back diffusion, and detoxification of chlorinated ethenes within an aquifer cell experiment packed with heterogeneous low permeability lens clusters.
- Measure the presence (total *Dhc*) and degradation metabolism capability (RDase genes) of dechlorinating microorganisms during enhanced in-situ bioremediation.
- Study the efficacy of a proprietary electron donor substrate (ERDenhanced) during bioremediation by measuring ethene production in a flowing 2D system.
- Calculate bioenhanced back-diffusion after simulated upgradient source zone treatment in a heterogeneous aquifer cell matrix.

Conclusions from this study will complement existing research while providing fresh insight into specific characteristics (soil type, electron donor, soil architecture) that contribute to chlorinated ethene bioremediation and mass transfer.

Chapter 2 – Background and Literature Review

2.1 Chemical Properties and Heath Risks of Chlorinated Ethenes

Chlorinated ethenes contain at least one chlorine atom covalently bonded to simple hydrocarbon chains and belong to a group of chemicals known as volatile organic compounds (VOCs). PCE, TCE, *cis*-1,2-dichloroethene (*cis*-DCE), and vinyl chloride (VC) are the most common chlorinated ethenes found in contaminated soil and groundwater. Parent compounds, such as PCE and TCE, exist as a dense non-aqueous phase liquid (DNAPL) at high concentrations which is denser than water and hydrophobic. After a DNAPL is released into an aquifer, capillary forces act to retain liquid ganglia or droplets within the porous media, which are immobile and do not travel downgradient under normal flow (Feenstra, Cherry et al. 1996). Substantial DNAPL volumes can also be retained and immobilized due to heterogeneous soils that can result in DNAPL pooling (Dekker and Abriola 2000). The density of TCE, the most commonly detected groundwater contaminant at Superfund sites (EPA 2023), is 1.4 g/L at 20°C (Sandmeyer 1981) and it has limited solubility in 18 MΩ Milli-Q™ deionized water of approximately 1,417 ppm (Knauss, Dibley et al. 2000). Chlorinated ethenes have industrial uses for degreasing, dry-cleaning, and military operations, and their unique properties made chlorinated ethenes a more popular choice over traditional petroleum products such as benzene, toluene, ethylbenzene, and xylene (BTEX). Use of TCE for dry-cleaning began in the 1930s and was slowly phased out and replaced by PCE in the 1950s (Doherty 2000). However, TCE continued as the main solvent used in metal cleaning applications through 1990 (Rusyn, Chiu et al. 2014). While large scale

use of TCE has slowed, it can still be found as a component in other chemical products like paint-strippers, adhesives, and PVC plastic (Doherty 2000, Hickman 2000, ATSDA 2017).

Chlorinated ethenes are among the most common soil and groundwater contaminates due to their widespread use and improper disposal methods (EPA 2023). Due to the persistent nature of these chemicals (non-flammable, chemically stable, low solubility), many historically contaminated sites still contain concentrations above the MCL issued by the United States Environmental Protection Agency (US EPA) (Huang, Lei et al. 2014). The MCL for PCE and TCE is 5 μg/L and 2μg/L for VC, and the US EPA has set a MCL goal of 0 μg/L for all three compounds (USEPA 2009). PCE and TCE are some of the most ubiquitous contaminants measured at concentrations above remediation goals at 69% and 59% of US Department of Defense sites, respectively (NRC 2013). This reality is largely due to low-permeable zones within heterogeneous aquifers that can adsorb high concentrations of contaminant mass - acting as a long-term reservoirs or secondary source zones (Grisak and Pickens 1980).

Exposure to chlorinated ethenes can occur through inhalation of vapors or consumption through contaminated groundwater. The negative health effects associated with exposure to chlorinated ethenes has resulted in a reduction in commercial use and an increase in regulations. The detrimental environmental and health effects of chlorinated ethenes gathered attention in the 1960s, and official EPA regulations began in the 1980s (Doherty 2000). TCE and vinyl chloride (VC) are listed by the International Agency for Research on Cancer (IARC) as class

1 carcinogens and are linked to kidney cancer, liver cancer, and non-Hodgkin's lymphoma (Wartenberg, Reyner et al. 2000, Guha, Loomis et al. 2012).

2.2 Techniques for Chlorinated Ethene Remediation

There are several physical methods available for remediation of sites contaminated with chlorinated ethenes including soil excavation, in-place containment, and groundwater extraction using pump and treat (Russell, Matthews et al. 2019). Additionally, techniques such as soil venting or thermal treatment can be used to remove vapor phase contaminants from source zone areas and groundwater plumes (Russell, Matthews et al. 1992, Sims, Suflita et al. 1992). Challenges associated with physical removal techniques include high costs, off-site disposal of extracted contaminants, and complications such aquifer heterogeneity, sorption to soils, and limited accessibility (Mackay, Roberts et al. 1985, Russell, Matthews et al. 1992). These challenges have shifted the focus to in-situ degradation technologies, like chemical oxidation and bioremediation, where contaminants are transformed into non-toxic products within the subsurface (Stroo, Leeson et al. 2012). In-situ chemical remediation can result in rapid transformation of chlorinated ethenes, but this technique is prone to rebound of contaminant mass once active treatment ends. This rebound occurs due to back diffusion from adsorbed mass in low-permeability media where sufficient contact was not achieved or from competing reactions in the subsurface. These challenges to remediation are also affected by the relatively short resident time of many chemical amendments into natural aquifers (Huling, Ross et al. 2017).

Biotic and abiotic processes often work together during remediation at complex sites (NRC 2013). Abiotic in-situ chemical reduction uses zerovalent iron (ZVI) technologies such as nanoscale iron and naturally occurring reduced minerals such as magnetite, green rust, and iron sulfides (Brown, Mueller et al. 2009). Products of abiotic dechlorination include dichloroacetylene, choroacetylene, and acetylene (Arnold and Roberts 2000). While these processes are often much slower and complex than biotic reductive dechlorination, it can assist in the overall process of removing contaminant mass (Tobiszewski and Namieśnik 2012).

An increasingly popular method for treating chlorinated ethene contaminated sites is using enhanced in-situ bioremediation (EISB) to transform chlorinated ethenes into ethene. EISB is a popular remediation technique since it is often a more sustainable approach, and less infrastructure is needed compared to techniques like pump and treat and thermal remediation. Monitoring wells allow access to specific locations within contaminated aquifers for monitoring, bioaugmentation, and biostimulation. Additionally, microbes utilizing EISB can continue dechlorination after initial bioaugmentation if conditions are favorable (neutral pH, electron donor available, anoxic), reducing the potential for contaminant rebound (Adamson and Newell 2009, McGuire, Adamson et al. 2016).

Bioremediation of chlorinated ethenes relies on the process of organohalide respiration to achieve microbial reductive dechlorination (MRD) that transforms toxic PCE, TCE, cis-DCE, and VC to benign ethene. This process is thermodynamically favorable under standard conditions, and microorganisms can gain energy from these reactions (Löffler, Ritalahti et al. 2013). The

chlorinated ethenes act as the electron acceptor and hydrogen is used as the electron donor (DeWeerd, Concannon et al. 1991). *Dehalobacter restrictus* was the first organism discovered that grew with PCE as the electron acceptor. However, dechlorination stopped at cis-DCE, so detoxification was not achieved (Holliger, Schraa et al. 1993, Holliger, Hahn et al. 1998). The discovery of *Dehalococcoides* proved that reductive dechlorination past cis-DCE to ethene existed (Freedman and Gossett 1989). This first isolate was named *Dehalococcoides ethenogenes* strain 195 and grew using PCE, TCE, and cis-DCE as electron acceptors, but VC was co-metabolically dechlorinated to ethene after all other polychlorinated ethenes were consumed (Maymó-Gatell, Nijenhuis et al. 2001). Another milestone discovery was the isolation of *Dehalococcoides sp*. strain BAV 1, which was the first isolate capable of organohalide respiration of VC to ethene (He, Ritalahti et al. 2003). Additional *Dhc* isolates including strain GT and VS followed and provided a diverse consortia of strains capable of reductive dechlorination to ethene (Müller, Rosner et al. 2004, Sung, Ritalahti et al. 2006). Currently, all known *Dehalococcoides* strains are classified under *Dehalococcoides mccartyi* (*Dhc*).

Dhc is a well-documented and widely used microbial species for EISB of chlorinated ethenes due to its ability to transform chlorinated ethenes to ethene (Duhamel, Mo et al. 2004). A commercially available microbial consortium containing *Dhc*, KB-1® (SiREM, Ontario, Canada), has been implemented numerous times for bioaugmentation at field sites (Cox, McMaster et al. 2002, Major, McMaster et al. 2002, Sleep, Seepersad et al. 2006, Richardson 2012). However, there are certain site conditions that are necessary to achieve successful remediation outcomes. KB-1 is an anaerobic consortium that requires a neutral pH (6.8-7.8) that is optimal

for dechlorination. Fermenters in the KB-1 consortium are capable of transforming lactate (a commonly used fermentable substrate) into acetate, propionate, and hydrogen that can be utilized as an electron donor by *Dhc*. Additionally, Dhc relies on other microorganisms (such as *Geobacter lovleyi*) that produce vitamin B12 which is necessary to promote *Dhc* activity (Yan, Ritalahti et al. 2012). The most observed degradation pathway associated with bioremediation using *Dhc* is shown in Figure 2.1. This flow chart outlines the stepwise dechlorination process from PCE to ethene. As dechlorination occurs, increased solubilities of daughter products can promote greater mass transfer from PCE and TCE source zones (Knauss, Dibley et al. 2000, Cápiro, Löffler et al. 2015). It has been reported that during biotransformation, cis-DCE is a more common intermediate than trans-DCE and 1,1-DCE (Bouwer 2017).

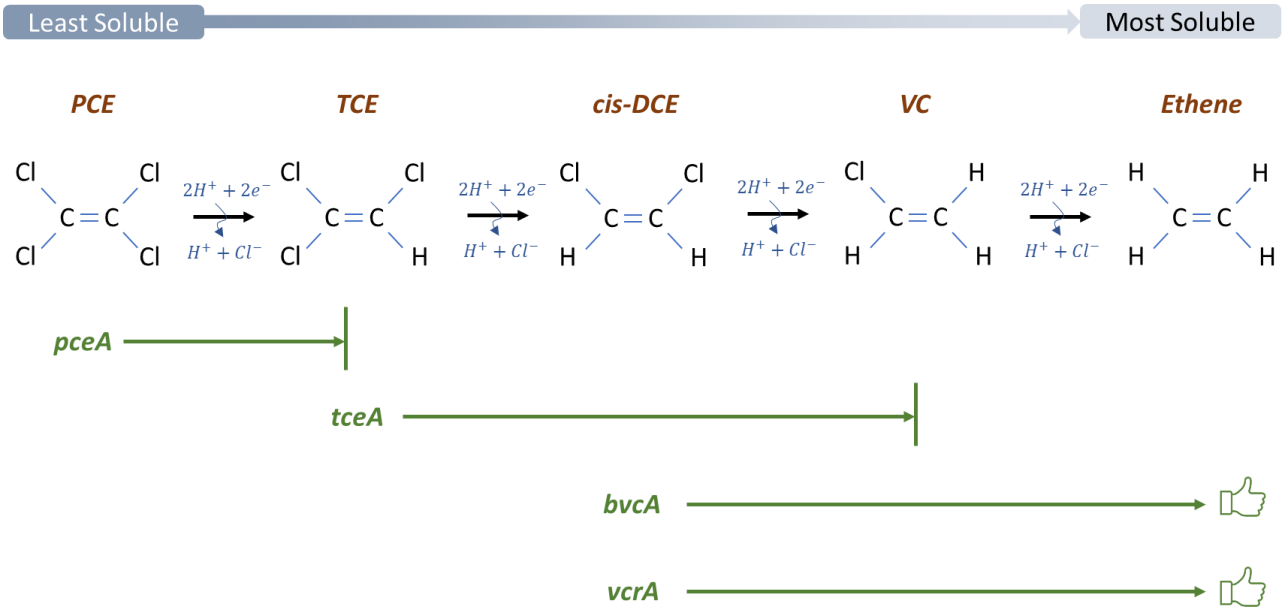

Figure 2.1 Chlorinated ethene chemical structure and dechlorination pathway [adapted from (Löffler and Edwards 2006)]

Specific RDase genes found in various strains within the *Dhc* community are indicators for different stages of dechlorination of PCE to ethene. Each strain of *Dhc* can transform specific chlorinated compounds, but only a few have been identified that are able to transform VC to ethene (Molenda, Tang et al. 2018). PCE reductase (*pceA*) catalyzes the first dechlorination step of PCE to TCE. TCE reductase (*tceA* gene) catalyzes the transformation of TCE to VC, vinyl chloride reductase (*vcrA* gene) and vinyl chloride reductase b (*bvcA* gene) catalyzes the transformation of *cis*-DCE and VC to ethene (Magnuson, Romine et al. 2000, Krajmalnik-Brown, Hölscher et al. 2004, Müller, Rosner et al. 2004, Futagami, Goto et al. 2008, Patil, Adetutu et al. 2014). Monitoring total *Dhc* 16S rRNA and RDase gene abundance can be a useful tool when predicting remediation performance. A positive correlation between total *Dhc* 16S rRNA gene and VC RDase (*bvcA and vcrA)* gene abundances greater than 10^7 and 10^6 gene copies/L, respectively and higher ethene concentrations has been established – indicating more complete transformation at this concentration threshold (Clark, Taggart et al. 2018). Additionally, incomplete dechlorination occurs when VC RDase genes are less than 10^5 gene copies/L, even if total *Dhc* 16S rRNA gene abundance is greater than 10^7 gene copies/L (Clark, Taggart et al. 2018). This emphasizes the need for adequate concentrations of dechlorinating microbes (containing the necessary RDase genes) for complete transformation to ethene. Measurement and documentation of RDase genes present at a site can give valuable insight into the capacity for a site to undergo successful bioremediation.

One of many challenges to EISB at complex sites includes selecting an electron donor source for different stages of a project's lifespan. Lactate is a commonly used fermentable substrate that

is used at field sites implementing EISB. Alternative electron donor sources that have a longer residence time in aquifers could prove to be more efficient in maintaining a more passive approach to remediation. Slow-release electron donors such as emulsified vegetable oil (EVO) (EOS Remediation; Research Triangle, NC; and RS®, TerraSystems, Inc), hydrogen releasing compounds (HRC) (Regenesis), and tetrabutoxysilane (TBOS) (Aldrich Chemical) could be beneficial for passive remediation techniques that desire a more hands off approach. The use of these slow-release substrates are especially beneficial for difficult sites with long-term remediation goals due to stored mass and back-diffusion from heterogeneous aquifers (Yu and Semprini 2002). Experiments have shown that sustained microbial dechlorination is possible for long periods of time for TBOS (>500 days), EVO (>900 days), and HRC (>300 days)(Adamson, McDade et al. 2003, Yu and Semprini 2009, Harkness and Fisher 2013). The benefit of slow-release electron donors include less amendments to the aquifer and a gradual provision of nutrients to decrease management costs and increase prolonged remediation processes (Joksimovich and Koenigsberg 2002).

2.3 Bioremediation Experimental Studies

Microcosm reactor studies have explored microbial reductive dechlorination and associated microbial population for many years (Hopkins, Semprini et al. 1993, Kranzioch, Ganz et al. 2015). These experimental studies have provided a crucial foundation for understanding the processes of microbial dechlorination. Microcosms are beneficial in isolating specific processes in a controlled environment. However, this method of research lacks the ability to observe complex interrelationships between soils, microbes, and contaminants that occur in

heterogeneous flowing systems. Column studies are better suited to analyze rate limited processes in a 1-D flow system. A column packed with porous media can capture sorption and desorption rates, biodegradation rates, and spatially relevant microbial community analysis (Harkness, Bracco et al. 1999, Evans, Nguyen et al. 2014, Mirza, Sorensen et al. 2016). All these processes are important for understanding the complex reactions that occur within a contaminated aquifer (Figure 2.2). An aquifer cell experiment can provide even more information on the interrelationships of chlorinated ethene transport, degradation, and microbial populations (Cápiro, Löffler et al. 2015). An aquifer cell can be packed with multiple soil types with a range of properties for insight into how bioremediation occurs within a complex soil matrix. Desorption and diffusion from low permeability zones and spatial variability of microorganisms can be analyzed to understand a more in-depth picture of how bioremediation takes place (Hnatko, Yang et al. 2020).

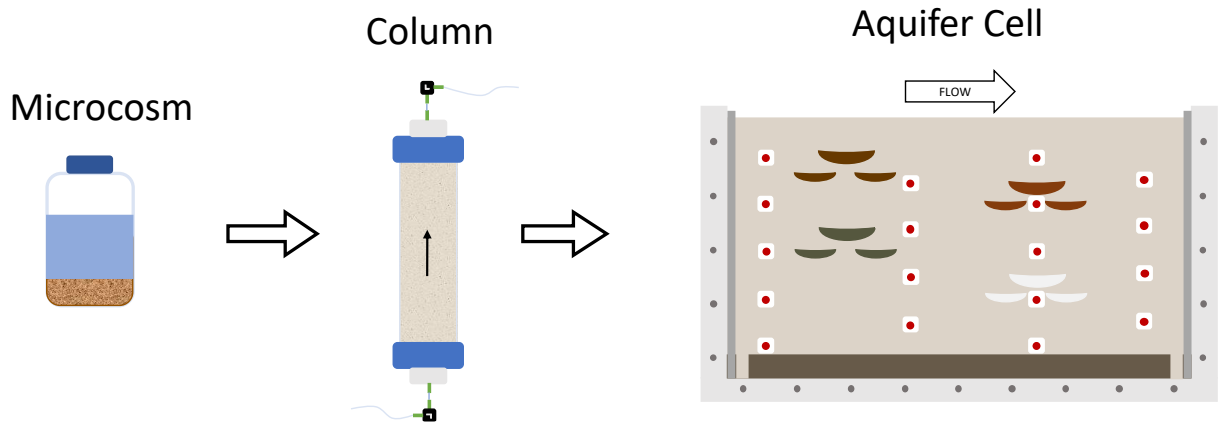

Figure 2.2 Experimental progression of increasing complexity from microcosm (0-D) to column (1-D) to aquifer cell (2-D)

Previous aquifer cells have studied the spatial and temporal dynamics of organohalide-respiring bacteria in relation to DNAPL source zones (Sleep, Seepersad et al. 2006, Glover, Munakata-

Marr et al. 2007, Haest, Springael et al. 2012, Cápiro, Löffler et al. 2015). Often, contaminant spills include a DNAPL source zone that remains in its separate phase within the aquifer. In this instance, studies have shown that *Dhc* cell abundance and growth was greater near the DNAPL source zone and dechlorination rates increased where microbes were attached to the soil. It is well documented that microbial processes can increase DNAPL mass transfer from 1.5 to 21-fold by converting them to more soluble byproducts compared to abiotic dissolution (Glover, Munakata-Marr et al. 2007, Haest, Springael et al. 2012, Philips, Van Muylder et al. 2013, Cápiro, Löffler et al. 2015). This emphasizes the dynamic microbial response to DNAPL source zones and the importance of understanding the impact aquifer source zone architecture has on remediation performance.

Less is known about the biogeochemical processes that dictate remediation performance of adsorbed chlorinated ethenes in low-permeable soils. Wanner, Parker et al. (2018) studied a field site with a history of long-term exposure to chlorohydrocarbons. While this study identified degradation pathways using carbon isotope analysis, modeling was used to predict abiotic mediated back diffusion fluxes up to 1.0×10^{-10} to 7.6×10^{-9} mmol/m^{2}s of chlorinated ethenes from a low-permeability aquitard. While abiotic processes can contribute to back diffusion, biotic processes are responsible for a majority of back diffusion in anaerobic environments (Major, McMaster et al. 2002, Hood, Major et al. 2008, Berns, Sanford et al. 2019). Berns, Sanford et al. (2019) utilized an aquifer cell packed with varying porous media to determine how abiotic and biotic processes affect TCE mass flux from low-permeability media. This study discussed that the highest impact on flux was near the interface between low-

permeability media and high permeability media. The interface is also where the available electron donor and electron acceptor concentrations were the highest. Results from this study support that biotic processes outperform abiotic processes when electron donor is available.

Puigserver, Herrero et al. (2022) studied the biotic and abiotic reductive dechlorination of chlorinated ethenes in aquitards by analyzing a field site. This study determined that bioremediation can promote back diffusion from low-permeability zones. While this process helps to remove stored contaminant mass, it can also be detrimental to the environment. If complete dechlorination does not occur, daughter products with higher solubilities and toxicities may diffuse from the low-permeability media and create a larger problem (Puigserver, Herrero et al. 2022). For this reason, it is important to know the remediation capacity of the entire aquifer to fully remediate a site.

A review of studies, performed by Blue, Boving et al. (2023), determined that only a small number field studies has been performed in detail sufficient enough to estimate the impact on bioenhanced back diffusion from low-permeability media. It is difficult to predict accurately estimate the extent of back diffusion due to multiple factors attributing to contaminant rebound and plume persistence. An example includes is the Naval Air Warfare Center (NAWC) Superfund site in West Trenton, NJ. This site was contaminated with TCE in an aquifer containing interbedded zones of low-permeability media containing high organic carbon soils. Amendments targeting these low-permeability zones increased mass removal, but several repeated rounds of bioaugmentation over many years would be needed for complete removal

(Blue, Boving et al. 2023). Estimating the duration required for remediation is difficult due to challenges in quantifying the effect bioremediation has on mass transfer in low-permeability zones. Studies have been performed to bridge this gap using multi-component transport modeling that accounts for mass flux in clay. Chambon, Broholm et al. (2010) determined that the time to remove 90% of contaminant can be reduced up to half when MRD occurs near the clay interface. Additionally, field studies have confirmed that microorganisms are able to effectively penetrate low-permeable zones to increase the mass transfer of chlorinated ethenes (Scheutz, Broholm et al. 2010).

A laboratory study that simulated the biological impact on back-diffusion, Hnatko, Yang et al. (2020), packed an aquifer cell with various low-permeability soil lenses to study how dissolved and adsorbed TCE interacts within a heterogenous aquifer. Dechlorinating microorganisms increase the mass transfer of chlorinated ethenes from low permeability porous media by increasing the difference in concentration gradient that drives the dissolution of chlorinated ethenes and increasing diffusivity with less chlorinated daughter products. An expression to quantitatively measure the enhanced back diffusion due to the presence of microorganisms was developed (Equation 1) (Hnatko, Yang et al. 2020).

$$\delta_{MRD} = \frac{CM_{exp} - CM_{sim}}{CM_{sim}} \times 100\% \qquad (\textit{Equation 1})$$

Where, δ_{MRD} measured the effective enhancement of TCE back diffusion, dissolution, and desorption attributed to microbial reductive dechlorination (MRD), CM_{exp} was the total chlorinated ethene molar mass calculated from biotic experimental measurements, and CM_{sim} was the total TCE molar mass calculated using model simulations to predict the same scenario

under abiotic conditions (Hnatko, Yang et al. 2020). While accounting for heterogeneity in physical and chemical properties, this study quantified local bioenhancement of back diffusion up to 53%. *Dhc* cells were capable of penetrating low-permeability porous media including clays, contributing to the enhanced back diffusion. This aquifer cell experiment was significant in determining that bio-enhanced back diffusion increases TCE mass transfer from low-permeability soils during EISB. Conclusions from the studies collectively suggest that mass transfer rates of DNAPL and adsorbed TCE increases with the presence of actively dechlorinating microorganisms (Amos, Suchomel et al. 2008, Cápiro, Löffler et al. 2015, Verce, Madrid et al. 2015, Berns, Sanford et al. 2019, Hnatko, Yang et al. 2020).

2.4 Knowledge Gaps

Much of the existing research on bioremediation of chlorinated ethenes is based on batch reactors or packed columns (Sleep, Seepersad et al. 2006, Amos, Suchomel et al. 2008). These experimental systems are unable to accurately represent 2D flow and back diffusion in a heterogenous aquifer. Additionally, dissolution of chlorinated ethenes from DNAPL source zones has been the primary focus for microbially enhanced mass transfer (Suchomel, Ramsburg et al. 2007, Cápiro, Löffler et al. 2015). These studies focus primarily on dissolution of a DNAPL source zone and not on the back diffusion of adsorbed mass to soils. Only a few studies to date have analyzed bioenhanced back diffusion from low-permeability media in a controlled aquifer cell experiment (Berns, Sanford et al. 2019, Hnatko, Yang et al. 2020). The Berns, Sanford et al. (2019) study analyzed the contribution of abiotic and biotic pathways during anaerobic MRD, but did not focus on the microbial community distribution within the varying permeability

zones. Field studies have determined that bioenhanced back diffusion is able to decrease clean up times, but isolating the impact MRD has on mass removal is challenging and multiple remediation efforts are often still needed (Blue, Boving et al. 2023). Hnatko, Yang et al. (2020) analyzed the effect microorganisms have on increasing the mass transfer of chlorinated ethenes out of low-permeability soil lenses. Inspiration from this previous study guided experimental set-up for the present research, but several key differences were established to improve upon the existing data base. A more in-depth discussion on the differences in experimental parameters and approach are listed below:

Soil type is an important parameter when analyzing chlorinated ethene remediation at contaminated sites. Specifically, organic carbon content (OC%) and hydraulic conductivity can have a large impact on the liquid-solid partitioning coefficient. This is traditionally measured by performing an adsorption isotherm experiment to determine the soil-water distribution coefficient (K_d). The K_d is specific to each contaminant and soil type and is used to determine the concentration of contaminant associated with the aqueous phase and solid phase; it is also crucial when estimating the quantity of contaminant mass stored in soils and can provide insight into the duration required to remove it. Different soils were used for the experimental set-up of the aquifer cell in the present experiment in order to provide a more realistic range for soil organic carbon (NRC 2000). Hnatko, Yang et al. (2020) used soils with an organic carbon range of 0.01% to 3.33%, and the present research analyzed a narrower range of organic carbon (0.01% to 0.91%) that is more representative of realistic aquifer conditions and might be found at a contaminated field site (NRC 2000).

Aquifer cell experiments are unique in that heterogeneous conditions can be established using various soil packing configurations. When studying adsorption and desorption of chlorinated ethenes from low-permeability lenses, the shape and surface area of these lenses likely play a significant role. Therefore, the soil lenses for this experiment were packed in three semicircular clusters instead of a singular rectangular block (Hnatko, Yang et al. 2020). This design increased the surface area of each soil lens by approximately 50%. Since bioenhanced back diffusion occurs at the interface of low-permeability media and bulk media, this change could increase the overall bioenhanced back diffusion for the aquifer cell.

Electron donor is one of the key ingredients that is needed at a site to achieve organohalide respiration using dechlorinating microorganisms such as *Dhc*. Naturally present organic carbon in soils offer low amounts of electron donor, thus biostimulation is often needed to achieve microbial growth in quantities needed to achieve remediation goals (NRC 2000). Hnatko, Yang et al. (2020) provided lactate continuously to the aquifer cell to encourage microbial productivity. Lactate pulses are common in field practice, but as sites transition to long-term management, a substrate that can remain in the aquifer and provide a slow release of electron donor may be a more desirable approach. When correctly implemented, the use of a long-term electron donor can decrease the frequency and cost of amendments while maintaining sustained remediation (ESTCP 2009). The current research utilized a proprietary electron donor substrate during EISB to explore the potential benefits of an alternative organic carbon source and biofilm formation within the soil matrix.

Chapter 3 – Bioenhanced Back Diffusion in a Heterogeneous Aquifer Cell

3.1 Introduction

Enhanced in-situ bioremediation (EISB) is one of the most common techniques used to treat chlorinated ethene contaminated sites (EPA 2020). Microorganisms such as *Dehalococcoides mccartyi* (*Dhc) and Geobacter* species *(Geo)* have been well studied for their ability to transform tetrachloroethene (PCE) and trichloroethene (TCE) to benign ethene. Use of EISB (bioaugmentation and biostimulation) has led to 90% removal of the original mass under favorable conditions (GeoSyntec 2004, McGuire, McDade et al. 2006). Microbial reductive dechlorination (MRD) of chlorinated ethenes occurs in a stepwise fashion where tetrachloroethene (PCE) is dechlorinated into trichloroethene (TCE), *cis*-1,2-dichloroethene (cis-DCE), vinyl chloride (VC), and ethene. However, a stall in dechlorination past cis-DCE has been observed in many instances (van der Zaan, Hannes et al. 2010). This can be attributed to several causes such as insufficient electron donor, low concentrations of *Dhc*, and lack of specific Reductive Dehalogenase (RDase) genes responsible for ethene production. Thus, more information is needed to better understand the complex processes occurring during bioremediation.

Adsorption into low-permeability media with high organic carbon [high soil-water distribution coefficient (K_d)] can lead to mass storage of chlorinated ethenes downgradient of the primary source zone (Hnatko, Yang et al. 2020). Engineered bioremediation has proven successful at reducing concentrations at the source zone, but long-term desorption and back diffusion from low-permeability media can lead to contaminate concentrations higher than remediation goals

(Parker, Chapman et al. 2008). MRD has shown to improve mass release (bioenhanced back diffusion) from low-permeability zones by up to 53% (Sleep, Seepersad et al. 2006, Berns, Sanford et al. 2019, Hnatko, Yang et al. 2020). This is attributed to an increased diffusivity with dechlorination and a change in concentration gradient that increases mass transfer from the low-permeability media.

To make remediation at complex sites more feasible, engineered remediation can be paired with a secondary, more hands-off approach (passive remediation). For this research, passive remediation is defined as decreasing amendments and/or relying on improved in-situ conditions for continued mass removal. Passive remediation can take many forms but must consist of significantly decreasing amendments to into the system (NRC 2013). Examples of this include utilizing a slow-release electron donor or ceasing the practice of groundwater re-circulation. Passive remediation is not to be confused with MNA which relies only on natural aquifer conditions to achieve remediation goals. This technique is becoming increasing popular at complex sites where contaminant concentration persists within low permeability media. While a transition to passive remediation was attempted with this research, it was not fully achieved since additional amendments were required to achieve complete dechlorination to ethene.

Biostimulation is a key step that is often needed at sites to achieve organohalide respiration using dechlorinating microorganisms such as *Dhc*. Naturally present organic carbon in soils may offer low amounts of electron donor; however, biostimulation is often needed to achieve

microbial growth in quantities needed to achieve remediation goals (NRC 2000). ERDenhanced is a proprietary electron donor substrate (Terrastryke; Andover, New Hampshire) that has potential to be used for biostimulation at chlorinated ethene contaminated sites. ERDenhanced is partially soluble and contains inactivated yeast and boron (an essential component for quorum sensing). Quorum sensing is how bacterial cells coordinate collective behavior and form biofilms (Coulthurst, Whitehead et al. 2002). In general, biofilms provide stability and protection for microorganisms and have been implemented in bioremediation applications (Sonawane, Rai et al. 2022). The formation of biofilms near low-permeability soils could promote the mass transfer of contaminates concentrated at soil lens interfaces (Sivadon, Barnier et al. 2019). Additionally, biofilm formation is thought to decrease the permeability of soils over time (Roth and Caslake 2019). This could provide a longer residence time and allow for microorganisms to fully dechlorinate to ethene. It was hypothesized that the low-solubility of ERDenhanced could prove beneficial in acting as a long-term, slow-release electron donor source compared to conventional products such as lactate. The use of ERDenhanced was selected to explore the potential for greater mass removal and sustained microbial productivity over time by utilizing the benefits of potential biofilm formation within and around low-permeability zones.

Challenges in remediation of chlorinated ethene contaminated sites include heterogeneous aquifers with low-permeability zones that can store contaminant mass for long periods of time – even after source zone removal. Field studies and modeling work have shown that the impact of bioenhanced diffusion can be significant when reducing contaminant mass and remediation

timeframes (Chambon, Broholm et al. 2010, Scheutz, Broholm et al. 2010, Blue, Boving et al. 2023). To further understand how physical heterogeneity and bioremediation effects the storage, release, and degradation of chlorinated ethenes, an aquifer cell experiment was performed. The aquifer cell was packed with five different low-permeability lenses to study the bioenhanced back diffusion and *Dhc* population distribution during engineering remediation and after simulated source zone removal. Results from this study add to the limited experiments that measure bioenhanced back diffusion from low-permeability media in a heterogeneous aquifer (Berns, Sanford et al. 2019, Hnatko, Yang et al. 2020, Blue, Boving et al. 2023). This research adds to the growing knowledge of how subsurface architecture, specifically surface area of low permeability lenses, impacts bioenhanced back diffusion of adsorbed chlorinated ethenes. An alternative electron donor substrate (ERDenhanced) was implemented to study the potential benefits of its use during bioremediation including prolonged release of organic carbon and biofilm formation. Additionally, bioenhanced back diffusion and spatially relevant *Dhc* and RDase gene abundances were measured to further understand how microorganisms impact mass flux of chlorinated ethenes from low-permeability lenses.

3.2 Materials and Methods

3.2.1 Porous Media Characterization and Preparation

The aquifer cell was constructed using six different soils with varying hydraulic conductivities (K) and organic carbon content (OC%) to create a heterogeneous aquifer configuration. A background media of ASTM 20/30 mesh Ottawa sand (US Silica Company; Ottawa, IL) was selected due to its relatively high hydraulic conductivity and low organic carbon content. Soils

including Arkport soil, Hudson soil, Appling soil, and Ottawa F-65 sand were added to create four low-permeability lenses. Clay taken from the Commerce St. Superfund site was placed at the bottom 3 cm to create a lower confining layer. These soils were chosen to study bioremediation over a range of different hydraulic conductivities, organic carbon contents, and adsorption coefficients (K_d). The properties of each soil used is shown below in Table 3.1. More detailed information about soil properties and procedures for soil testing can be found in the Appendix (Section A.2).

Table 3.1 Properties of soils used in aquifer cell experiment

Material	Hydraulic Conductivity (m/day)	Organic Carbon (%)	Adsorption Isotherm K_d(L/kg)
Commerce Street Clay	0.05[b*]	0.27	1.47
ASTM 20/30	200[b]	N/M[g]	N/M[g]
Arkport	1.64[a]	0.16[a]	0.11*
Hudson	0.04[a]	0.91[a]	0.56
Appling	10.2[c]	0.75[a]	0.83[d]
F65 Sand	19.01[h]	0.01[e]	0.006[f]

a: Values measured by Harry Vaslo
b: Hnatko, Yang et al. (2020) - model fitted value
b*: Hnatko, Yang et al. (2020) – value reported from clay at same site but different location
c: Pennell, et al. 1995
d: Calculated by $K_d = Orgranic\ Carbon\ Content * K_{OC}$ using the organic carbon content from Marcet, Cápiro et al. (2018) and K_{OC} = 126 L/kg for TCE from Pankow, Luo et al. (1996)
e: known value for F95 sand was assumed similar to F65 sand Marcet, Cápiro et al. (2018) based on grain size distribution
f: Joo, Shackelford et al. (2008) value for F95 assumed similar to F65 sand based on grain size distribution
g: N/M = not measured
h: Bastidas (2016)
*: non-linear Langmuir model constants q_m = 13.41, K_L = 0.11

The only natural soil with an unknown value for organic carbon was the Commerce St. clay, so this was the only soil measured for this experiment. All other soil OC% was measured by Harry Vaslo (Masters student in Dr. Natalie Cápiro's Lab at Auburn University) or Tyler Marcet (Marcet, Cápiro et al. 2018). Methods for determining OC% can be found in Section A.2.1. Batch adsorption and desorption experiments were performed on the Commerce St. Clay, Hudson soil, and Arkport soil to measure the adsorption coefficient (K_d) and better understand TCE adsorption and desorption within the aquifer cell (Sections A.2.2 and A.2.3). The Appling soil was calculated using OC% and K_{oc}, which could potentially cause differences if the Appling soil used for this experiment had varying properties or does not maintain a linear K_d.

Prior to emplacement into the aquifer cell, the soils (Arkport, Appling, Hudson, and Commerce St. Clay) were ground with a mortar and pestle and passed through a #20 mesh sieve. The Commerce St. Clay was pre-saturated with TCE to allow for maximum penetration into the low-permeability soil and decrease the total time required to fully saturate the aquifer cell while flowing. The clay was air-dried, ground with a mortar and pestle, passed through a #20 mesh sieve, and saturated with a 0.76 mM (100 ppm) TCE solution in 1-L mason jars. The jars contained 240 grams of clay and 700 ml of synthetic groundwater (Section A.1). After waiting approximately 4 months to allow for equilibration, methanol extraction was performed on the clay to measure TCE concentration in the clay (Section A.3.3).

3.2.2 Construction of the Aquifer Cell

The aquifer cell (63.5 cm length x 38 cm height x 1.4 cm thickness) was constructed using an aluminum frame with two glass panels on each side. The back glass panel is solid while the front-facing panel (shown in Figure 3.1) contains 18 glass ports with bleed and temperature optimized (BTO) septa (Restek, Bellefonte, PA) that were pierced with a 25-gauge BD PrecisionGlide 1 ½" needle (VWR, Radnor, PA) and sampled to provide spatially relevant VOC and biomass information throughout the aquifer cell experiment. Two aluminum well screens were attached on each side to allow flow from left to right through the aquifer cell without fines leaving the system.

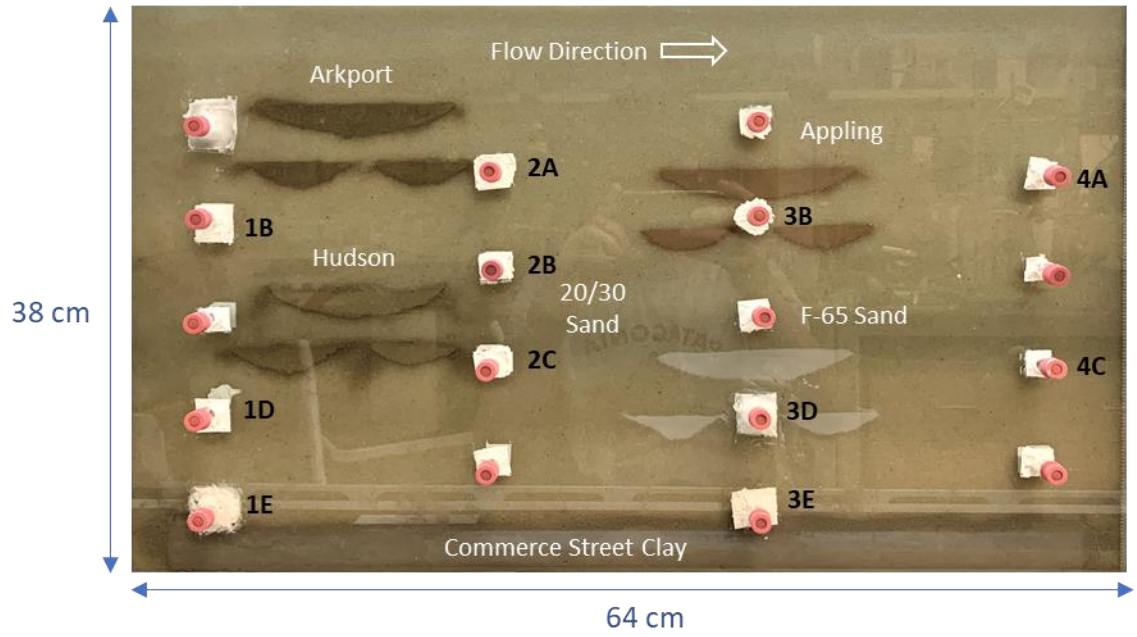

Figure 3.1 Image of aquifer cell showing actual configuration and size of soil lenses

A total mass of 416.6 g TCE pre-saturated Commerce St. clay slurry (225 g dry weight) was placed into the bottom 3 cm of the aquifer cell first, and the remaining aquifer cell was packed under a head of synthetic groundwater to ensure full saturation of all the soils. An ASTM 20/30 Ottawa mesh sand buffer of about 2 cm was added on each side of the clay layer to prevent any

fines from infiltrating the well screens. The lenses were created using a metal weighing spatula attached to a dowel rod to create a crater in the sand. The soil for the lens was added using a funnel from the top of the aquifer cell and background sand was folded over the soil lens to prevent saturated soil from dispersing into the head of water. After each lens cluster was created, the background sand was added until it was just above the top of the well screen slots (about 2 cm from the top of the aquifer cell). The total mass of each porous media that was added to the aquifer cell during the packing process is listed in Table 3.2.

Table 3.2 Mass of porous media added to aquifer cell during packing

Soil	Dry mass added to aquifer cell (g)
ASTM 20/30 Sand	5067.83
Arkport	71.61
Appling	67.77
Hudson	39.47
F-65 Sand	64.95
Commerce St. Clay	225

The aquifer cell was driven by a difference in head between the influent and effluent reservoirs (Figure 3.2). Stainless steel tubing (1/8” diameter) was lowered inside the well screens to simulate screened pumping wells into the aquifer. Argon gas was constantly introduced to a 4-L Mariotte influent bottle through an open rubber stopper. Since argon is heavier than ambient air, the introduction of argon created a gas buffer to minimize volatilization of TCE as the water level decreased over time. This configuration also assisted in maintaining anaerobic conditions within the influent bottle by preventing mixing of air near the liquid-headspace interface. The

effluent line was configured with a 20-ml glass sampling bulb so that samples could be extracted without volatilization of chlorinated ethenes and to maintain redox conditions. A flow rate of 1 ml/min (60 cm/day) in the aquifer cell was established by adjusting the height of the influent and effluent reservoirs using lab-jacks. A 3-way ball valve was used for switching the influent bottles, and a Hamilton 3-port valve was used for the effluent sample collection during the experiment.

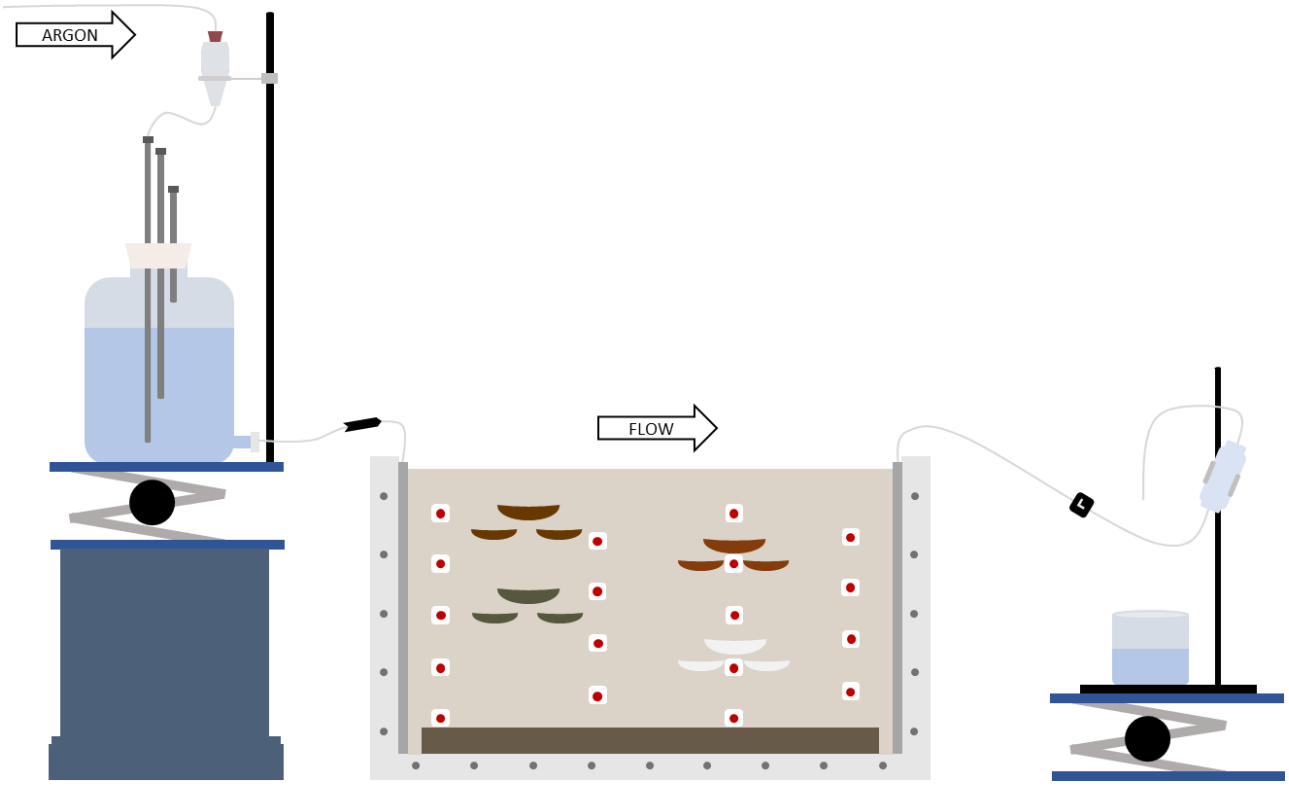

Figure 3.2: Aquifer cell experimental schematic including influent and effluent

3.2.3 Operation of the Aquifer Cell

Table 3.3 outlines each phase of the aquifer cell experiment including the duration, flow rate, influent solution, and sampling locations.

	Non-Reactive Tracer		Natural Conditions		EISB			Passive Remediation		
Phase	Develop Bromide Plume	Bromide Flushing	Develop Bromide/ TCE Plume	Natural Flushing	Develop TCE Plume	BIOAUGMENTATION & ERD	Establish Community	TRANSITION FROM EISB → PASSIVE	No Amendments	ϟ Complete Source Zone Removal
Duration (PV)	0.37	1.5	42	18	18.5		8.9		12.1	3
Flow Rate (ml/min)	2.28	2.28	1	1	0.27		0.23✕		0.23	0.23
Influent Solution	10 mM NaBr 20 mM NaCl 0.06 mM Erioglaucine A Dye	30 mM NaCl	0.38 mM TCE (50 ppm) 30 mM NaCl	**0.02 mM TCE (3 ppm)** 30 mM NaCl	0.38 mM TCE (50 ppm) 5 mM Lactate		0.38 mM TCE (50 ppm) 6 g/L ERD		**0.02 mM TCE (3 ppm)**	0 mM TCE (0 ppm) 1 mM Lactate
Sampling Location	Effluent	Effluent	Effluent/ Ports	Effluent/ Ports	Effluent/ Ports	1	Effluent/ Ports 2 3	4	Effluent/ Ports	Effluent/ Ports 5

Table 3.3: Aquifer Cell Experimental Timeline

- Durations and flow rates were determined based on modeling (VT) and experimental objectives. Numbers on the bottom correspond to phases listed in Figure 3.11.

✕ *A 48-hour flow interruption at PV 4.2 was performed to provide a longer residence time*

ϟ *Samples from this point forward were taken with assistance from Harry Vaslo, Savannah Cummins, and Temitope Popoola*

3.2.3.1 Non-Reactive Tracer

A bromide and erioglaucine A (blue dye) tracer test was performed to determine hydraulic parameters [pore volume (PV) and average porosity] and illustrate flow paths throughout the aquifer cell. The influent contained low ionic strength (IS) synthetic groundwater with 10 mM NaBr, 20 mM NaCl, and 0.06 mM blue dye. More information about the ingredients and preparation of groundwater solutions can be found in Section A.1. The ionic strength for the current research was maintained at 30 mM for the entire experiment to provide a consistent environment for controlling the solubility of chemicals and fines. The tracer test was performed at an average flow rate of 2.28 ml/min (143 cm/day) and 570 mL (0.37 PV) of the bromide/dye was injected into the aquifer cell. Samples were collected using a Spectrum Labs CF-2 fraction collector (Spectrum Chemical, New Brunswick, NJ) and bromide was measured using a Thermo Scientific Orion Dual Star pH/ISE meter (Thermo Fisher Scientific, Waltham, MA) with a combination ion-selective electrode probe (Cole-Parmer; Vernon Hills, IL) and an ion chromatograph (IC) (see Section A.3.1 for more details).

3.2.3.2 TCE Saturation

To simulate TCE mass storage in the low-permeability lenses, after the tracer test, the aquifer cell was saturated with 0.38 mM TCE and 20 mM bromide at a flow rate of 1 ml/min (i.e., seepage velocity of 60 cm/day) for 42 PVs. Bromide was introduced along with TCE as a reference to investigate the adsorption and desorption of TCE, and to identify slow flow regions Influent and effluent samples were collected every PV, and port samples were collected every other PV for the measurements of bromide and TCE during the saturation phase. Port samples

were extracted using a Fusion 200 syringe pump (Chemyx; Stafford, TX) at a rate of 5% of the background flow to prevent disrupting flow paths in the aquifer cell. To achieve a concentration of 0.38 mM TCE in the influent, a stock of approximately 6 mM (800 ppm) TCE was prepared in low IS solution. The stock was measured prior to preparation of the influent so that the appropriate amount of stock was added each time to achieve 0.38 mM TCE. The duration of TCE saturation phase was determined by modeling from collaborators at Virginia Tech University based on physical properties (organic carbon and soil-water partitioning coefficient (Kd)) of the soils, flow properties (from tracer test), and TCE concentrations measured in the aquifer cell. During the TCE saturation, samples analyzing volatile organic compounds (VOCs) and bromide were collected to track the influent mass and recovered mass for TCE and bromide.

3.2.3.3 Natural Flushing

Following the TCE saturation, the natural flushing phase of the aquifer cell was performed to investigate the desorption of TCE from the low-permeability zones. The goal of this phase was to establish background desorption prior to the EISB phase. During the natural flushing phase, the TCE concentration in the influent was decreased from 0.38 mM to 0.02 mM to simulate upgradient source zone treatment and to monitor flushing of TCE from the low permeability lenses and clay layer. VOC samples were taken from the influent and effluent every PV and from the ports every other PV. The natural flushing phase lasted for 18 PVs until TCE concentrations in the effluent changed less than 0.008 mM (1 ppm), over one PV. It was discovered that significant losses in TCE mass were measured (>50%) from port samples – likely

due to a long contact time (>30 minutes) between the sample and plastic syringe. To fix this problem, a 2.5 mL Hamilton Gastight PTFE Luer-Lok syringe (Hamilton Company; Reno, NV) was used for all future sampling. An average of 64% TCE mass difference was measured when comparing glass and plastic syringes. Therefore, the TCE concentrations in the ports during the flushing phase of the experiment were increased by 64% to account for losses from the plastic syringe.

3.2.3.4 TCE Re-Saturation

After the natural flushing phase, the aquifer cell was re-saturated with 0.38 mM TCE to prepare for the EISB phase. The duration of re-saturation (18.5 PV) was determined based on TCE and bromide measurements taken from the aquifer cell in the initial TCE saturation phase and model simulations by Virginia Tech that used soil-water distribution coefficient values and influent TCE concentrations to predict adsorbed mass in the soils. The goal of re-saturating the aquifer cell was to establish TCE concentrations in each of the lenses and clay that were comparable to the natural flushing experiment. After 12 PVs of TCE re-saturation, a modified anaerobic DCB-1 medium (detailed in Section A.1) including 5 mM lactate and 0.38 (50 ppm) TCE was introduced to prepare the aquifer cell for bioaugmentation. This medium was used as it has been proven to support microbial dechlorination and contains realistic ingredients for a bioremediation field sites (Amos, Suchomel et al. 2008, Cápiro, Löffler et al. 2015, Hnatko, Yang et al. 2020). The ionic strength of the DCB-1 medium was lowered from 60 mM to 30 mM by adding 50% of the 100x salt solution and 10 mM of sodium bicarbonate buffer. The ionic strength was modified to provide more realistic in-situ groundwater conditions. The anaerobic

medium was measured for pH and adjusted as needed to maintain 7.2-7.4 – the optimal range for *Dhc* activity (He, Ritalahti et al. 2003). Anoxic conditions were established in the aquifer cell to create an environment realistic to a saturated aquifer and a suitable environment for anaerobic microorganisms prior to bioaugmentation. An ORP of less than approximately -100 mV was confirmed using a resazurin indicator that turns pink when exposed to oxygen. Additionally, a black precipitate was visualized in the aquifer cell (Figure 3.10 in Section 3.3.3), which was likely resulted from the reaction between the iron naturally present in the soils and sulfide in the medium, forming iron sulfide. This provided additional support that the aquifer cell was maintained in an anoxic and reduced environment (Section A.1). Background levels of VOCs, dissolved total organic carbon (DOC), volatile fatty acids (VFAs), and biomass samples were taken every PV to document conditions prior to microbial activity. Further Discussion of this data can be found in Section A.6.

3.2.3.5 Bioaugmentation *(PV 0-6)*

After 18.5 PV of re-saturation (6.5 PV of anaerobic medium), the aquifer cell was bioaugmented with KB-1® (SiREM, Ontario, Canada), a commercially available PCE-to-ethene dechlorinating microbial consortium. For consistency and ease of reference, bioaugmentation will be referred to as PV 0 for the duration of this research, and all other PVs are in reference to bioaugmentation. KB-1® contains three *Dehalococcoides mccartyi* (*Dhc*) strains, which are known to dechlorinate using the reductive dehalogenase genes *tceA*, *vcrA*, and *bvcA* (Löffler, Yan et al. 2013). The 16S rRNA gene was measured using a real-time quantitative polymerase chain reaction (qPCR) to determine the total number of cells of *Dhc* in the stock solution sent by

SiREM. The concentration of *Dhc* was equal to $1.54 \times 10^{11} \pm 1.59 \times 10^{10}$ 16S rRNA gene copies per liter. Since *Dhc* have one copy of 16S rRNA gene per cell, the concentration of *Dhc* is equal to 1.54×10^{11} ($\pm 1.59 \times 10^{10}$) cells per Liter (Ritalahti, Amos et al. 2006). The KB-1® stock was then diluted to 4.3×10^{7} *Dhc* cells per Liter in a second stock solution before inoculation so that the total concentration in the aquifer cell would be equal to 1.0×10^{7} cells per Liter. This concentration was used based on data from studies that found a correlation between higher ethene concentrations and total *Dhc* concentrations greater than 10^{7} copies/L (Clark, Taggart et al. 2018). A Fusion 200 syringe pump (Chemyx; Stafford, Texas) was used to add 20 ml of concentrated KB-1 to each of the 18 ports on the aquifer cell at a rate of 0.1 mL/min. After bioaugmentation, the flow rate in the aquifer cell was slowed to 0.23 mL/min (14 cm/day) to establish a more realistic flow rate through the porous media. This adjustment, along with a 48-hour flow interruption at PV 4.2 after bioaugmentation, allowed the microorganisms to acclimate to the new environment, attach to soil particles, and more effectively dechlorinate for the duration of the experiment.

3.2.3.6 ERDenhanced Addition *(PV 6-8.9)*

No microbial dechlorination past cis-DCE (i.e., no detectable concentrations of VC or ethene) was measured in the effluent or any of the ports approximately 6 PV after bioaugmentation. At this stage, ERDenhanced (Terrastryke; Andover, New Hampshire) was introduced to the aquifer cell to monitor how a transition in electron donor source would alter the dechlorination and microbial population. A concentration of 6 g/L in the aquifer cell was suggested by Terrastryke for TCE concentrations of 10 mg/L to 100 mg/L, thus a total of 9 grams of ERDenhanced was

added into the aquifer cell (PV = 1535 mL). ERDenhanced was added into ports 1A, 1C, 1E, 2B, and 2D (Figure 3.3)

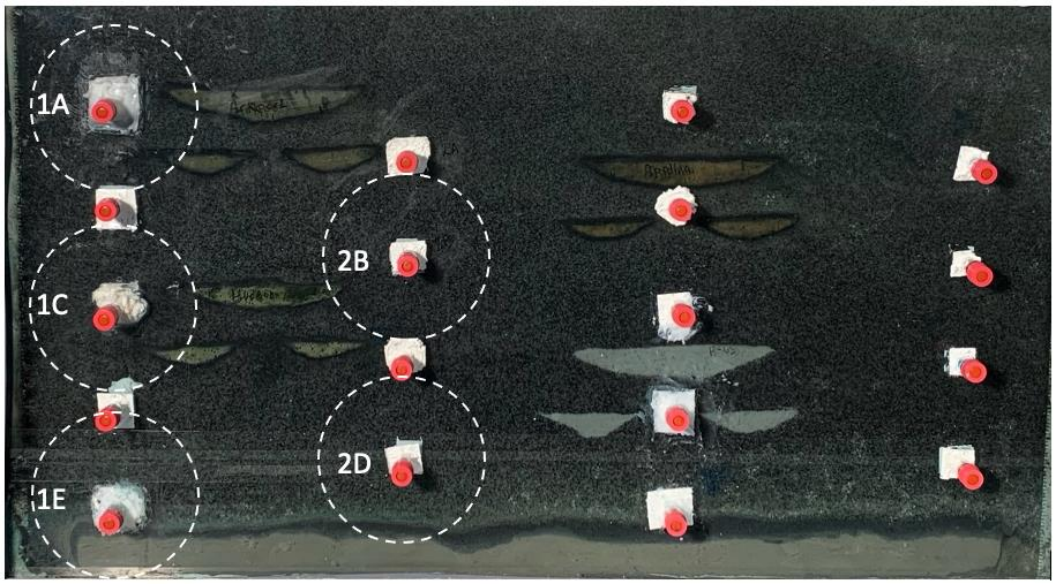

Figure 3.3: Locations of ERDenhanced addition into the aquifer cell including estimated area impacted by each port injection

to provide complete coverage to the first half of the aquifer cell assuming downstream ports would receive electron donor from the upstream ERDenhanced addition. The injection of ERDenhanced was accomplished using a peristaltic pump equipped with 2 PTFE lines (Figure 3.4). A concentration of 15 g/L ERDenhanced was constantly stirred using a magnetic stir bar to prevent settling and bubbled with ultra-zero grade nitrogen to maintain anaerobic conditions (Airgas, Radnor, PA). The injection was performed at a flow rate of 0.1 ml/min for a total flow rate in the aquifer cell of 0.47 ml/min (30 cm/day) for a duration of 0.64 PV. An 18-gauge, 1.5-inch needle was used to allow for larger particulates to enter the aquifer cell and prevent clogging in the influent lines. Since ERDenhanced is not fully soluble, particulates near the ports were observed, which could have slowed the flow rate down locally. Additionally, insoluble

particles likely settled to lower regions in the aquifer cell attributing to a greater availability of electron donor. More information about the solubility and physical characteristics of ERDenhanced can be found in Section A.4.

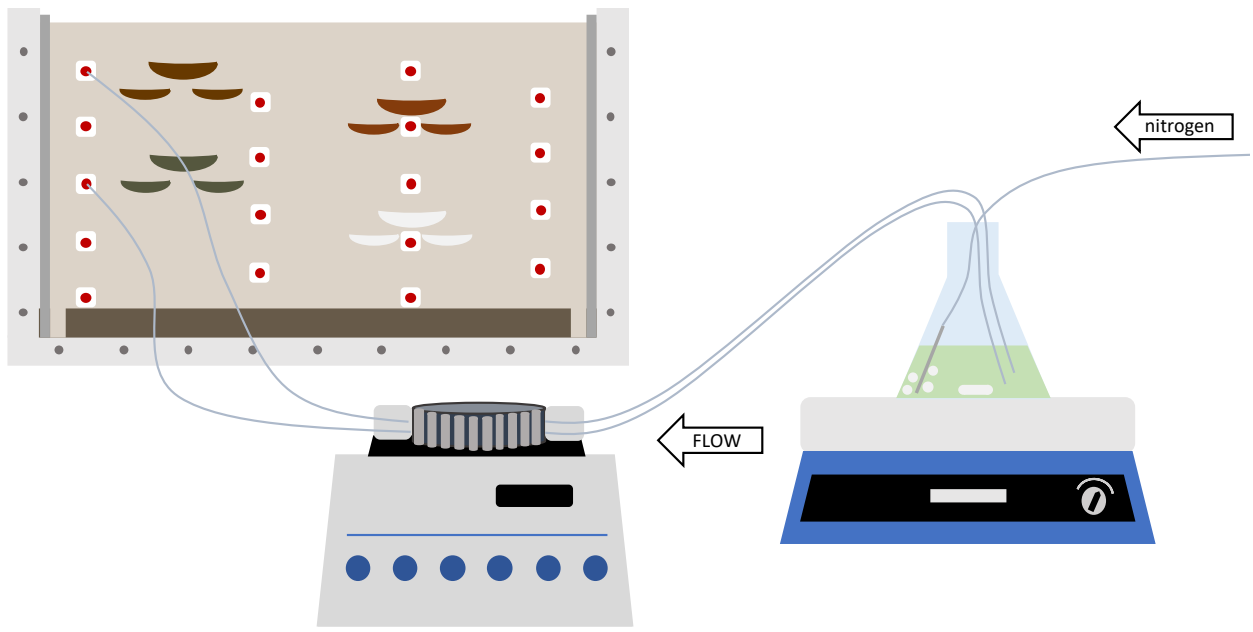

Figure 3.4: ERDenhanced injection experimental set-up including aquifer cell, peristaltic pump, and magnetic stir plate (left to right)

3.2.3.7 Biotic Flushing *(PV 8.9-20)*

The TCE concentration in the influent was lowered to approximately 0.02 mM (3 ppm) at PV 8.9 for the investigation of potential bioenhanced back diffusion. This reduction in TCE simulated upgradient source zone removal and created the opportunity for back diffusion and desorption of TCE from the low-permeability soil lenses to occur. Samples for VOCs were taken every PV, and biomass samples were taken every other PV in the influent, effluent, and the 11 selected ports throughout the remainder of the experiment. These ports were selected due their

proximity to the low-permeable soils – especially the locations immediately downgradient of the soil lenses (2A, 2C, 4A, 4C) and near the clay (1E and 3E) (see port locations in Figure 3.1). Other ports were not sampled as frequently due to time constraints of sampling and so that no more than 5% of the background flow was being extracted from the aquifer cell for sampling. A volume of 1ml was taken for DNA extraction and qPCR analysis before and after important changes throughout the experimental phases (methods discussed in Section A.3.4). The biotic remediation phase continued without introducing additional electron donor for 12.5 PV and with an average influent concentration of 0.02 mM TCE.

At approximately PV 18.5, the remaining experimental procedure was performed with the assistance of Harry Vaslo, Savannah Cummins, and Temitope Popoola. VOC data from this phase of the experiment is presented here, but microbial analysis and solid phase chlorinated ethene extractions are not discussed for the purpose of this research. Rebound of TCE At PV 18.5 was detected in the effluent and all ports except for 2C. This indicated that the microorganisms were decreasing in efficiency due to a lack in electron donor availability.

3.2.3.8 Continuing Remediation *PV 20-24)*

At PV 20, the influent TCE concentration was reduced to an average of 0.01 mM (1.5 ppm) to simulate complete source zone removal. This created an even lower background TCE concentration to draw remaining TCE from the soil lenses. Due to the contaminant rebound at PV 18.5, a low concentration of lactate (1 mM) was reintroduced at PV 21.5 for the remainder

of the experiment. This was needed to support additional electron donor to the microbial community and maintain full dechlorination in the aquifer cell.

A final round of VOC and biomass samples were taken prior to deconstructive sampling of the aquifer cell at PV 24. At PV 24.2, the flow was stopped in the aquifer cell and the remaining liquid was drained to prepare for solid phase sampling. The front glass pane was removed, and soil samples were taken throughout the bulk media and at strategic locations near the soil lenses. These samples were collected to measure TCE adsorbed to the low-permeability media, and to collect biomass samples to measure *Dhc* and RDase gene abundances at specific locations.

3.3 Results and Discussion

3.3.1 Soil Preparation and Tracer Test

Adsorption isotherm experiments were performed on the Commerce St. Clay, Hudson soil, and Arkport soil to predict TCE adsorption and desorption more accurately in the aquifer cell (Section A.2.3). The Linear soil-water distribution coefficient (K_d) value for Commerce St. Clay and Hudson Soil was measured as 1.47 and 0.56 L/kg, respectively. The Arkport soil was calculated using a non-linear Langmuir isotherm approach, and the K_L value was determined as 0.11 L/kg (Figure 3.5).

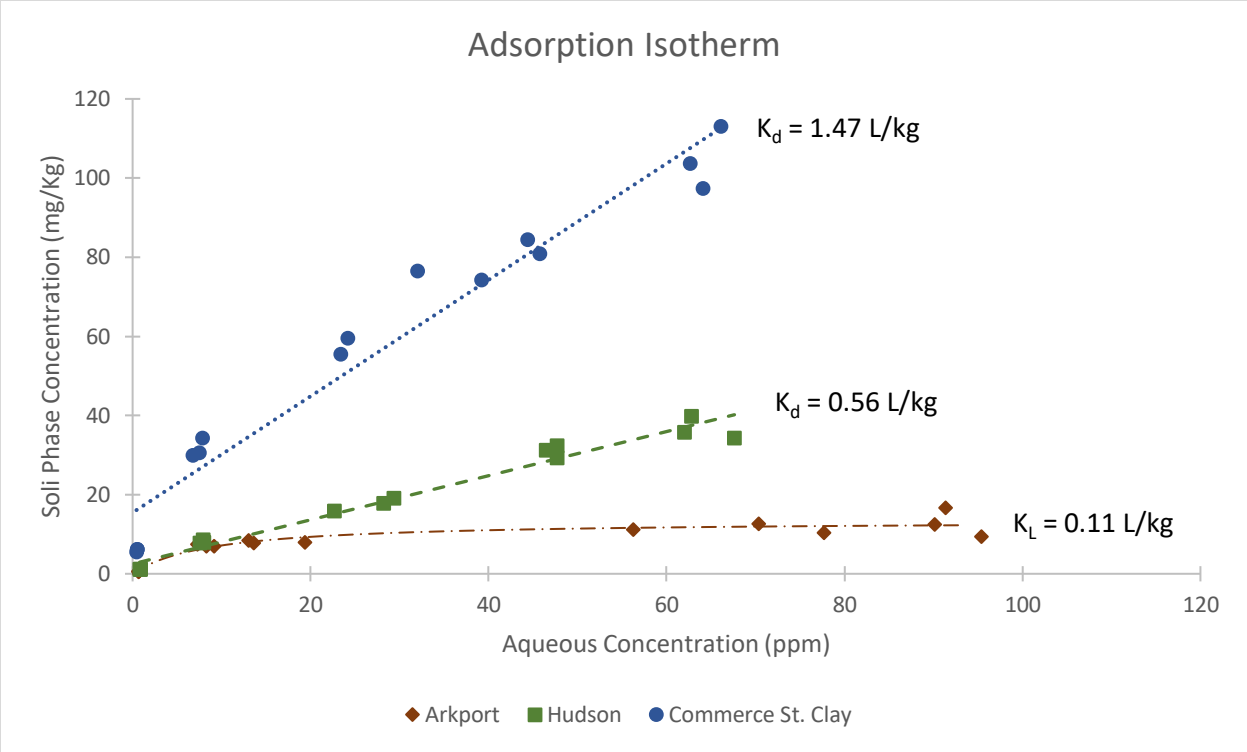

Figure 3.5: Adsorption Isotherm for Arkport soil, Hudson soil, and Commerce St. Clay. The relationship between the concentrations associated with the solid phase and the aqueous (slope of the linear isotherm) yields the K_d.

Based on the bromide mass recovery during the test, as illustrated in Figure 3.6, the pore volume of the aquifer cell was determined as 1,535 mL. The pore volume was determined as the cumulative volume in which half of the total bromide mass introduced into the system had been detected in the effluent.

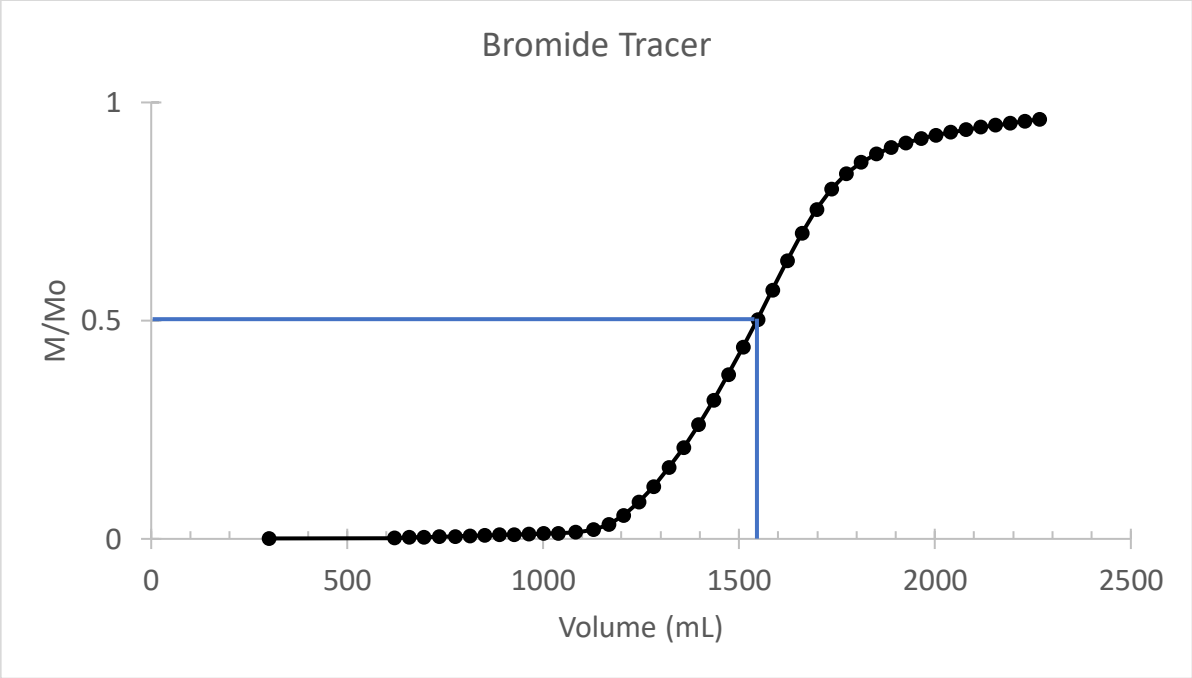

Figure 3.6: Bromide tracer mass recovery. Y-axis is cumulative bromide mass over total mass introduced. X-axis is cumulative volume flushed through the aquifer cell. Pore volume was determined where 50% of influent bromide mass was measured in the effluent (1535 mL)

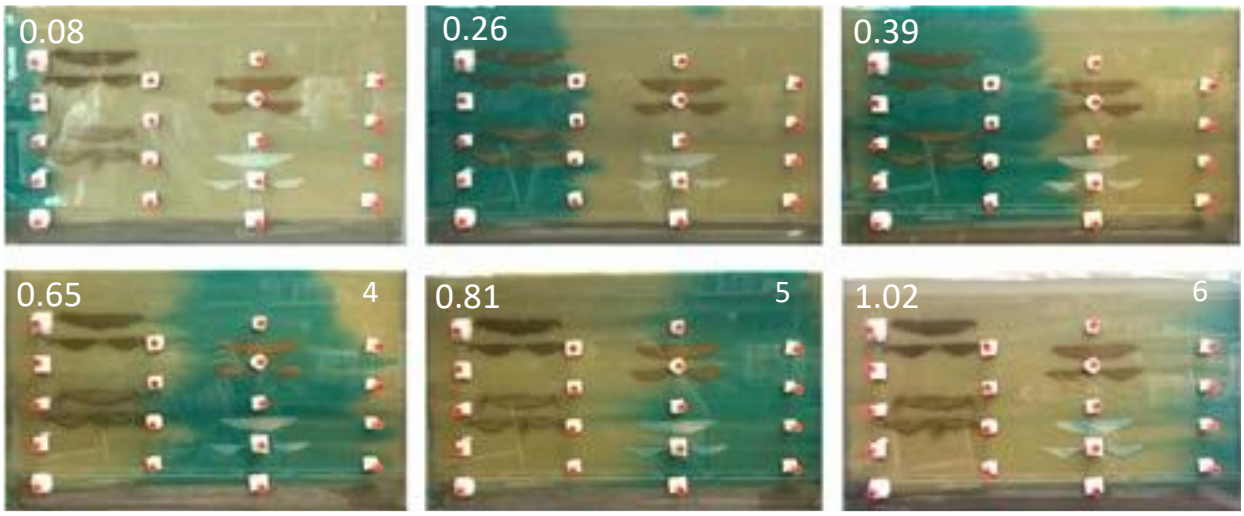

Figure 3.7: Blue dye tracer photos visually indicating flow paths. This describes the uniformity of flow through the aquifer cell and confirms slower flow through the low-permeability soil lenses (Numbers in the top left indicate PV after introduction).

Images showing the progressive flow of dye through the aquifer cell are shown in Figure 3.7.

The comparison in the dye flow rate was calculated using the dimensions of the aquifer cell and

visual observation of the blue dye. Flow was relatively uniform in the first quarter of the tracer experiment (PV 0.08 to PV 0.26), while the flow was observed to be around 33% faster in the bottom 10 cm of the aquifer cell than the top 10 cm at PV 0.39. At PV 0.65, the flow in the bottom 20 cm of the aquifer cell was flowing 25% faster than top 10 cm (Figure 3.7). After PV 0.65, the flow started to lag near the low permeability lenses and the clay/sand interface. The blue dye confirmed that flow was up to 50% slower in the 2 cm above the clay layer and directly downgradient of the soil lenses. This was expected due to the lower hydraulic conductivities of the clay and soils compared to the background sand. In addition, it appeared that the influent flowed through all soil lenses but not the bottom clay regions, since no blue coloration was visualized at the bottom 2 cm of the aquifer cell (Figure 3.7).

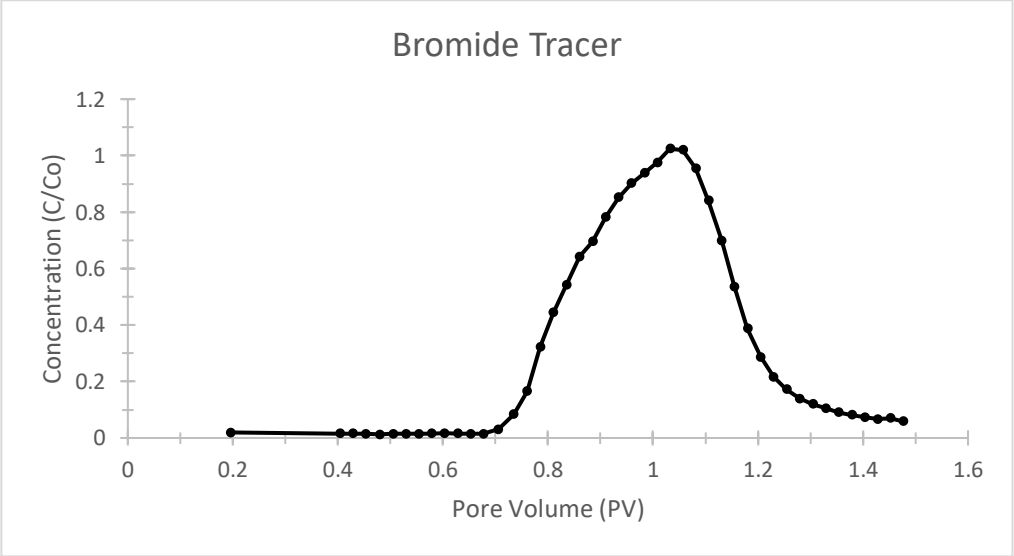

Figure 3.8: Bromide tracer breakthrough curve. Y-axis is bromide concentration measured over initial bromide concentration introduced; x-axis is measured in pore volumes determined from Figure 3.6. This shows the uniformity of flow through the aquifer cell as a whole

Bromide concentrations in the effluent were measured and compared to the initial influent concentration. In Figure 3.8, at PV 0.7, the bromide concentration was 3% of the influent

concentration. At PV 1, the effluent was measuring exactly the influent concentration (C/Co = 1). At PV 1.3, the C/Co concentration continued to measure 12% of the influent concentration (4X higher than at PV 0.7). This concentration measurement verified the visually observed slower flow regions throughout the heterogenous system. This supports the idea that bulk flow through the aquifer cell was impacted by the low permeability media due to lower flow rates near the soil lenses, and that is why the bromide concentration is higher on the back end of the breakthrough curve. In Figure 3.7, it is clearly seen that residual dye is diffusing out from the low permeability lenses at PV 0.81 and 1.02. Results from the bromide tracer and images of the dye provided data to collaborators at Virginia Tech that helped guide durations for the remaining experimental phases using chemical transport and hydrological modeling.

3.3.2 Desorption and Diffusion under Natural Conditions

After completing the tracer test, complete saturation during the TCE plume development was confirmed by modeling performed at Virginia Tech. Following TCE saturation, data collected during the natural flushing period determined baseline desorption and back diffusion of TCE from each of the regions near low-permeability soils. The concentration of TCE and bromide were reduced (0.38 mM to 0.02 mM TCE; and 20 mM to 0 mM bromide) to create a concentration gradient and measure back diffusion. Figures 3.9 shows experimental TCE and bromide concentrations compared to modeled TCE concentrations for port 3E, 4C, and 4A. These ports were chosen since they measured the greatest amount of back diffusion under natural conditions, and it was hypothesized that these ports would also experience the greatest amount of bioenhanced back diffusion. The model (Virginia Tech) was used to account for

varying TCE concentrations during the initial decrease in concentration, and bromide concentrations were used to calibrate the model to measure TCE desorption and diffusion. The goodness of fit between the modeled and experimental TCE values were 0.92, 0.91, and 0.97 for ports 3E, 4C, and 4A respectively. The agreement between modeled and experimental measurements indicates that the model can capture measured TCE back diffusion under natural conditions. For all three of the selected ports, the TCE recovery was higher than the bromide recovery after decreasing the concentrations. On average (from PV 0 to 21) the TCE recovery was higher than bromide by 24% in port 3E, 17% in port 4C, and 28% in port 4A

The greater recovery of TCE compared to bromide is evidence that back diffusion from the low-permeability lenses had occurred. To quantify this difference, natural back diffusion (NBD%) was calculated by subtracting the bromide mass recovery (BMR%) from the TCE mass recovery (TCE REC%) and dividing that by the bromide mass recovery (BMR%).

$$\mathrm{NBD\%} = \frac{\mathrm{TCE\ REC\%} - \mathrm{BMR\%}}{\mathrm{BMR\%}} \qquad \textit{(Equation 2)}$$

NBD% represents the mass of chlorinated ethenes released from the low permeability soil lenses by back diffusion under natural conditions. NBD% was also used later in the experiment as a baseline to calculate bioenhanced back diffusion (BBD%) (see Section 3.3.4).

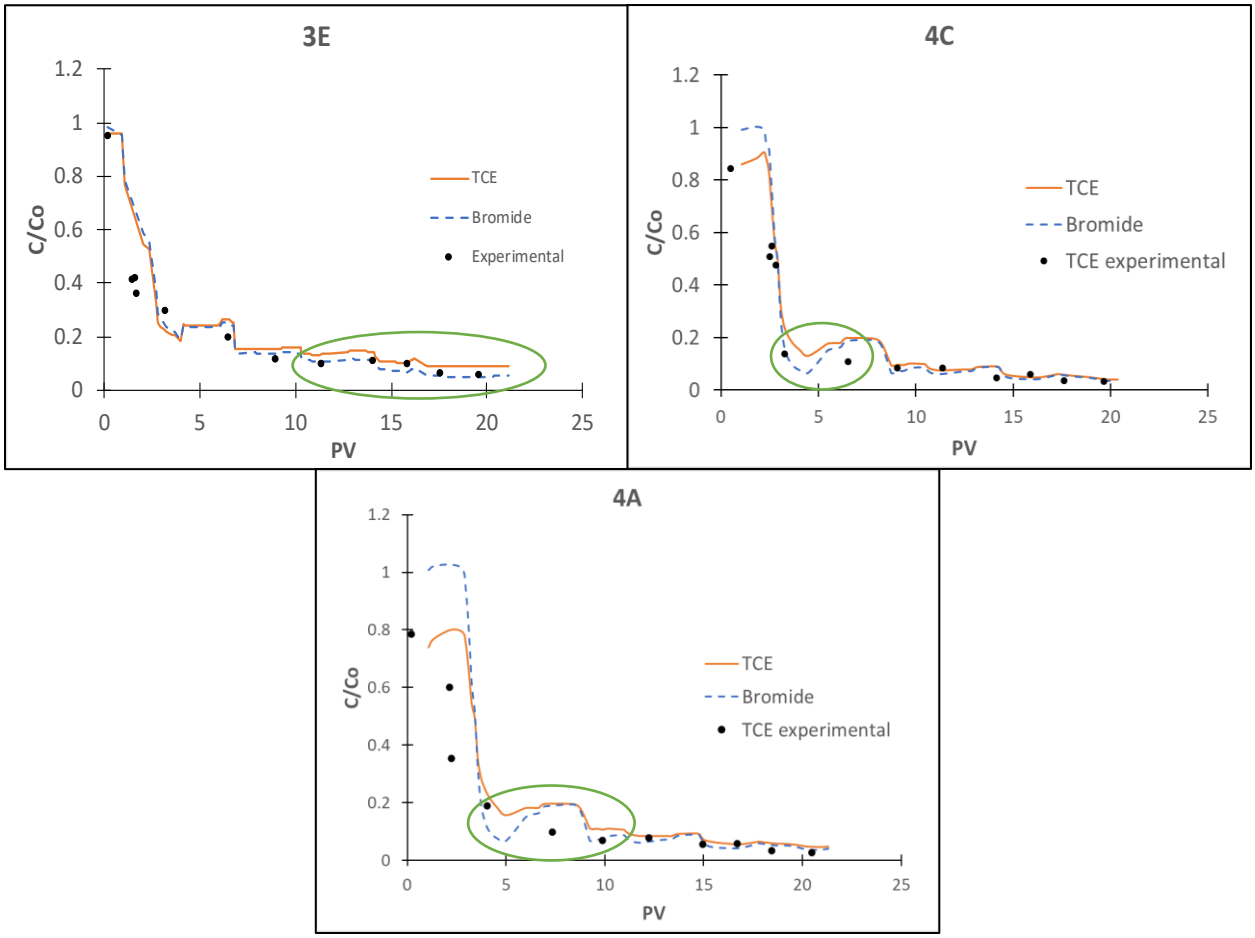

Figure 3.9 Natural flushing modeled vs. experimental for port 3E, 4C, and 4A near the Commerce St. Clay. TCE concentrations were reduced from 0.38 mM to 0.02 mM. TCE and bromide modeled values are shown as the solid and dashed line respectively. The green outline highlights where the most back diffusion was observed.

Port 3E is near the clay layer which has a low permeability and high adsorption coefficient (1.47 L/kg) compared to the background sand. Over 40% NBD was measured in port 3E from PV 14.7 to PV 21 with a maximum of 74% higher TCE diffusion at PV 20 (Figure 3.9). Port 4C experienced more NBD% earlier in the natural flushing phase than 3E with the highest diffusion occurring between PV 3.2 and 4.5 – measuring 102% at PV 4. Port 4C is located downgradient of the Hudson soil and immediately downgradient of the F65 lens. The experimental TCE recovery is lower than bromide for port 4C at approximately PV 7. Theoretically, TCE recovery should

always be higher than bromide recovery if back diffusion is occurring. This discrepancy is accounted for in the modeled values, but it is noteworthy to mention that results from this phase are relying heavily on the accuracy of the modeled data.

Additionally, port 4A experienced the highest NBD% near the beginning of the natural flushing phase between PV 3.7 and PV 5. Port 4A is located directly downgradient of the Appling soil lens which has the second highest organic carbon content (0.75%) and a K_d of 0.83 L/kg. The soil-water distribution coefficient for the Appling soil was the only value calculated directly using organic carbon content and K_{oc}. Since this method assumes a linear relationship between K_d and organic carbon, it could be flawed in accounting for non-linear adsorption of contaminant (like the Arkport soil). Over 100% NBD was measured between PV 4 and PV 5, with the highest diffusion measured as 142% at PV 4.5. A more pronounced second wave of diffusion (44% to 67%) was measured in port 4A between PV 9.2 and PV 10. This was most likely due to variances in influent TCE concentration which acted as a secondary loading of TCE into the aquifer cell. Overall, data from the natural flushing confirmed that more sorption occurred near lenses with higher organic carbon content and low permeability. Data from this phase of the experiment provided abiotic back diffusion values that were compared to later biotic experimental data to calculate bioenhanced back diffusion.

3.3.3 Microbial Reductive Dechlorination

TCE concentrations during the re-saturation phase were measured with an average of 80% TCE recovery in the effluent and 70-100% TCE recovery in the ports. During this phase, a black

precipitate was observed in the aquifer cell that was assumed to be iron (II) sulfide formation. This type of phenomena has been observed in previous experiments (Marcet 2014), and the difference in head for the aquifer cell was adjusted to maintain a consistent flow rate. More information (including groundwater medium and soil components) about this process can be found in Section A.1. Figure 3.10 shows the progression of the black precipitate starting at 4.1 PV after the introduction of anaerobic medium (PV -2.4). The aquifer cell was completely covered with black precipitate after approximately 9.4 PV of anoxic conditions (PV 2.9) as seen in Figure 3.10.

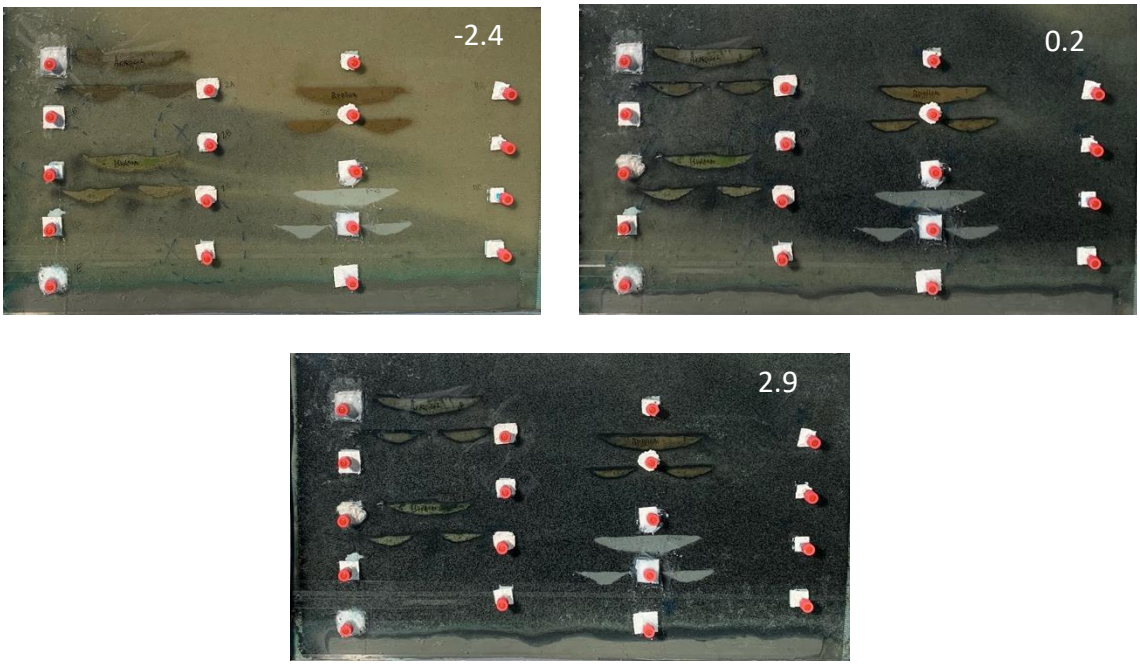

Figure 3.10: Progression of black precipitate (likely iron sulfide) formation (PV 0 = bioaugmentation)

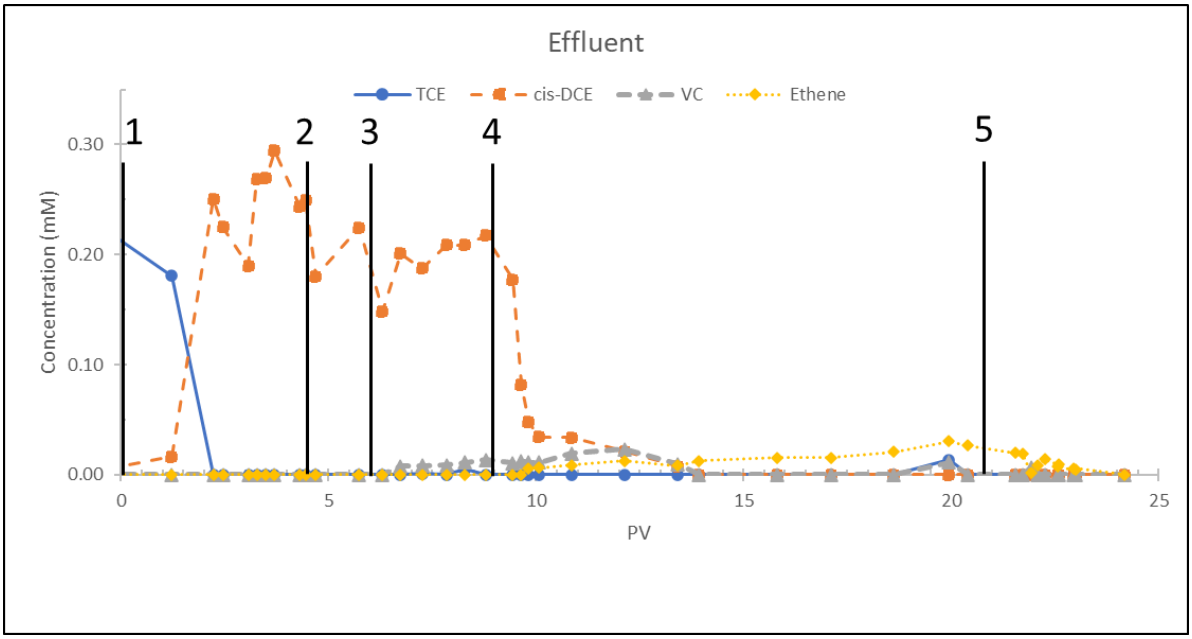

Figure 3.11: Effluent Biotic VOC Concentrations at intervals 1-5 (1) bioaugmentation, (2) flow interruption, (3) ERDenhanced addition, (4) TCE reduction #1 (0.38 mM to 0.02 mM), (5) Lactate amendment and TCE reduction #2 (0.01 mM to 0 mM).
(Experimental parameters for each phase are shown in Table 3.3)

Table 3.4 Stages 1-5 of the aquifer cell experiment and the corresponding VOC concentrations that were measured in the effluent

Stage	PV	Significance	VOCs
1	0	Bioaugmentation	100% TCE
2	4.2	Flow Interruption	100% cis-DCE
3	6	ERDenhanced Addition	100% cis-DCE
4	8.9	TCE Reduction #1 (50 ppm to 3 ppm)	94% cis-DCE, 6% VC
5	21	Lactate Amendment & TCE Reduction #2 (1.5 ppm to 0 ppm)	100% Ethene

Starting at 0.22 PV after bioaugmentation, the formation of cis-DCE from MRD of TCE was observed in the effluent. At 2.46 PV, TCE was no longer detected in the effluent; however, during the first 4 PV after bioaugmentation, no dechlorination past cis-DCE was observed in the

effluent or any of the ports. To evaluate the impact on mass transfer limitations due to residence time, a flow interruption was performed at PV 4.2 which lasted for approximately 48 hours. This was done based on previous studies that determined bioenhanced mass transfer from DNAPL source zones can be increased up to 7.8-fold following a flow interruption (Cápiro, Löffler et al. 2015). Immediately following the flow interruption, chlorinated ethene mass in the effluent was measured 60% higher than the influent concentration at PV 4.3 (Figure 3.12). The increased chlorinated ethene measurements after the flow interruption confirmed that a longer residence time leads to increased dechlorination in the aquifer cell. This finding supports previous studies that have attributed incomplete dechlorination to insufficient residence time from DNAPL source zones (Amos, Suchomel et al. 2008, Cápiro, Löffler et al. 2015). Additionally, this data indicates that MRD of TCE could be limited by residence time for this aquifer cell system. However, this improvement was short lived as chlorinated ethene mass measured in the effluent decreased below the influent TCE concentration by PV 4.7 – indicating a slight decrease in remediation performance compared to immediately following the flow interruption.

Methane was detected immediately following the flow interruption in the effluent and ports and caused gas bubbles to form in the aquifer cell – specifically near the clay layer and second half of the aquifer cell. Methane was measured at concentrations up to 0.4 mM, 0.22 mM, and 0.12 mM in the effluent, port 3E, and port 4A, respectively. This confirms anoxic conditions in the aquifer cell and suggests that methanogenic microorganisms within the KB-1® consortium, or in the natural soils, are utilizing part of the electron donor (lactate) or a byproduct (acetate,

propionate, or hydrogen). Also, the substantial formation of methane observed here is in agreement with a prior study that reported significantly greater methane concentrations in samples with *Dhc* abundances greater than 10^7 16S rRNA gene copies per Liter at bioaugmentation and biostimulation field sites (Clark, Taggart et al. 2018) More information about methane production in the aquifer cell can be found in Section A.5.

VC was detected for the first time in the following pore volume after adding ERDenhanced (PV 6-7) in ports 1E, 3E, and the effluent. There are several reasons that could prompt this result and it should not be credited solely to the addition of ERDenhanced. During ERDenhanced addition, the microorganisms were given more time to acclimate to the aquifer cell since the entire process lasted 48 hours. This additional time, and local accumulation of ERDenhanced particles causing a decrease in flow rate, would allow *Dhc* more time to dechlorinate cis-DCE to VC. The VC production was initially measured near the clay layer, providing supporting evidence to these hypotheses. The 2 cm above the clay layer in the aquifer cell had the slowest flow rate visually according to the dye tracer test – likely due to the low hydraulic conductivity of the Commerce St. Clay (Section 3.3.1). All these factors worked in combination to create a productive dechlorinating environment, and ERDenhanced continued to provide adequate electron donor through PV 18.5. Further in-depth analysis of ERDenhanced performance can be found in Section 3.3.6.

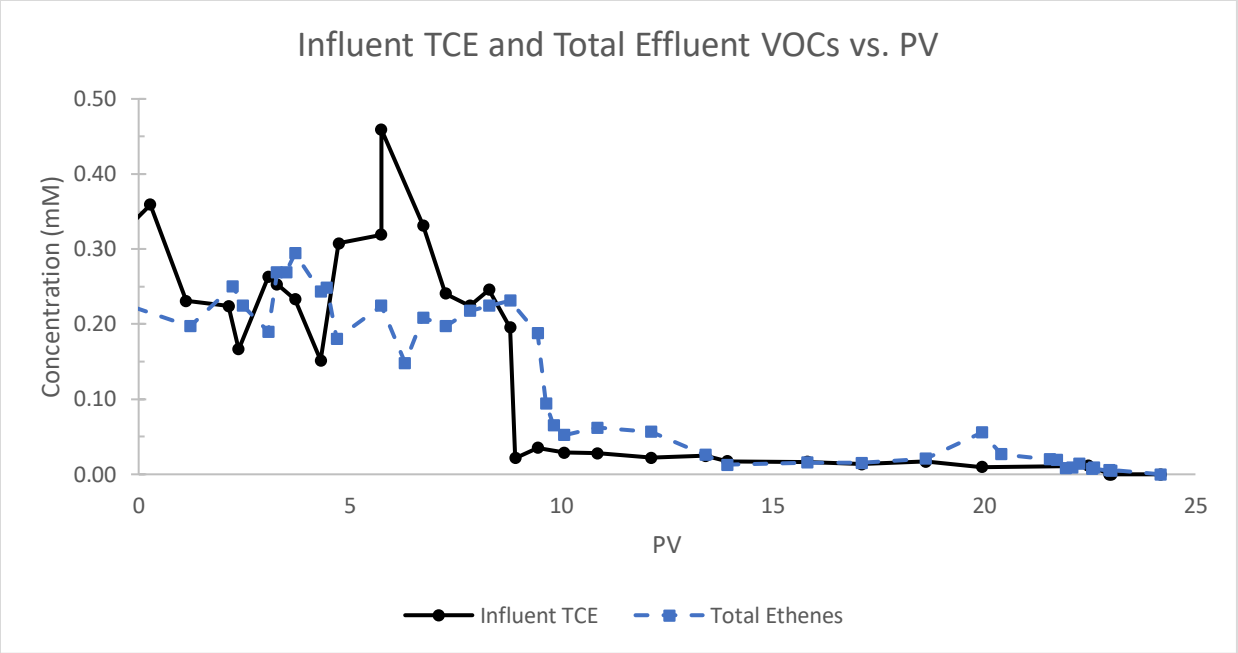

Figure 3.12 Influent TCE and Total Effluent VOCs vs. PV during biotic remediation where bioaugmentation occurred at PV 0

To measure the biological impact on mass transfer of chlorinated ethenes in the aquifer cell, the concentrations of total chlorinated ethenes and ethene were measured. Figure 3.12 shows the influent TCE concentration compared to the molar mass of TCE and all daughter products measured in the effluent. Before reducing the TCE concentration, PV 0 to PV 8.9, the influent TCE concentration was higher than the total chlorinated ethene concentrations in the effluent by 3% (± 28%). The difference in mass introduced into the system and mass recovered in the effluent is attributed to the adsorption into soil lenses. However, a shift was observed after the decrease in TCE concentration from 0.38 mM to 0.02 mM in the influent at PV 8.9. After this transition, the effluent total chlorinated ethenes and ethene were 104% (± 171%) higher than the influent TCE concentration, with over 400% total mass recovered in the effluent at PV 9.4 and PV 20. The relatively high standard deviation when comparing average influent and effluent concentrations is attributed to fluctuation in the influent concentration and varying effluent

concentrations attributed to back diffusion on mass from the low-permeability zones. The shift in chlorinated ethene mass recovery indicates that the chlorinated ethenes adsorbed to soils during the saturation phase was being extracted after reducing influent TCE concentration. Additionally, lesser-chlorinated transformation products have higher diffusivities and lower sorption coefficients than TCE (Jin, Rolle et al. 2014). Along with microbial dechlorination, these physical processes likely account for the increase in mass removal from the aquifer cell soil lenses (Glover, Munakata-Marr et al. 2007, Hnatko, Yang et al. 2020).

Complete reductive dechlorination was observed in all the ports by the end of the experiment (PV 24.2). In general, a similar dechlorination performance was observed in most ports (except for Port 3E, discussed below), and Port 2C was selected to represent data from other ports (Figure 3.13). A rapid transformation from TCE to cis-DCE within 5 PV after bioaugmentation was observed (Figure 3.13). This continued through the primary decrease in TCE concentration (8.9); VC was detected at PV 15 and ethene at approximately PV 20.

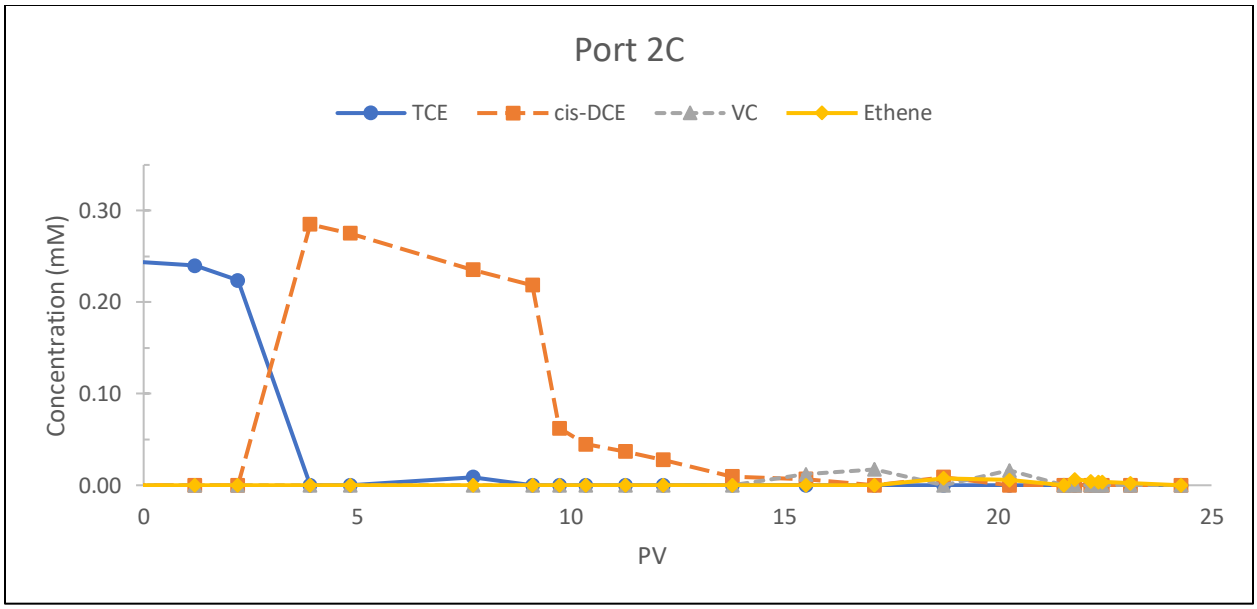

Figure 3.13 VOC Concentrations during biotic remediation for port 2C near the Hudson soil. PV 0 represents bioaugmentation and TCE concentration was reduced in the influent from 0.38 mM to 0.02 mM at PV 8.9.

Unlike other ports, port 3E produced VC and ethene concentrations quicker and in greater quantity (Figure 3.14). VC was measured after PV 5 and ethene concentrations were measured after PV 10. Port 3E had the highest concentrations of VC and ethene compared to all ports with over 700% greater VC and over 600% greater ethene concentrations compared to port 2C. This increased performance is most likely due to the slower flow velocity near the clay interface (see tracer test in Section 3.3.1) and electron donor availability. The area near port 3E provided a conducive environment to MRD and sufficient residence time needed for complete transformation. Additionally, the relatively high concentrations of daughter products could be a result of upgradient transformation which was also measured in port 4C.

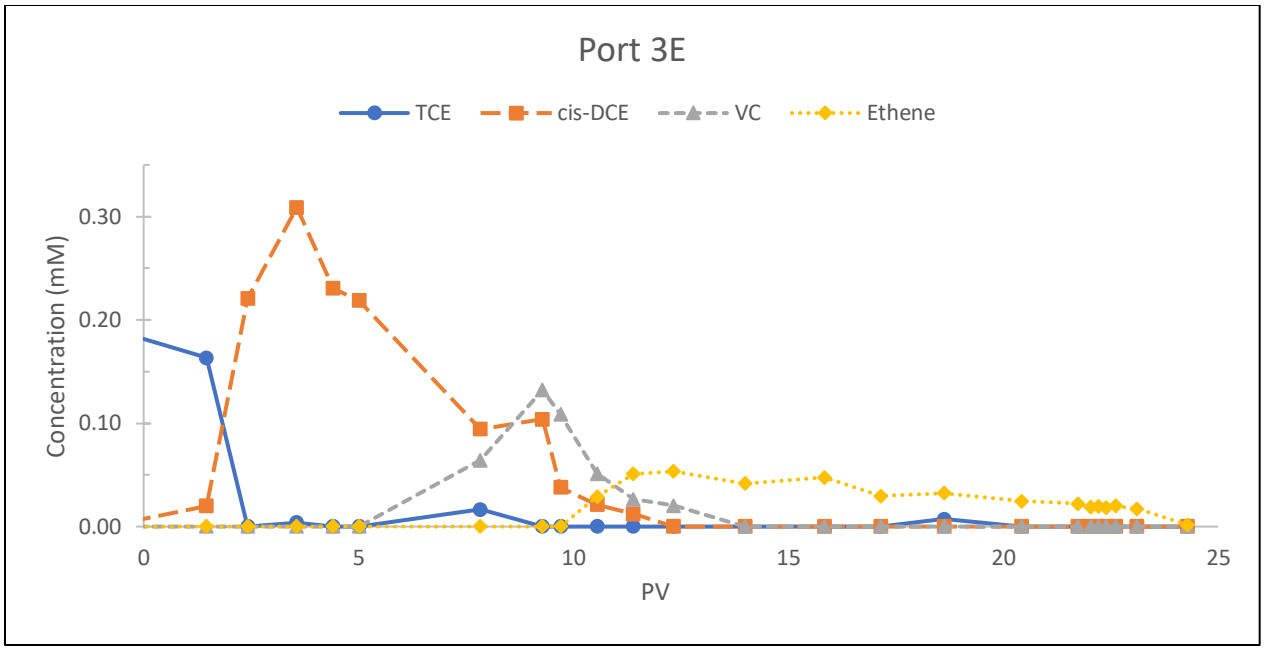

Figure 3.14 VOC Concentrations during biotic remediation for port 3E near the Commerce St. Clay. PV 0 represents bioaugmentation and TCE concentration was reduced in the influent from 0.38 mM to 0.02 mM at PV 8.9.

3.3.4 Biologically Enhanced Back Diffusion

The bioenhanced back diffusion for 11 locations throughout the aquifer cell was calculated by comparing the recovered contaminant mass during phase 4 (EISB after TCE reduction #1) with the TCE mass recovered during the natural flushing phase (Figure 3.15) . Data for this calculation was taken from time of decreasing the TCE concentration (PV 8.9) to the end of the aquifer cell experiment (PV 24.18). Bioenhanced back diffusion was calculated using Equation 3 below.

$$\mathrm{BBD\%} = \frac{\mathrm{BMR\ \% - AMR\ \%}}{\mathrm{AMR\ \%}} \qquad (\textit{Equation 3})$$

This equation calculates the bioenhanced back diffusion percent (BBD%) by subtracting the biotic mass recovery (BMR%) of total chlorinated ethenes and ethene during the biotic phase of the experiment by the abiotic mass recovery (AMR%) of TCE during the natural flushing phase

and dividing by the AMR%. These values are shown as percentages since the cumulative mass of VOCs collected were divided by influent mass of TCE during that time frame. This method of comparing VOC mass to influent TCE mass was used to normalize variances in influent concentrations during the natural phase and the biotic phase.

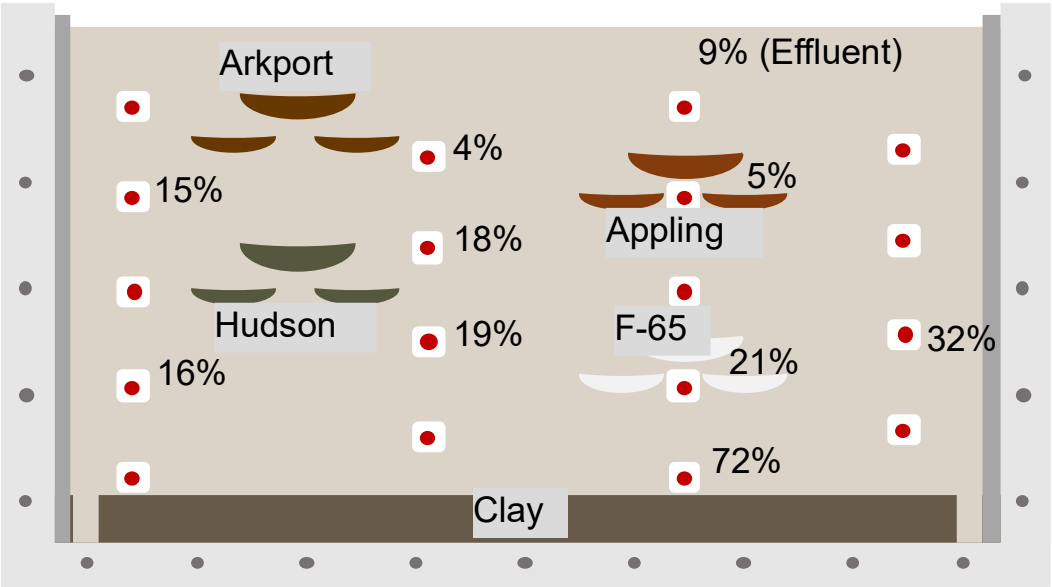

Figure 3.15 Bioenhanced back diffusion for the port and effluent after decreasing influent TCE concentration from 0.38 mM to 0.02 mM

The BBD% was used as a metric to determine how much MRD attributed to the increase in mass flux out of the low-permeability lenses (Figure 3.15). The BBD% varied from 0% to 72% where the maximum amount of bioenhancement was measured near the clay (72%). Downgradient of the Hudson soil, and near the F-65 sand, 18-32% bioenhancement was measured. The clay and the Hudson soil have the lowest hydraulic conductivities of the soils used (0.05 m/day and 0.04 m/day, respectively), and the Hudson soil has the highest organic carbon content (0.91%). These properties contributed to the increased microbial degradation that was able to draw out more contaminant mass than other areas. Although high BBD% was

measured near the F-65 lens, this is likely a result from higher MRD near the Hudson soil leading to products with higher diffusivity that were eventually measured downgradient near the F-65 lens. Similar observations were also reported by Hnatko, Yang et al. (2020) in which bioenhanced back diffusion (27%-28%) was measured directly downgradient of a high conductivity sand similar to F-65 used in the current research. The relatively low organic carbon and high hydraulic conductivity compared to other lenses suggests a less conducive environment for mass storage, microbial growth, and bioenhancement near the F-65 lens. It is likely, in this study and Hnatko, Yang et al. (2020), that the bioenhancement is a result of upgradient mass transfer.

3.3.5 Microbial Population and Distribution

Microbial analysis was performed using quantitative polymerase chain reaction (qPCR) to measure for total 16S rRNA *Dhc* and RDase genes (*tceA*, *bvcA*, and *vcrA*). All samples were analyzed in triplicate according to procedures outlined in Section A.3.4. Like the bioenhancement results, downgradient of the Hudson soil and near the clay (ports 2C and 3E, respectively) saw the greatest number of *Dhc* and RDase gene populations (Figure 3.16). The greater microbial population in ports 2C and 3E likely resulted from a higher availability in electron donor from the organic carbon in the soils and electron acceptor from back diffusion near the low-permeability lenses. Although the RDase populations often outnumbered *Dhc*, the concentrations followed the same general trend (Figure 3.18). These measurements indicate that there are other sources of RDase genes other than *Dhc* alone. Previous studies have reported similar observations and more research is needed to determine the source of the

additional RDase gene copies (van der Zaan, Hannes et al. 2010, Damgaard, Bjerg et al. 2013, Cápiro, Löffler et al. 2015). The primary RDase gene measured was the *tceA* gene throughout the entire experiment.

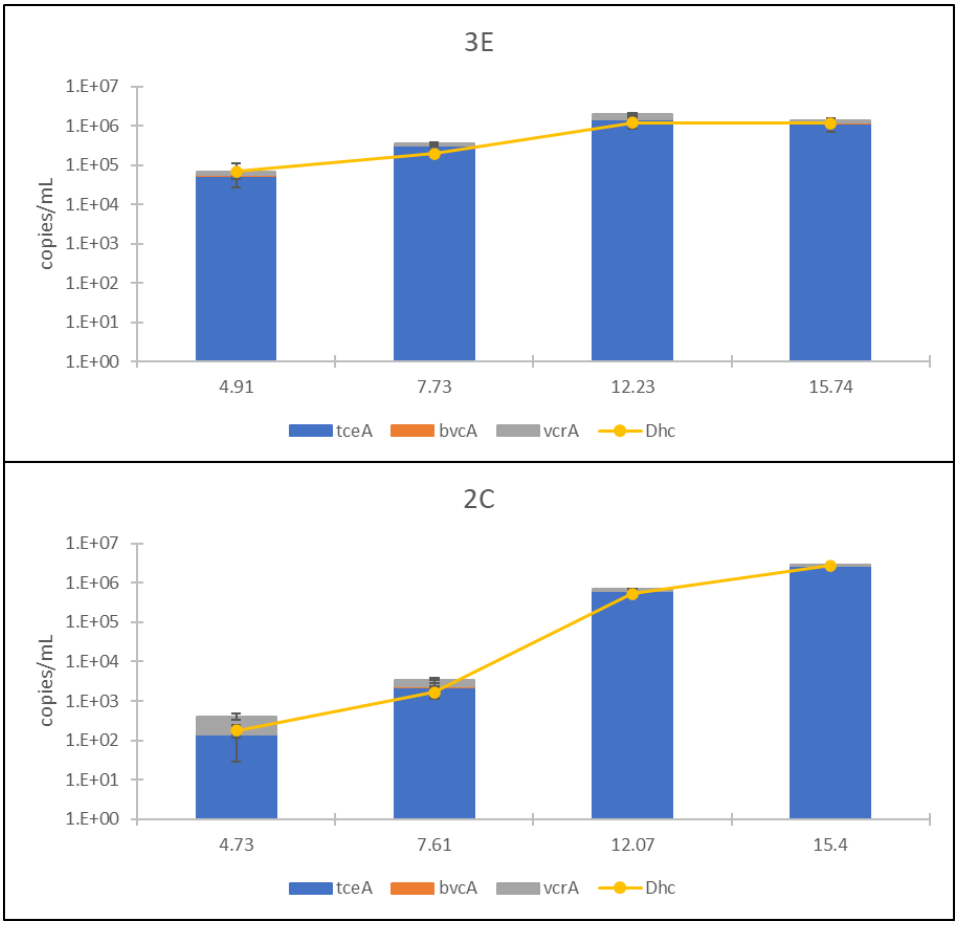

Figure 3.16 Port 3E and 2C Dhc and RDase gene abundances from PV 4.73 to PV 15.74 with standard deviation error bars

Port 3E had the overall highest microbial populations at (10^5 *Dhc*, 10^5 *tceA*, 10^3 *bvcA*, 10^4 *vcrA* – gene copies/mL) and the highest bioenhancement value (72%) (Figure 3.16). This location near the Commerce St. Clay also had the highest ethene production and greatest availability of electron acceptor – due to the pre-saturation of clay. Near the clay, the microorganisms had favorable conditions promoting higher population growth, dechlorination, and bioenhancement

results. However, the largest increase in *vcrA* gene (94X) was in port 2C near the Hudson soil (Figure 3.18). This is important to acknowledge since the *vcrA* gene is largely responsible for ethene production. The Hudson soil has the highest organic carbon and measured high bioenhancement downgradient of the lens (18-32%). The combination of adsorbed mass (high organic carbon correlates to high K_d), available electron donor (ERDenhanced and organic carbon from the Hudson soil), and high measurements of microbial populations (>10^3 copies/mL *Dhc*) creates an environment that supports and encourages high bioremediation performance (Dragun 1998, Clark, Taggart et al. 2018).

Table 3.5 shows the increase in concentration (gene copies/mL) that occurred between pore volume 7.5 and 15.5. These two time points are critical in the experimental timeline because PV 7.5 represents the microbial community prior to reducing the TCE concentration, and PV 15.5 represents the microbial community after reducing the TCE concentration (representing up gradient source zone removal). Samples taken at PV 7.5 captured the microbial abundances after bioaugmentation (PV 0) and biostimulation (PV 6), but before reducing the TCE concentration (PV 8.91). Samples taken at PV 15.5 measured *Dhc* and RDase concentrations after reducing the TCE concentration, and complete transformation to ethene had been observed in several ports (1E, 3E, and 4C). Samples from these stages in the experiment were analyzed in detail to provide the best information prior and after important milestones in the aquifer cell lifespan. Results specific to these two time points are included in Table 3.5, Figure 3.17, and Figure 3.18. Biomass from additional time points were not included due to poor DNA

recovery from errors in sample collection and preservation. However, the microbial information shown provides sufficient information to support the following conclusions (Section A.7).

Table 3.5 Microbial Increase after comparing before (PV 7.5) and after (PV 15.5) TCE reduction from 0.38 mM to 0.02 mM

X Increase in Concentration from PV 7.5 --> 15.5					
PORT	***Dhc***	***tceA***	***bvcA***	***vcrA***	**TOTAL RDase**
1B	6	4	365	5	5
1D	1	1	2	4	2
1E	9	6	11	26	8
2A	32	15	3	16	15
2B	62	43	61924	46	52
2C	1638	1202	168	94	827
3B	445	391	629	25	274
3D	7	5	18	2	4
3E	6	4	44	6	4
4A	1	1	0	0	0
4C	262	130	16	74	106

Data from Table 3.5 shows that port 2C showed the greatest increase in *Dhc*, *tceA*, *vcrA*, and total RDase gene abundance. Port 2B experienced a greater increase (61924X) in *bvcA* concentrations compared with port 2C. Port 2C and 2B are downgradient of Hudson soil which measured high bioenhancement values (18-19%). This links high bioenhanced back diffusion to an increase in microbial populations and ethene production. Port 3E had the highest overall microbial population at pore volume 7.5, and port 2C measured the highest microbial population at PV 15.5. Ethene production was highest in port 3E which also measured the highest bioenhancement and highest microbial population at PV 15.5. Microbial abundance values for all measured ports are shown in Figures 3.17 and 3.18 for PV 7.5 and PV 15.5, respectively.

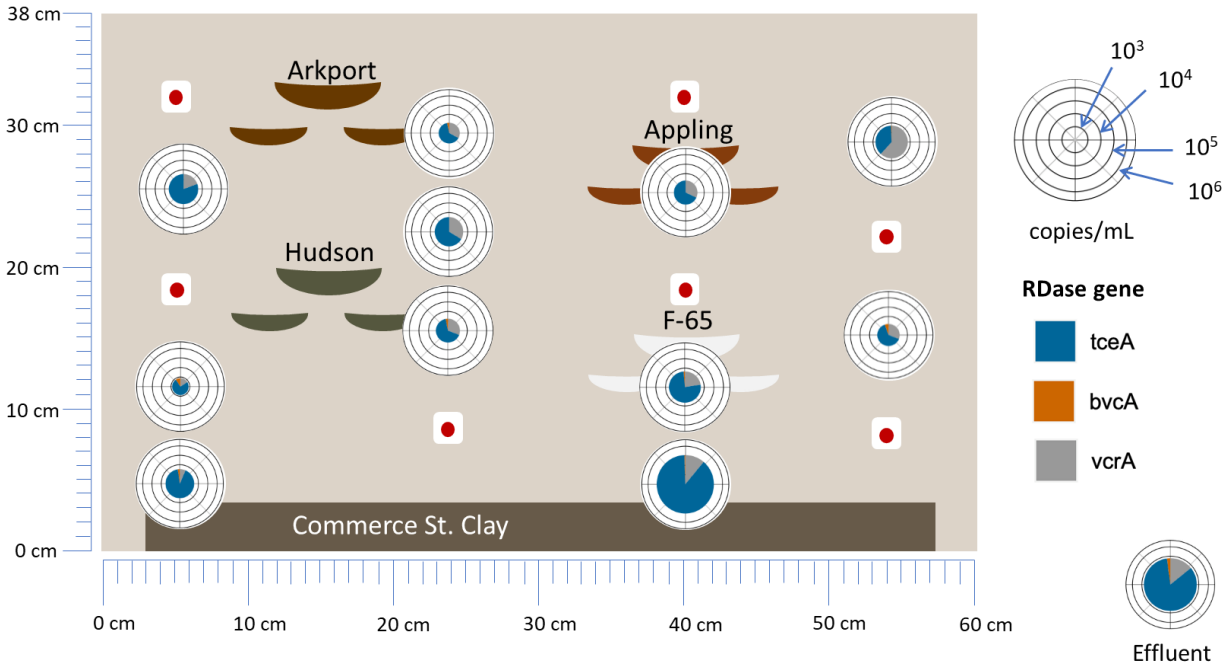

Figure 3.17 RDase Gene Abundance 7.5 PV after bioaugmentation and 1.4 PV prior to decreasing the TCE concentration from 0.38 mM to 0.02 mM

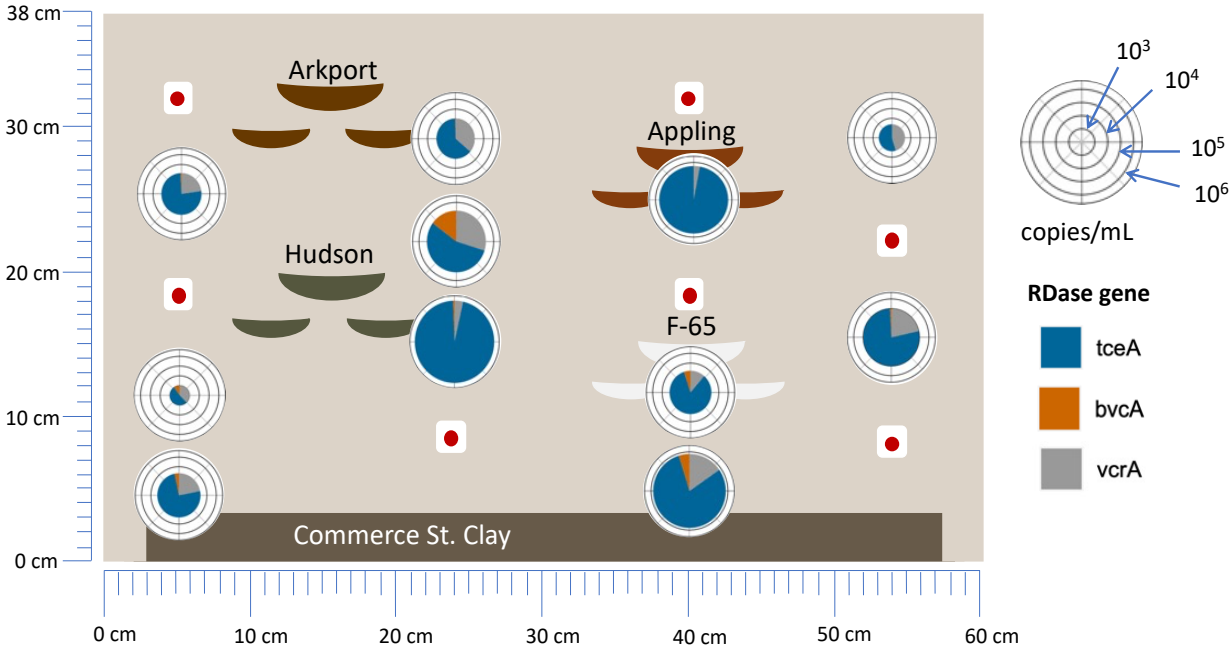

Figure 3.18 RDase Gene Abundance 15.5 PV after bioaugmentation. This is 6.6 pore volumes after the TCE concentration was reduced from 0.38 mM to 0.02 mM at PV 8.9.

For both time points, the *bvcA* gene contributed to a very small percentage of the total RDase gene population except for in port 2B where it measured 15% at PV 15.5. This area corresponds to the middle of the contaminant plume where cis-DCE was the most available electron acceptor for the previous 11.6 pore volumes – which confirms similar findings (Hnatko, Yang et al. 2020). The greatest overall abundances were in port 2C, 3E, and 3B which are near the Hudson soil, Commerce St. clay, and Appling soil, respectively. The highest *vcrA* percentage was measured in port 4A at 45% of total RDase genes. The correlation between electron acceptor availability and specific RDase abundance supports why the *vcrA* gene was detected in greater quantities later in the aquifer cell where transformation of VC to ethene was the predominant reaction. While port 4A had the highest percentage of the *vcrA* gene at PV 7.5, the quantity (10^2 copies/mL) was not as high as other ports (>10^3), which may explain the outperformance when measuring BBD%. The relationship between electron acceptor availability and prevalence of RDase gene has been documented and the results from this study provide additional support to those findings (Hnatko, Yang et al. 2020). Additional studies have shown that longer exposure to electron acceptor is linked to a greater prevalence of specific RDase genes. For example, longer exposure to TCE would correspond to a greater prevalence of the *tceA* gene (Liang, Molenda et al. 2015). This helps to further explain why the *tceA* gene was measured near stored TCE, and why the *vcrA* gene experienced the greatest increased later in the experiment (PV 15.5) after more prolonged exposure to VC. Additionally, the Appling soil adsorption coefficient was calculated instead of measured, so the high K_d may not be accurate if Appling soil has a non-linear soil-water partition relationship. This would explain the lower BBD% values

and the greater presence of *vcrA* gene – assuming a correlation between higher *vcrA* gene abundance and greater availability of TCE daughter products.

3.3.6 Performance of ERDenhanced

Two electron donors were used throughout this experiment. Lactate was used to verify the viability of the KB-1® consortium at the beginning of the EISB phase (PV -1 to 5) to facilitate acclimation to the experimental system and confirm microbial activity. ERDenhanced replaced lactate at PV 6 and was injected into select ports so that a total concentration of 6 g/L was introduced into the aquifer cell (Figure 3.3). ERDenhanced was successful at providing sufficient substrate to the KB-1 consortium to achieve full dechlorination to ethene. This experiment marked the first time the effectiveness of ERDenhanced in a controlled laboratory 2D flow system was measured. Dechlorination was observed until PV 18.6 when MRD started to stall and rebound in several ports (Figures 3.13 and 3.14). TCE was detected in the effluent and in all ports except port 2C ranging from 0.003 mM (0.4 ppm) in port 1D and 0.02 mM (3 ppm) in port 4C (Figure 3.12). It was determined that supplementation of ERDenhanced with a reintroduction of lactate at PV 21.5 was necessary to continue studying microbial enhanced diffusion. While ERDenhanced lasted approximately 12.5 PV, ethene was detected in all ports after transitioning back to lactate. The quick resurgence of ethene formation following electron donor supplementation indicated that ERDenhanced had been depleted and lack of electron donor was a limiting factor. Therefore, while ERDenhanced may not compare with slow-release electron donors such as HRC or EVO, it supported full dechlorination to ethene for shorter

durations (12.5 PV) in this specific experiment (Adamson, McDade et al. 2003, Harkness and Fisher 2013).

3.4 Conclusions

A heterogeneous aquifer cell packed with five low permeability soils was saturated with TCE to simulate long-term chlorinated ethene exposure at a complex site. Following saturation, the influent was decreased to measure back diffusion of the adsorbed contaminant mass out of the low-permeability zones. This change in concentration represented source zone removal and provided the opportunity to quantify the impact of back diffusion. A flushing phase was performed under natural conditions to establish baseline data to compare with the biotic portion of the experiment. Following the natural flushing phase, the aquifer cell was saturated with TCE again and prepared for EISB. Bioremediation was performed using bioaugmentation of KB-1 microbial consortium and biostimulation with lactate and ERDenhanced. The influent concentration was reduced to simulate upgradient source treatment and bioenhanced back diffusion was measured.

Microbial dechlorination contributed to an average of 9% more BBD% (effluent) with localized enhancement of up to 72% near the confining clay layer. Soil properties, such as high organic carbon content (0.91%) and a low hydraulic conductivity (0.04 m/day), in the Hudson soil correlated to high bioenhanced back diffusion (18%-19%) compared to 9% in the effluent. Organic carbon content is known to influence adsorption into the solid phase (Dragun 1998).

Therefore, the high bioenhancement performance was made possible due to the high prevalence of stored chlorinated ethene mass near the Hudson Soil.

Complete transformation of TCE to ethene was detected by termination of the aquifer cell (PV 24.2) in the effluent and all ports. Locations with low hydraulic conductivities (Commerce St. Clay and Hudson soil) accounted for higher concentrations of TCE transformation products and measured ethene concentrations in less pore volumes (10 PV after bioaugmentation) compared with other soils (20 PV). The more rapid transformation could be caused by longer residence times through the low-permeability lenses – giving microorganisms the time needed to fully dechlorinate.

Locations with the highest organic carbon content measured the greatest increase in *Dhc* and RDase gene abundance (Hudson, Arkport, and Clay). This confirms that organic carbon is an important factor in providing an environment for dechlorinating microorganisms to increase in numbers high enough for full dechlorination ($>10^3$ copies/mL) (Clark, Taggart et al. 2018). Appling soil had the second highest organic carbon (0.75%), but a hydraulic conductivity of 10.2 m/day – higher than the clay and Hudson soils. The Appling soil measured bioenhancement values of 5% (in port 3B) and 0% downgradient in port 4A. This information suggests that high organic carbon and low hydraulic are conjunctively needed to increase the removal of stored contaminate mass beyond natural processes.

Port 3E, near Commerce St. Clay, had the highest microbial populations (10^5 *Dhc*, 10^5 *tceA*, 10^3 *bvcA*, 10^4 *vcrA* – gene copies/mL) and the highest bioenhanced back diffusion. This supports that bioremediation near low permeability media helps remove contaminant mass faster than abiotic processes alone (Berns, Sanford et al. 2019). On average, the overall abundance of RDase genes exceeded the concentration of *Dhc* 16S rRNA genes, which is consistent with other studies (van der Zaan, Hannes et al. 2010, Cápiro, Löffler et al. 2015, Hnatko, Yang et al. 2020). RDase gene concentrations greater than *Dhc* values indicate that there are still unknown factors besides *Dhc* cells that are contributing to RDase gene abundances.

ERDenhanced provided sufficient nutrients to support reductive dechlorination for approximately 12.5 PVs before additional electron donor was needed. Results from this study provided new data on ERDenhanced viability in a flowing experimental system. More information is needed on detection and quantification to track ERDenhanced more accurately in heterogeneous flowing systems. Additionally, potential biofilm formation should be studied to determine if any additional benefits to enhanced microbial dechlorination can be found.

This is one of only two known studies that have analyzed bioenhanced back diffusion from low-permeability media in a heterogeneous aquifer cell experiment. The Hnatko, Yang et al. (2020) study measured bioenhancement values ranging between 6%-53% with the highest enhancement measured near the Commerce St. clay. The aquifer cell in the current research measured higher overall bioenhancement (72%) which could be attributed to several different aspects of the experimental set-up. For example, modeled values were used for calculating

bioenhancement in the Hnatko, Yang et al. (2020) study; for this experiment, data from the natural flushing phase was used since modeling data was not available for calculating BBD%.

Additionally, the surface area of each lens increased by approximately 50% which likely contributed to the increased mass transfer of chlorinated ethenes – since back diffusion occurs at the low-permeability interface. Microbial data confirmed that specific RDase abundances increased when and where the required electron acceptor was available (Hnatko, Yang et al. 2020). The high abundances of *tceA* genes in this experiment could be due to higher back diffusion of adsorbed TCE from the low-permeable lenses. Additionally, increases in *vcrA* gene abundances increased as TCE was removed and cis-DCE, VC, and ethene were more predominant. Further analysis of the soil in the aquifer cell after decommissioning is needed for complete analysis of the microbial community and any remaining adsorbed contaminant mass.

A transition from EISB to passive remediation was attempted by introducing a singular pulse of ERDenhanced as an electron donor (instead of continuous lactate addition). Biostimulation with ERDenhanced represented treatment using a combined remedy - which is increasingly recommended at complex field sites (EPA 2020). While healthy microbial populations and complete dechlorination was measured for the first 12.5 PV, a low amendment of lactate was needed to achieve ethene production in all ports without TCE rebound. More information is needed to quantify ERDenhanced in-situ so that accurate predictions can me made about the duration of remediation performance.

Chapter 4 - Engineering Implications and Recommendations

The goal of this research was to better understand the interrelationships between TCE bioremediation and complex heterogeneous aquifers. The impact of bioremediation process on mass transfer of chlorinated ethenes out of low-permeable zones as a function of soil properties (organic carbon, hydraulic conductivity) was investigated. Data from this aquifer cell experiment adds to the larger knowledge base of information that can be used to calibrate models for accurate remediation predictions and offers new insights into which conditions are favorable for achieving remediation goals.

Key Findings:

- Organic carbon content, hydraulic conductivity, and lens shape are driving factors when predicting bioenhanced back diffusion of chlorinated ethene mass from low-permeability zones.
- Microbial reductive dechlorination contributed to greater back diffusion from low-permeability soils (9% average and up to 72% locally) than natural aquifer conditions.
- The distribution of RDase genes was correlated to available electron acceptor.
    - A greater fraction *tceA* gene was measured where TCE was primarily available near the beginning of the plume and near saturated zones.
    - The *bvcA* gene composed a greater fraction where cis-DCE was available (near the middle of the contaminant plume).

    - *vcrA* genes increased in abundance near areas with the most ethene formation near the end of the plume.
- ERDenhanced was used to fully dechlorinate TCE in a heterogeneous flowing 2D experimental system without amendments for 12.5 PV.

Ongoing work includes analysis of qPCR data that was collected after PV 15.5 to study the more prolonged effects microbial communities during later stages of remediation. Solid phase soil samples and aqueous VOC samples collected during the deconstruction of the aquifer cell could provide additional insights to specific locations of *Dhc* and RDase genes and account for attached vs. unattached cells. Further analysis of this additional data is important in understanding if complete mass removal was achieved from any or all the soil lenses. These next steps would gain an even more specific understanding between the solid and liquid phases of bioremediation performance within the aquifer cell.

Data collected during this experiment is being modeled with collaborators at Virginia Tech to develop predictive tools that can be used for field scale applications (SERDP ER20-1079). This information will be help calibrate models that can accurately predict where the highest bioenhancement, *Dhc* populations, and RDase populations would be within complex aquifers and recommend which sites are promising candidates for transitioning from EISB to passive remediation.

Guidance for Future Work:

- Measure the impact of biofilm formation on increased mass removal and detoxification of chlorinated ethenes, especially within low-permeability zones.
- Create a system that better represents realistic field site conditions. Natural aquifer bulk media is more complex than ASTM 20/30 sand, and various shapes of lenses could offer additional insight into the effect subsurface architecture and surface area has on bioenhanced back diffusion.
- Different introduction methods for ERDenhanced could prove to be more effective at improving microbial growth and remediation. There is not much information on application and measurement of ERDenhanced in experiment systems, so creating a more field-like addition would be beneficial.
- An experiment with larger lenses and greater mass storage could result in a longer release of TCE and more accurate predictions for field scale extrapolation

There is still much to be learned about the behavior and classification of dechlorinating microorganisms. *Dhc* was thought to be the only microorganisms capable of complete dechlorination of chlorinated ethenes to ethene until *Dehalogenimonas (Dhgm)* was discovered (Yang, Higgins et al. 2017). The abundance of RDase genes often outnumbers total 16S rRNA of *Dhc,* suggesting that additional microorganisms and RDase genes may contribute to dechlorination (van der Zaan, Hannes et al. 2010, Damgaard, Bjerg et al. 2013, Cápiro, Löffler et al. 2015). Future studies are needed to measure how *Dhc* and other dechlorinating microorganisms (e.g., *Dhgm*) work together in a heterogenous subsurface matrix. Field sites are

complex environments where understanding the interactions between microorganisms and adsorbed contaminant mass could prove extremely beneficial when predicting clean-up times and engineering remediation techniques.

Appendix A: Supplementary Material

Appendix A includes pertinent information that was not included in the main section to be concise and direct. Information included in Appendix A includes information on chemicals and soils used in the experiments outlined above. Methods used and results for soil properties such as organic carbon, rate to adsorption, and soil-water distribution coefficient are discussed in further detail. Chemical and biological analytical methods and instrument operating procedures are listed. Information about an additional study using ERDenhanced in a flowing column provides supporting information for ERDenhanced transport. Finally, information on methane measured in the aquifer cell is discussed along with supporting figures.

A.1 Chemicals, Synthetic Groundwater, and Soils

Sodium bromide and sodium chloride used for the natural flushing phase of the experiment was purchased from Fisher Scientific, Hampton, NH. Erioglaucine A (blue dye) used for visually observing transport through the aquifer cell was obtained from Fluka Chemical; Seelze, Germany. TCE (ACS reagent, >99.5%) was used for calibration curves for the GC-FID, and GC-ECD, for saturating the aquifer cell, and for adsorption/desorption experiments (Sigma Aldrich; St. Louis, MO). Methanol (LC-MS grade, >99.9%) was used for methanol extraction measurements on the GC-ECD. Ultrapure 18.2 MΩ deionized water was used for all aqueous solutions using an Evoqua water purification system (Evoqua Water Technologies).

Three recipes for groundwater solutions were primarily used for the current research.

1) Synthetic Groundwater

2) Anaerobic Medium

3) Aerobic Medium

1) Synthetic groundwater containing 30 mM NaCl (VWR; Solon, Ohio) and ultrapure water was used for the tracer, TCE saturation, and natural conditions in the aquifer cell. Occasionally bromide (NaBr) was introduced for tracer tests, so NaCl was reduced to maintain an overall ionic strength of 30 mM unless specified otherwise. 2) Anaerobic medium was used to prepare for bioaugmentation (starting at PV -2.4) and thereafter in the aquifer cell. Anaerobic medium was prepared using a modified recipe according to (Loffler, Sanford et al. 1996, Sung, Ritalahti et al. 2003, Amos, Suchomel et al. 2008, Cápiro, Löffler et al. 2015). The original recipe had an ionic strength of 60 mM, and the recipe was modified using half of the 100x salt solution and 10 mM sodium bicarbonate to achieve an ionic strength of 30 mM. This was done to create an environment that was more realistic to groundwater found at field sites. 3) An aerobic version of medium including the same ingredients as the anaerobic medium was used for the ERDenhanced preliminary experiments. These experiments were abiotic, so anoxic conditions did not matter for this portion of the research. All three solutions maintained an ionic strength of 30 mM for consistency in solubility of chemicals and fines.

ASTM International Standard 20/30 mesh sand (US Silica Company; Ottawa, IL) was used as the background sand for the aquifer cell. The aquifer cell consisted of four lenses including: Appling soil (<30 cm depth, University of Georgia Agricultural Experiment Station; Eastville, GA), a loamy coarse sand with a pH of 4.6; Hudson soil (60-104 cm depth, Allegany County, NY), a silty clay with a pH of 5.8; Arkport soil (114-142 cm depth, Orleans County, NY), a loamy fine sand with a

pH of 5.5 (USDA); and F-65 Ottawa sand (KyMudworks; Lexington, KY), a uniform sand with 0.17% fines (Bastidas 2016). The clay used to establish a lower confining layer in the aquifer cell was collected from the Commerce St. Superfund site (Williston, VT) at a depth of 38.5-40 ft. The percent organic carbon for the Commerce Ct. clay was measured as 0.27%. A value of 0.3% organic carbon was taken from clay at the Commerce St. Superfund site (Hnatko et al 2020), and the slight difference in clay properties was attributed to variances with sample collection depth and location. All soils except for the Commerce St. Clay were stored at room temperature in a sealed container. The Commerce St. Clay was preserved in a 4^{o}C refrigerator in sealed plastic bags prior to preparation for introduction to the aquifer cell. The clay was removed from the refrigerator, air dried, and sieved for more consistent results throughout all experiments.

Iron (II) sulfide precipitation was visually observed in the aquifer cell (Figure 3.10 in Section 3.3.3). Sodium sulfide was used in medium preparation to maintain anaerobic conditions and iron is a natural component of soils used in the aquifer cell. Iron content in Hudson soil was measured by the Auburn University soil lab as 16.68 (±4.24) ppm. The head elevation for the effluent was lowered approximately 4 cm over the duration of the experiment to account for the decrease in permeability in the aquifer cell. This equates to a drop in average hydraulic conductivity for the aquifer cell up to 18%.

A.2 Soil Characterization

A.2.1 – Organic Carbon Analysis

Organic Carbon was measured using a Shimadzu SSM-5000A Solid Sample Module (SSM) and Shimadzu TOC-L Total Organic Carbon Analyzer (Shimadzu; Columbia, MD). All natural soils were air dried and passed through a #20 mesh sieve to be consistent with soil preparation for the aquifer cell. For total carbon analysis, 10-20 mg of soil was added to a ceramic weigh boat and placed into the SSM furnace for measurement. For inorganic carbon analysis, 10-20 mg of soil and 400 μL of phosphoric acid were added before measurement. Organic carbon was calculated by subtracting the total carbon from the inorganic carbon.

A.2.2 – Rate to Adsorption

A rate to adsorption experiment was performed for the Commerce St. Clay to guide the duration of the following adsorption isotherm experiments for each soil. The clay was chosen since it was predicted to have the longest duration to achieve adsorption of all the soils. The goal of performing this experiment was to verify that TCE adsorption had reached equilibrium between the aqueous and solid phases prior to deconstructive sampling. The clay was air-dried and passed through at #20 mesh sieve. A clay slurry was made using a 1:1 mass ratio of clay to 18.2Ω ultra-pure water and allowed to sit overnight (Figure A.1). The use of clay slurry aimed to avoid clay expanding and breaking the 20 ml glass crimp top vials once sealed (Agilent Technologies; Santa Clara, CA).

Figure A.1 Commerce St. clay slurry

The experimental set-up consisted of 36 vials (27 with clay slurry as the experimental group, 9 without slurry as the control group) that were destructively sampled over 10 days according to Table A.1. Triplicate vials in the experimental group were prepared for each sampling point so that an average and standard deviation could be calculated. Control vials were used to account for any TCE losses due to volatilization. Approximately 3 grams of slurry was weighed and added to 20 ml crimp-top glass vials. A 30 mM synthetic groundwater solution spiked with 100 ppm TCE was added until no headspace remained in the vial. The rate to adsorption experiment was performed using a 100 ppm TCE solution since that was the highest concentration to be used in the adsorption isotherm experiments. The vials were crimp-sealed with a grey PTFE stopper to limit TCE adsorption to the septa. The water content of the clay was measured and used to adjust the dry mass of clay and total concentration of TCE in the solution. All the vials were placed on an oscillating shaker under a snorkel for additional safety.

Table A.1 Rate to Adsorption Sample Matrix

Day	# Vials	# Control
0	3	1
0.25	3	1
0.5	3	1
1	3	1
2	3	1
3	3	1
4	3	1
7	3	1
10	3	1

For each sampling event, triplicate experimental group vials and one control group vial were taken off the shaker and centrifuged at 1,500 rpm for 5 minutes. An aqueous sample of 1 mL was measured using a gas chromatographer equipped with a flame ionization detector (GC-FID) for aqueous TCE analysis. Afterwards, methanol extraction was performed on the clay to measure TCE concentrations in the solid phase (Section A.3.3).

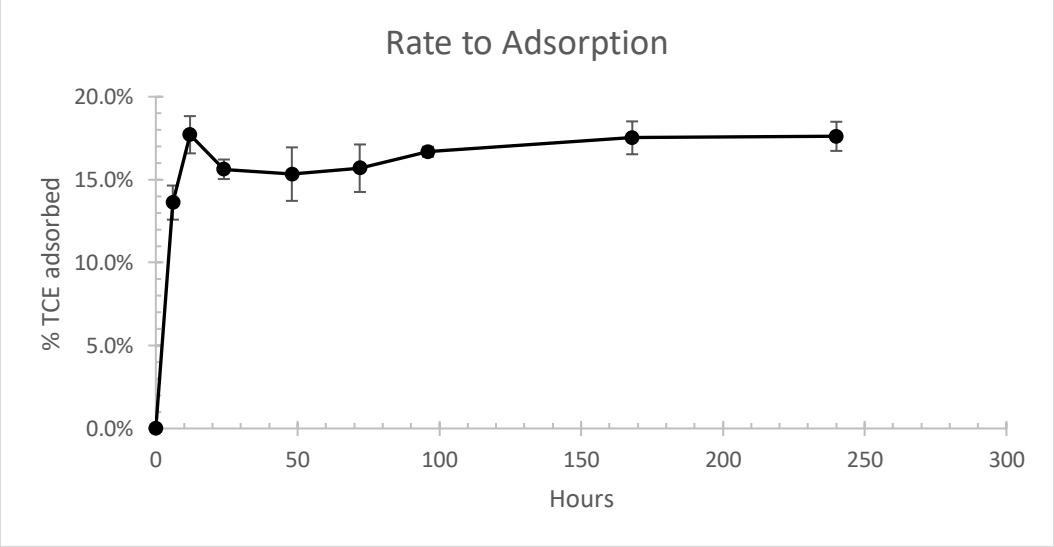

Figure A.2 Rate to Adsorption - Commerce St. Clay

Results from the rate to adsorption show that the TCE adsorption equilibrium between the aqueous and solid phases was achieved after 168 hours or 7 days (Figure A.2). At equilibrium, approximately 17.5% of the total mass of TCE in the system was adsorbed to the solid phase.

A.2.3 – Adsorption Isotherm

Adsorption isotherm experiments were performed on the Commerce St. Clay, Hudson soil, and Arkport soil to predict TCE adsorption and desorption more accurately in the aquifer cell. Approximately 3 grams of soil were added to 20 ml crimp-top vials containing a 30 mM synthetic groundwater with 5 different concentrations of TCE ranging from 1 ppm to 75 ppm in triplicate (Table A.2).

Table A.2 Adsorption isotherm sample matrix

TCE Concentration (ppm)	# Vials	# Control
1	3	1
10	3	1
25	3	1
50	3	1
75	3	1

The vials were placed on an oscillating shaker for 7 days (determined from Section A.2.2) before measuring aqueous and adsorbed TCE concentrations according to methods discussed in Section A.3.

The soil-water distribution coefficient values for the soils were necessary when estimating experimental time frames for saturating the aquifer cell with TCE. Modeling by Dr. Mark

Widdowson and Dr. Hamed Mohammadnejad at Virginia Tech, along with experimental data, provided estimated durations for each phase of the aquifer cell experiment. Based on these results, the Commerce St. clay was saturated with 0.76 mM (100 ppm) TCE prior to emplacement into the aquifer cell. The final concentration of TCE in solid phase was determined as 0.086 (±0.005) mg/g and was measured using the methanol extraction procedure outlined in Section A.3.3.

A.3 Analytical Methods

A.3.1 Chemical Analytical Methods

Aqueous chlorinated ethenes and ethene concentrations were measured using an Agilent 8890 GC system equipped with a 60-centimeter DB-624 column (Agilent Technologies, Santa Clara, CA). A 1 ml aqueous sample was placed in a 20 ml headspace crimp-top vial and sealed with a PTFE septa and aluminum crimp cap. Vials were placed onto a Teledyne TEKMAR HT3 Headspace autosampler (Teledyne Technologies; Thousand Oaks, CA) to be introduced to the GC. The autosampler method consisted of a constant heat equilibration time of 30 minutes and a mass flow rate of 50 mL/min at 70°C. The GC method included an initial temperature of 60°C for 4 minutes, a ramp of 25°C/min until reaching 200°C and holding for 2 minutes. A splitless method using helium as the carrier gas at 23.8 psi was used for the FID detector. Bromide samples were measured using a Thermo Scientific Orion Dual Star pH/ISE meter (Thermo Fisher Scientific, Waltham, MA) with a combination ion-selective electrode probe (Cole-Parmer; Vernon Hills, IL). Smaller volume bromide samples (from the aquifer cell ports) were measured using a Dionex Aquion ion Chromatograph equipped with an IonPac™ AS22 column (4 × 250

mm) and IonPac™ AG22 guard column (4 × 50 mm) (Thermo Fisher Scientific, Waltham, MA). VFA (lactate, acetate, and propionate) samples were measured using an Agilent 1260 Infinity II high-performance liquid chromatograph (HPLC) equipped with a Bio-Rad Aminex HPX-87H column (300 mm × 7.8 mm) (Agilent; Santa Clara, CA).

Methane was measured using the same method as aqueous chlorinated samples. A calibration curve was established by injecting 0 to 20 ml pure methane gas into 100 ml 18 MΩ ultra-pure water in 160 ml sealed serum bottles. Standards were created at five different concentrations prepared in triplicate. Samples were allowed to equilibrate on a shaker for 48 hours before 1 ml aqueous sample was added to a 20 ml headspace vial and measured on the GC-FID.

A.3.2 ERDenhanced Measurement

ERDenhanced was quantified using dissolved organic carbon (DOC). A calibration curve was established by adding ERDenhanced with concentrations ranging from 0 to 8 g/L into 10 ml of an aerobic medium solution in 15 ml centrifuge tubes. The centrifuge tubes were placed on an oscillating shaker for 48 hours to allow for maximum dissolution of ERDenhanced. The tubes were then centrifuged at 2000 rpm for 5 minutes and 1 ml of aqueous sample was collected for DOC measurement on Shimadzu TOC-L Total Organic Carbon Analyzer (Shimadzu; Columbia, MD). The calibration curve had an R^2 of 0.99 and was used to quantify ERDenhanced during the column transport study (Figure A.3).

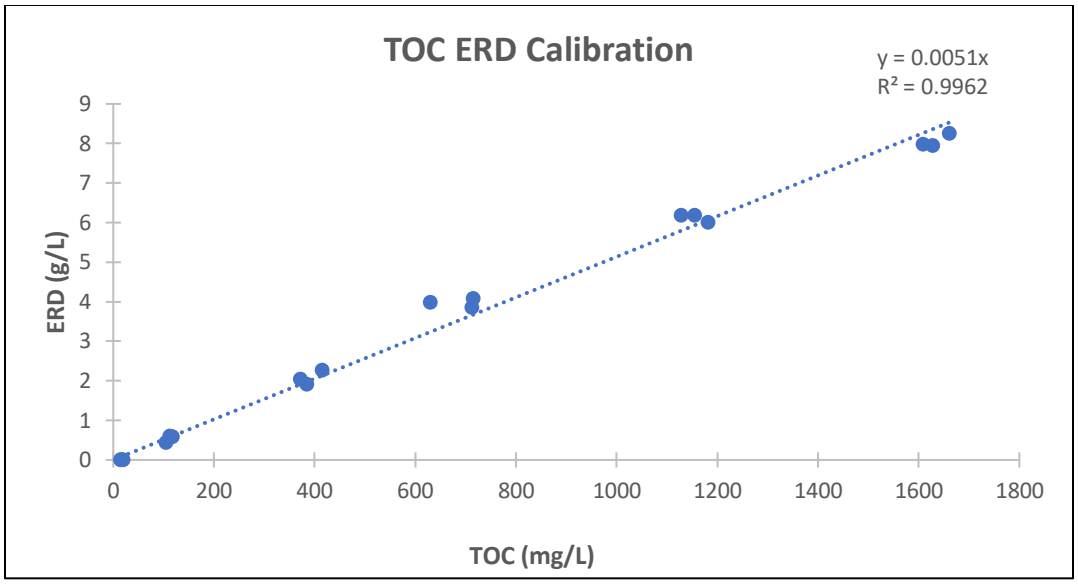

Figure A.3 Calibration curve using total organic carbon to measure the dissolved phase of ERDenhanced

A.3.3 Methanol Extraction

Solid phase TCE samples were measured using a modified methanol extraction method (Costanza 2005). This method was used for sampling solid phase TCE after saturating the clay, during the rate to adsorption experiment, and during the adsorption isotherm experiment. Extraction of TCE was performed on a slurry sample of saturated soil and synthetic groundwater. After 1 ml supernatant was take for liquid phase TCE analysis, the remaining TCE solution was decanted and replaced with ten milliliters of LC-MS grade methanol for each vial. Each vial was placed on a tilt shaker for 24-48 hours to equilibrate. After equilibrium, the vials were centrifuged at 1,500 rpm for 5 minutes. Two milliliters of supernatant were transferred into microcentrifuge tubes and centrifuged at 15,000 rpm for 10 minutes to remove any remaining soil particles. One milliliter of supernatant was collected and analyzed on an Agilent 8890 gas chromatographer equipped with an electron capture detector (GC-ECD) to measure

the TCE concentration associated with the solid phase (Agilent Technologies, Santa Clara, CA). The remaining supernatant in the vial was removed and replaced with 10 mL of LC-MS grade methanol. The extraction process was repeated until the total mass recovery was greater than 99%.

A.3.4 Biological Analytical Methods

Biological samples were taken from the aquifer cell using a syringe pump and a 1 ml sample was placed into a 1.7 ml microcentrifuge tube. The sample was immediately centrifuged at 15,000 rpm for 15 minutes to concentrate the biomass pellet at the bottom of the centrifuge tube. The remaining liquid was removed, and the sample was stored at -20^{o}C for future analysis. A DNA extraction procedure was performed using a QIAGEN DNeasy PowerSoil Pro Kit (QIAGEN; Hilden, Germany). Total DNA was measured to verify the success of the DNA extraction process using a Qubit 2.0 Fluorometer (Thermo Fisher Scientific; Waltham, MA). After the DNA extraction process was complete, the *Dhc* cell abundance was quantified by qPCR analysis targeting the *Dhc* 16S rRNA gene as well as the *tceA, vcrA,* and *bvcA* RDase genes. All qPCR analyses were measured in triplicate using a QuantStudio 3 (Applied Biosystems; Foster City, CA) under standard operating conditions and TaqMan- based chemistry. Methods for qPCR analysis were performed using established protocols (Ritalahti, Amos et al. 2006, Cápiro, Wang et al. 2014). Primers and probes were obtained from IDT Technologies (Coralville, IA) or ThermoFisher and the TaqMan Universal PCR Master Mix from Applied Biosystems (Foster City, CA).

A.4 ERDenhanced Column Study

A proprietary electron donor substrate, ERDenhanced (Terrastryke; Andover, New Hampshire), was used in the aquifer cell experiment to test dechlorination rates and biofilm growth in a 2D flowing system. ERDenhanced contains inactivated yeast and boron that can potentially promote quorum sensing and biofilm growth. ERDenhanced has a green color when mixed with water and small particles settle to the bottom if not continuously mixed. ERDenhanced arrived in solid form from Terrastryke with sand-like qualities and does not fully dissolve into solution. Due to the mentioned properties of ERDenhanced, it may have long-term effects on the release and availability of electron donor substrate in flowing systems. No work to date has been done to measure ERDenhanced in-situ, so a column study was performed to better understand transport through flowing systems.

A.4.1 – Bromide Tracer

An abiotic column study was performed to study the transport of ERDenhanced through porous media. The glass column (15cm L x 2.5cm D) was packed with 20/30 mesh Ottawa sand (Figure A.4) (Kimble-Chase Vineland, NJ). The column was then flushed with carbon dioxide for 30 minutes to remove any oxygen from the pore space and saturated for 10 PV with a 10 mM NaCl solution to mimic natural groundwater.

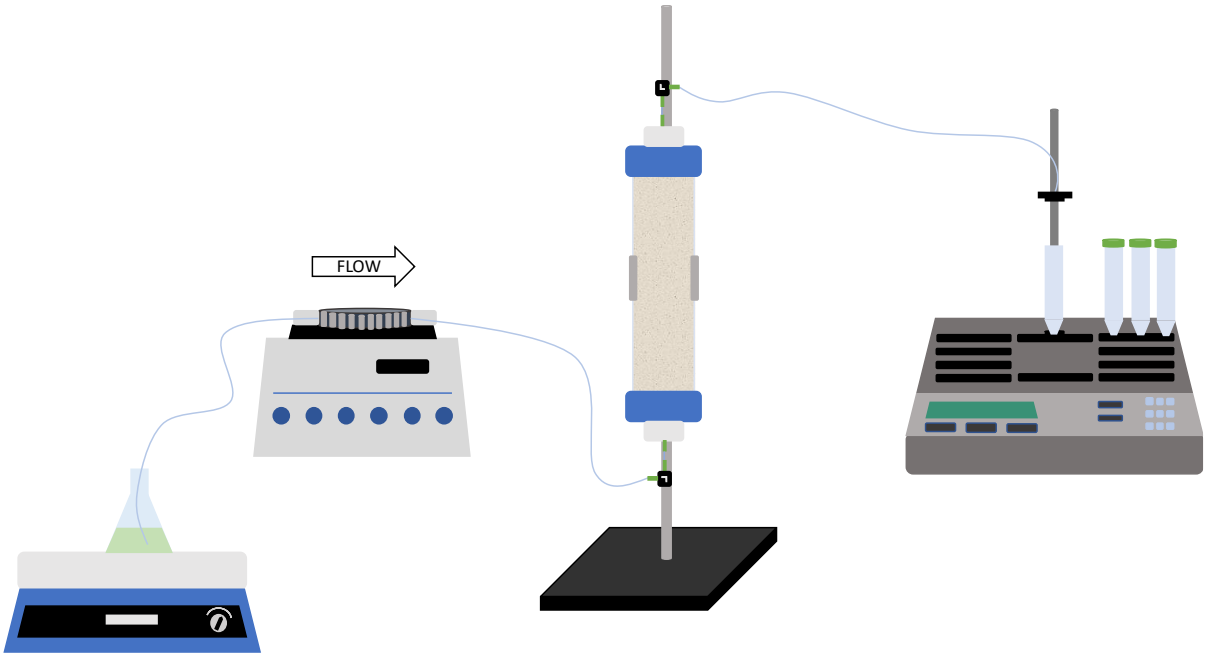

Figure A.4 Column Experimental Set-up

Next, a non-reactive bromide tracer test was performed with a 10 mM sodium bromide solution (Figure A.5). Bromide was injected at 1 ml/min using a peristaltic pump for approximately 2 pore volumes, and then flushed with 2 PV of NaCl to monitor the release of bromide from the column. Samples were collected (5 per PV) using a Spectrum Labs CF-2 fraction collector (Spectrum Chemical, New Brunswick, NJ) for bromide measurement (Section A.3.1). The breakthrough curves of bromide and ERDenhanced were analyzed using the Code for Estimating Equilibrium Transport Parameters from Miscible Displacement Experiments (CFITM) as a part of Studio of Analytical Models (STANMOD) Version 2.2 (available through USDA-ARS U.S. Salinity Laboratory; http://www.ars.usda.gov). Results from STANMOD helped determine a working pore volume (25.2 ml) and a porosity (0.34) for the column.

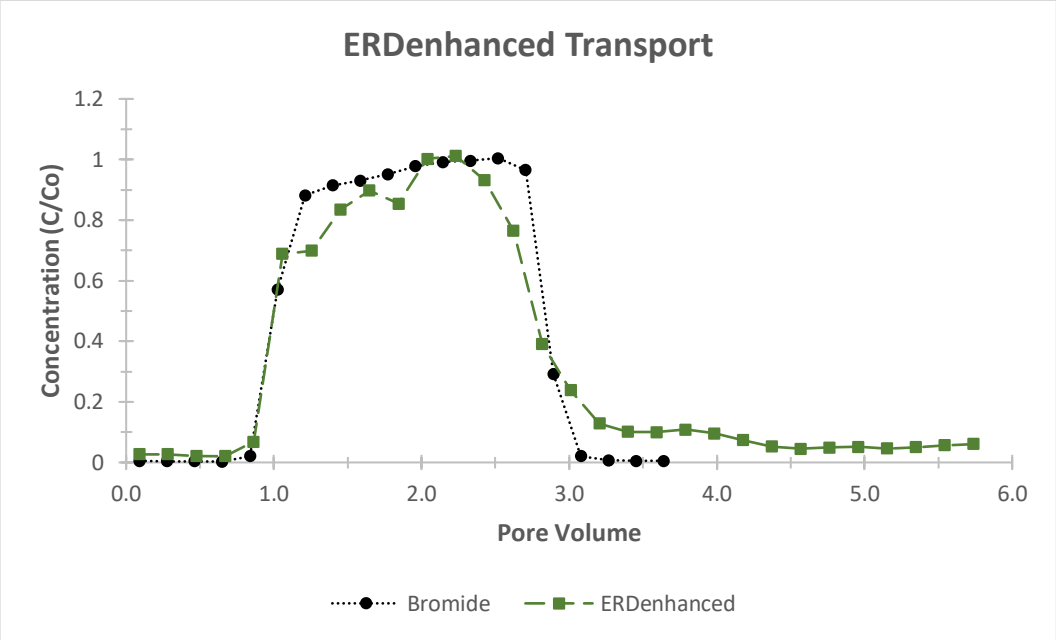

Figure A.5 ERDenhanced transport for column study

A.4.2 - ERDenhanced Transport

Following the bromide tracer test, 2 PV of aerobic medium (Section A.1) was flushed through the column to prepare for the introduction of ERDenhanced. To begin the ERDenhanced pulse, a 6 g/L ERDenhanced in aerobic medium was prepared and stirred on a stir plate for 1 hour to allow even particle distribution. The ERDenhanced solution was injected at a rate of 0.036 ml/min (32 cm/day) while continuously stirring for 2 PVs. The column influent was then switched back to the aerobic medium for an additional 3.5 PV for a total ERDenhanced mass recovery of 100%. To measure ERDenhanced, samples were collected using a fraction collector (shown in Figure A.4), centrifuged at 2000 rpm for 5 minutes, and analyzed on the TOC-L machine (Section A.3.2). To measure retardation of ERDenhanced, the PV in which 90% cumulative mass was measured in the effluent was determined for bromide and ERDenhanced as a comparison. Bromide mass was 90% recovered at PV 2.8 and ERDenhanced measured 90%

recovery at PV 3.1. This equates to approximately 11% retardation of ERDenhanced through the column compared with bromide. This study was successful in measuring transport of ERDenhanced through porous media which has not been demonstrated prior to the current research. Since ERDenhanced is not fully soluble, this method is constrained in that it only measures the dissolved phase.

A.5 Methane Production in the Aquifer Cell

Following a 48-hour flow interruption in the aquifer cell (4.2 PV after bioaugmentation), gas formation was visualized in the lower portion of the aquifer cell (Figure A.6). Methane was measured highest in port 3E and the effluent at concentrations of 0.4 mM and 0.22 mM, respectively at PV 4.2 (Figure A.7). Methane was measured in all other ports at concentrations ranging from 0.01 mM to 0.21 mM.

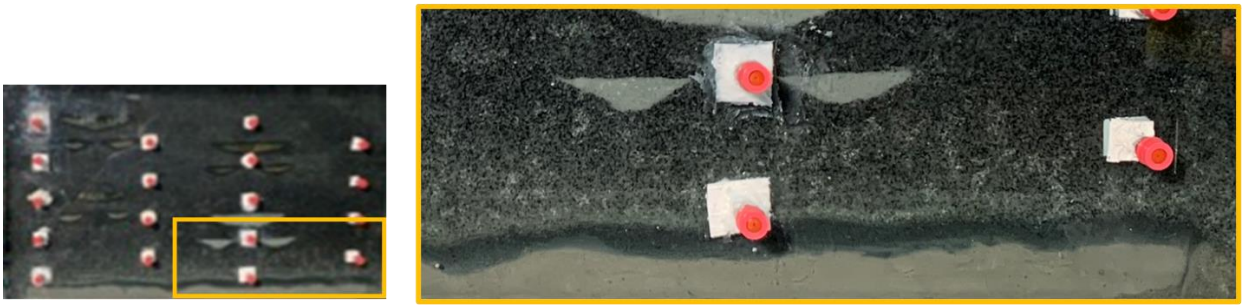

Figure A.6 Methane Production in Aquifer Cell

Methane was measured using GC-FID as discussed in section A.2.1. Most ports measured a spike in methane concentrations that decreased within 3 pore volumes (as represented by port 4A in Figure A.7). However, methane concentrations slowly decreased in the effluent and port 3E for over 10 PV after the flow interruption (Figure A.7). These results demonstrate that the increase and decrease of methane production is a function of residence time.

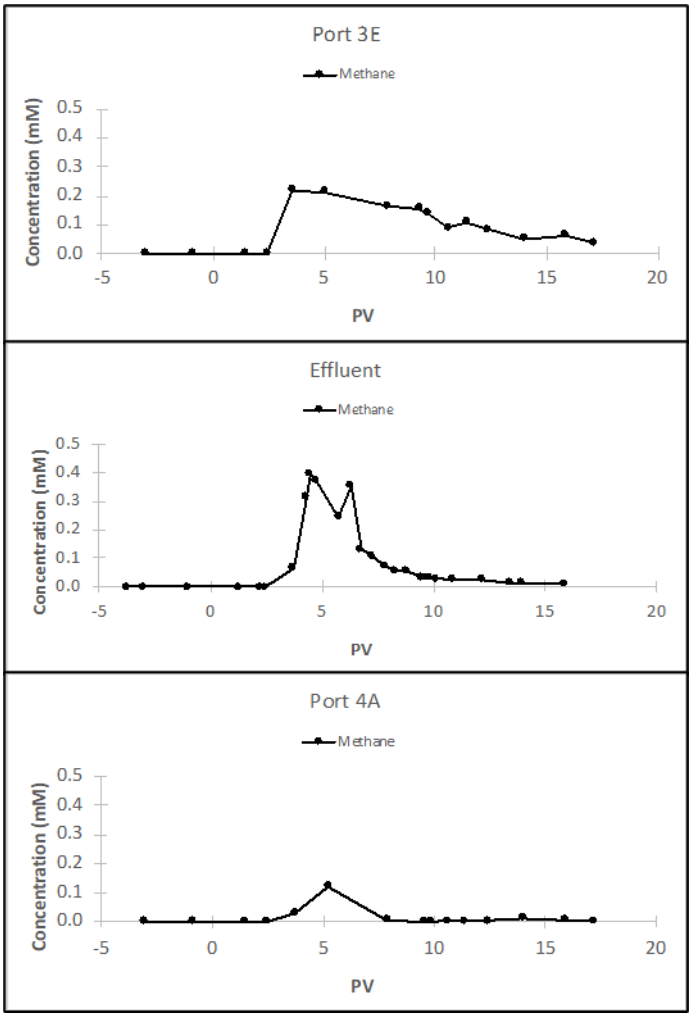

Figure A.7 Methane Production in Ports 3E, Effluent, and 4A where (PV 0 = bioaugmentation)

Previous studies have observed an increase in methane production after bioaugmentation of KB-1, specifically near the bottom of the aquifer cell and with high concentrations of chlorinated ethenes (Sleep, Seepersad et al. 2006). In the current research, ports with the highest methane production also had the highest ethene production – linking increased dechlorination and methanogenesis. The buildup of gas bubbles resulted in reduced flow through the aquifer cell, and the flow rate in the aquifer cell had to be adjusted. Port 3E measured the most sustained ethene production and highest concentrations of methane.

However, the highest concentration of methane was measured at approximately PV 5, and ethene production was not measured until PV 10.5 in port 3E.

A.6 DOC and VFAs in Aquifer Cell

Samples were taken from the aquifer cell influent and effluent to monitor the presence of volatile fatty acids (VFAs) including lactate and its daughter products (acetate and propionate) during the initial stages of bioaugmentation (PV -1 to PV 6).

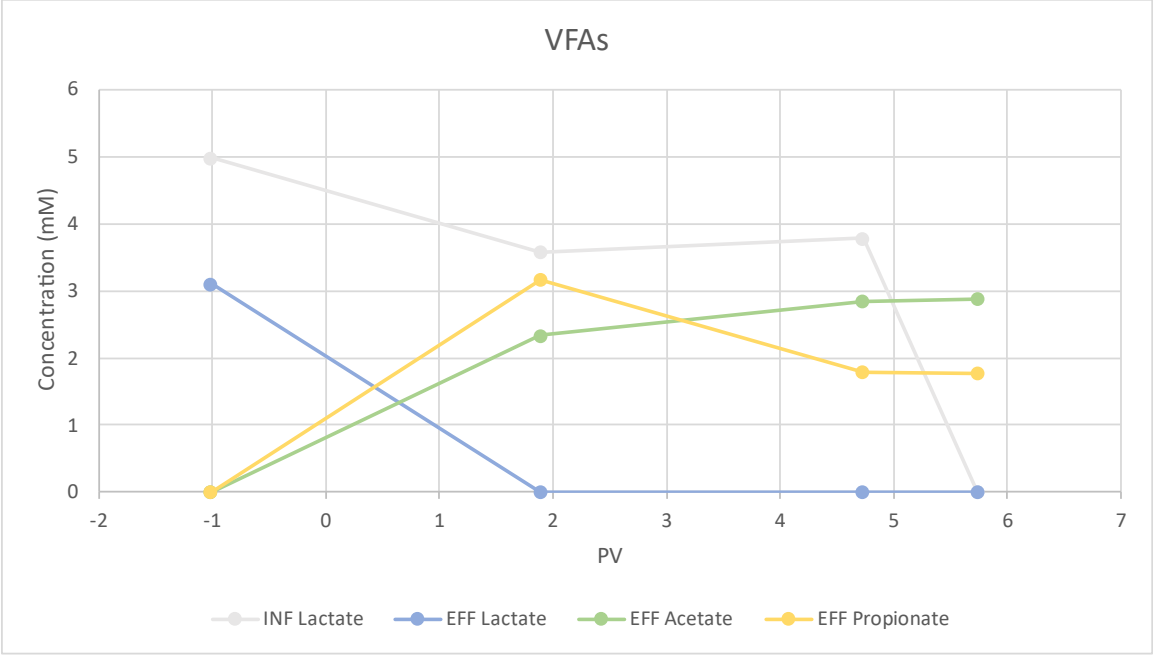

Figure A.8 Volatile Fatty Acids (VFAs) in the influent and effluent of the aquifer cell before bioaugmentation (PV -1) and prior to ERDenhanced addition (PV 6).

Figure A.8 shows that lactate was not detected in the effluent after bioaugmentation at PV 0 while acetate and propionate were measured in the effluent at 2.9 mM and 1.8 mM respectively at PV 5.7. The conversion of lactate to acetate and propionate confirmed microbial growth in the aquifer cell prior to addition of ERDenhanced.

Dissolved organic carbon (DOC) was measured in the influent, effluent, and select ports to determine the effect ERDenhanced addition had on the overall DOC in the aquifer cell. Figure A.9 shows the influent and effluent DOC concentrations.

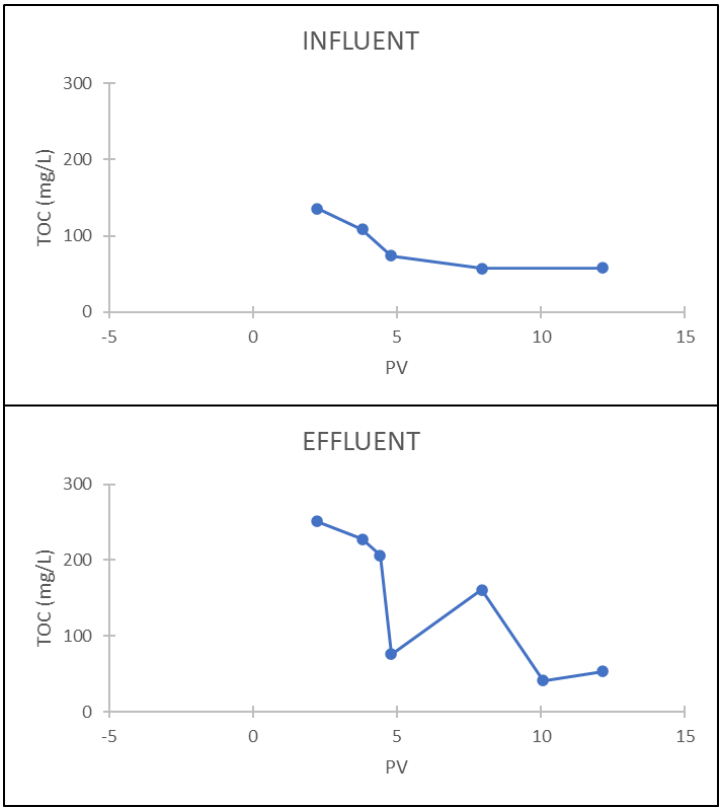

Figure A.9 Dissolved organic carbon in the influent and effluent of the aquifer cell after bioaugmentation (PV 0) and ERDenhanced addition (PV 6) until PV 12.

The influent has DOC concentrations of less than 200 mg/L from the 5 mM lactate that was introduced prior to PV 5.7. The Effluent concentration is higher than the influent but remains below 300 mg/L. DOC in the effluent is attributed predominantly to the byproducts of lactate consumption (acetate and propionate) and ERDenhanced addition.

After ERDenhanced addition, primarily near the first and second columns of ports (1 and 2), the DOC in port 3E increases from approximately 200 mg/L to over 1000 mg/L (Figure A.10). This was attributed to a multitude of factors including increased microbial growth, ERDenhanced addition, increased methane production, and DOC naturally present in the Commerce St. clay soil. However, the increase in DOC can most likely be attributed to the addition of ERDenhanced.

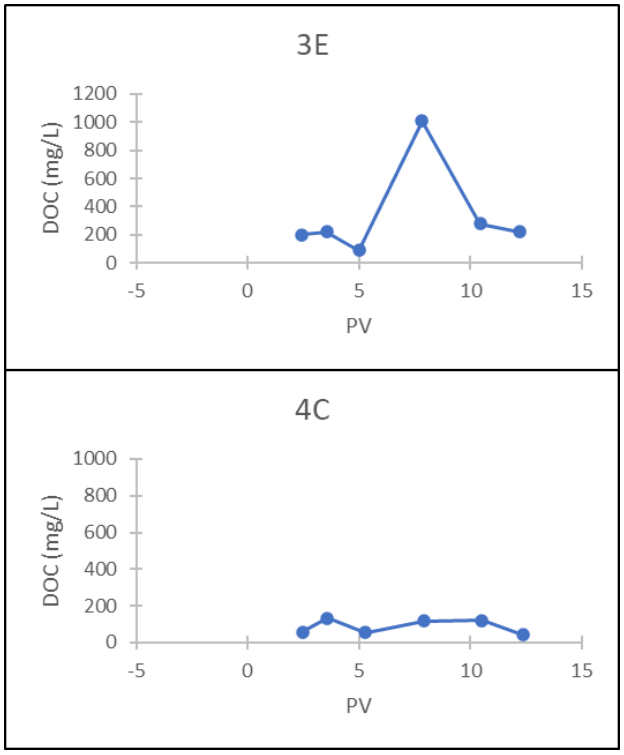

Figure A.10 Dissolved organic carbon in ports 3E and 4C of the aquifer cell (near the F-65 lens) after bioaugmentation (PV 0) and ERDenhanced addition (PV 6) until PV 12.

Port 4C is located downgradient of the F-65 soil lens and does not show an increase in organic carbon even after ERDenhanced addition at PV 6 (Figure A.10). ERDenhanced addition occurred in the first 2 columns of ports, and it remained in the aquifer cell since the effluent and later ports (illustrated by port 4C) did not experience a large spike in DOC.

A.7 Microbial Data from the Aquifer Cell

Microbial biomass samples were taken from each of the 11 ports and the effluent at PV 5, 7.5, 12.5, and 15.5. Total *Dhc* and RDase genes (*tceA*, *bvcA*, and *vcrA*) were targeted for each sample and measured in triplicate. Bar graphs for port 1E and port 4C are shown below in Figure A.11. These ports were chosen to provide additional microbial population data that is supportive of previously discussed conclusions, but data from these ports are more representative of the overall processes occurring in the aquifer cell. These graphs show the RDase gene distribution along with the total *Dhc* plotted as a line across each PV. Port 1E is directly above the clay in the first column of ports, and port 4C is downgradient of the Hudson soil and directly downgradient of the F-65 sand lens.

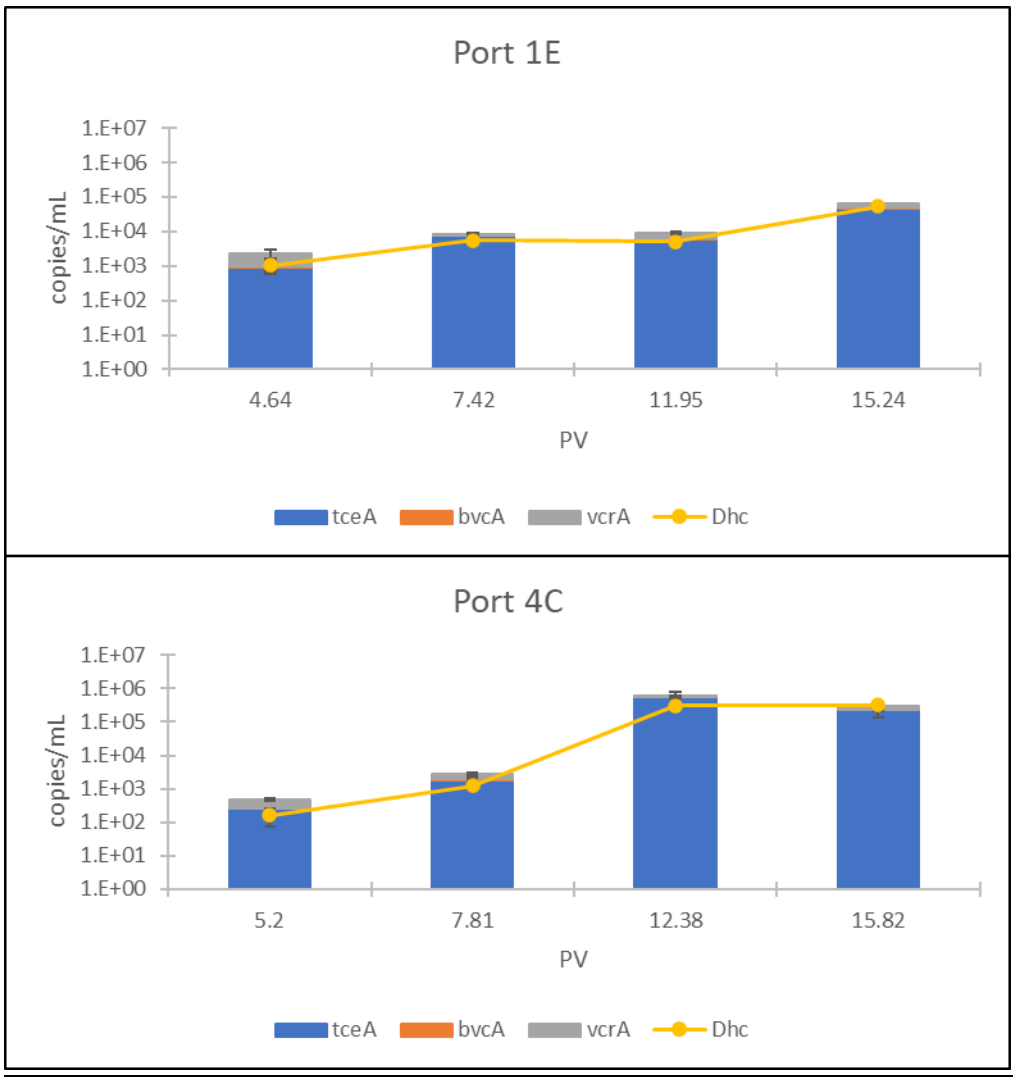

Figure A.11 Microbial population graphs showing Dhc and RDase genes from PV 5 to PV 15.5 after bioaugmentation in port 1E and 4C

Port 1E measured microbial concentrations ranging from 10^3 to 10^5 copies per mL and port 4C ranged from 10^2 to 10^5 copies per mL. It is evident that the *tceA* gene was predominant throughout the experiment in both ports. It is interesting to note that total RDase outnumbered Dhc in most of these sampling points. Images showing the relative abundance of each RDase gene at each port for PV 5 and 12.5 are shown below in Figure A.12 and Figure A.13.

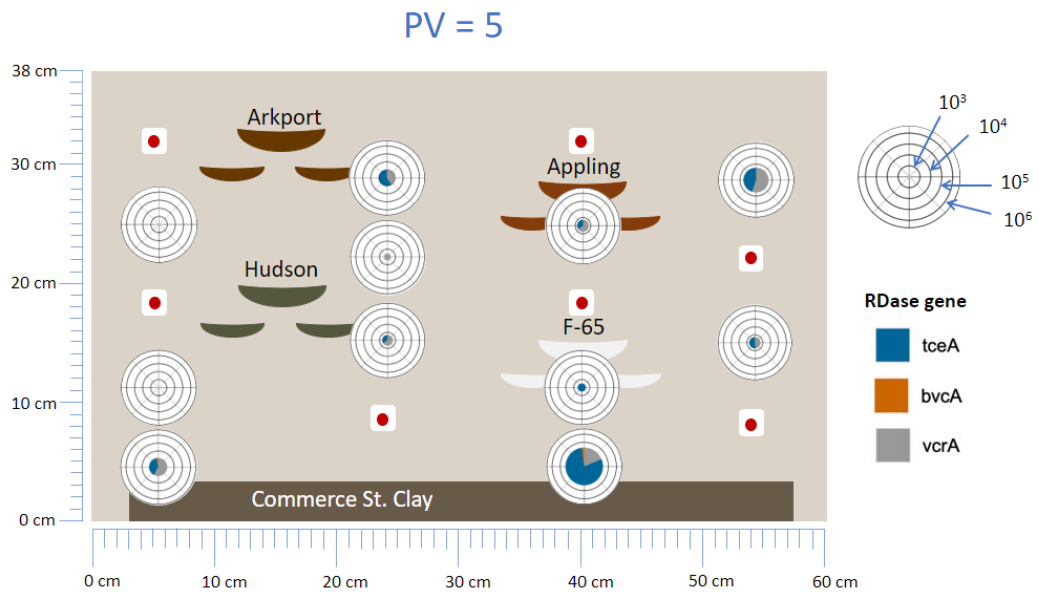

Figure A.12 RDase gene distribution at PV 5 after bioaugmentation (PV 0) and before decreasing the TCE concentration (PV 8.9)

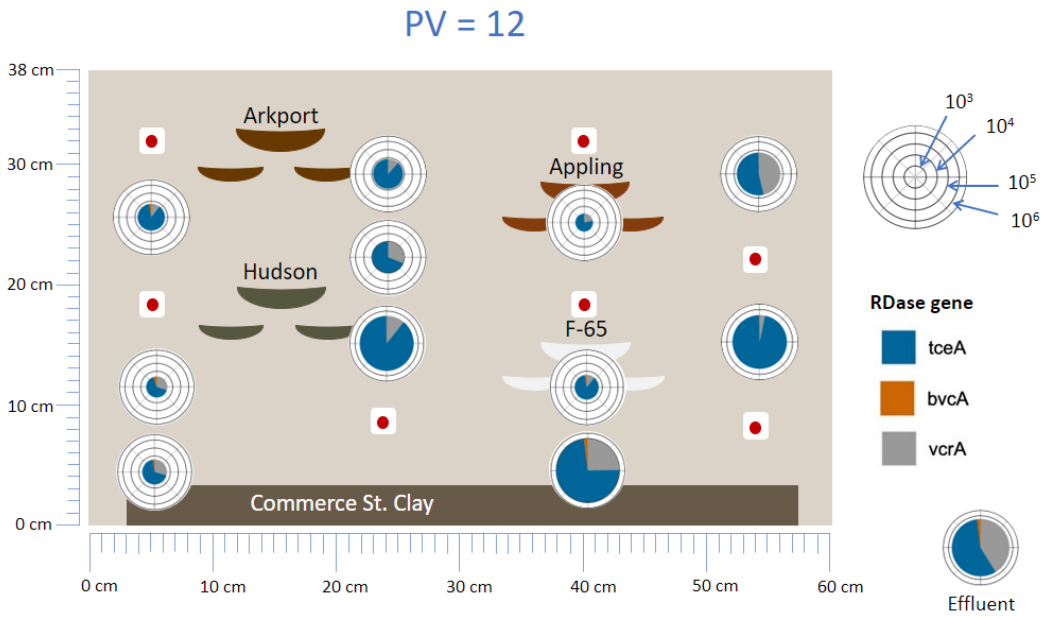

Figure A.13 RDase gene distribution at PV 12 after bioaugmentation (PV 0) and after decreasing the TCE concentration from 0.38 mM to 0.02 mM (PV 8.9)

These figures provide additional information that help fill in the gaps around PV 7.5 and PV 15.5 that were discussed in Section 3.3.5. On average, low (0 to 10^4) microbial concentrations were

measured at PV 5. This is attributed to imperfect biomass sample collection at the beginning of the experiment, and these values were not used for making conclusions about the data set as a whole. Additionally, microbial data from PV 12 occurred 3.1 PV after decreasing the TCE concentration from 0.38 mM (50 ppm) to 0.02 mM (3 ppm) in the aquifer cell. Microbial data from this time point was counted as intermediate data, as PV 15.5 captured a more complete picture of the state of the microbial population after decreasing the TCE concentration. Overall, increase in microbial populations were measured with up to 4 orders of magnitude increase from PV 5 to PV 15.5 in the aquifer cell.

References

Abriola, L., J. Christ, K. Pennell and C. Ramsburg (2012). Source remediation challenges. Delivery and Mixing in the Subsurface, Springer**:** 239-276.

Adamson, D. T., J. M. McDade and J. B. Hughes (2003). "Inoculation of a DNAPL source zone to initiate reductive dechlorination of PCE." Environmental Science & Technology **37**(11): 2525-2533.

Adamson, D. T. and C. J. Newell (2009). "Support of source zone bioremediation through endogenous biomass decay and electron donor recycling." Bioremediation Journal **13**(1): 29-40.

Amos, B. K., E. J. Suchomel, K. D. Pennell and F. E. Löffler (2008). "Microbial activity and distribution during enhanced contaminant dissolution from a NAPL source zone." Water research **42**(12): 2963-2974.

Arnold, W. A. and A. L. Roberts (2000). "Pathways and kinetics of chlorinated ethylene and chlorinated acetylene reaction with Fe (0) particles." Environmental Science & Technology **34**(9): 1794-1805.

ATSDA (2017) "Trichloroethylene (TCE) Overview."

Aulenta, F., M. Majone and V. Tandoi (2006). "Enhanced anaerobic bioremediation of chlorinated solvents: environmental factors influencing microbial activity and their relevance under field conditions." Journal of Chemical Technology & Biotechnology: International Research in Process, Environmental & Clean Technology **81**(9): 1463-1474.

Bastidas, A. M. P. (2016). Ottawa F-65 sand characterization, University of California, Davis.

Berns, E. C., R. A. Sanford, A. J. Valocchi, T. J. Strathmann, C. E. Schaefer and C. J. Werth (2019). "Contributions of biotic and abiotic pathways to anaerobic trichloroethene transformation in low permeability source zones." Journal of contaminant hydrology **224**: 103480.

Blue, J., T. Boving, M. E. Tuccillo, J. Koplos, J. Rose, M. Brooks and D. Burden (2023). "Contaminant Back Diffusion from Low-Conductivity Matrices: Case Studies of Remedial Strategies." Water **15**(3): 570.

Bouwer, E. J. (2017). Bioremediation of chlorinated solvents using alternate electron acceptors. Handbook of bioremediation, CRC Press**:** 149-176.

Brooks, M. C., E. Yarney and J. Huang (2021). "Strategies for managing risk due to back diffusion." Groundwater Monitoring & Remediation **41**(1): 76-98.

Brown, R. A., J. G. Mueller, A. G. Seech, J. K. Henderson and J. T. Wilson (2009). "Interactions between biological and abiotic pathways in the reduction of chlorinated solvents." Remediation Journal: The Journal of Environmental Cleanup Costs, Technologies & Techniques **20**(1): 9-20.

Cápiro, N. L., F. E. Löffler and K. D. Pennell (2015). "Spatial and temporal dynamics of organohalide-respiring bacteria in a heterogeneous PCE–DNAPL source zone." Journal of contaminant hydrology **182**: 78-90.

Cápiro, N. L., Y. Wang, J. K. Hatt, C. A. Lebrón, K. D. Pennell and F. E. Löffler (2014). "Distribution of organohalide-respiring bacteria between solid and aqueous phases." Environmental Science & Technology **48**(18): 10878-10887.

Chambon, J. C., M. M. Broholm, P. J. Binning and P. L. Bjerg (2010). "Modeling multi-component transport and enhanced anaerobic dechlorination processes in a single fracture–clay matrix system." Journal of Contaminant Hydrology **112**(1-4): 77-90.

Chapman, S. W. and B. L. Parker (2005). "Plume persistence due to aquitard back diffusion following dense nonaqueous phase liquid source removal or isolation." Water Resources Research **41**(12).

Christ, J. A., C. A. Ramsburg, L. M. Abriola, K. D. Pennell and F. E. Löffler (2005). "Coupling aggressive mass removal with microbial reductive dechlorination for remediation of DNAPL source zones: a review and assessment." Environmental Health Perspectives **113**(4): 465-477.

Clark, K., D. M. Taggart, B. R. Baldwin, K. M. Ritalahti, R. W. Murdoch, J. K. Hatt and F. E. Löffler (2018). "Normalized quantitative PCR measurements as predictors for ethene formation at sites impacted with chlorinated ethenes." Environmental science & technology **52**(22): 13410-13420.

Costanza, J. (2005). Degradation of tetrachloroethylene and trichloroethylene under thermal remediation conditions, Georgia Institute of Technology.

Coulthurst, S. J., N. A. Whitehead, M. Welch and G. P. Salmond (2002). "Can boron get bacteria talking?" Trends in biochemical sciences **27**(5): 217-219.

Cox, E., M. McMaster and D. Major (2002). "Successful Field Demonstrations of Bioaugmentation to Remediate Trichloroethene in Groundwater." Remediation of Chlorinated and Recalcitrant Compounds, Monterey, California.

Damgaard, I., P. L. Bjerg, J. Bælum, C. Scheutz, D. Hunkeler, C. S. Jacobsen, N. Tuxen and M. M. Broholm (2013). "Identification of chlorinated solvents degradation zones in clay till by high resolution chemical, microbial and compound specific isotope analysis." Journal of contaminant hydrology **146**: 37-50.

Dekker, T. J. and L. M. Abriola (2000). "The influence of field-scale heterogeneity on the infiltration and entrapment of dense nonaqueous phase liquids in saturated formations." Journal of contaminant hydrology **42**(2-4): 187-218.

DeWeerd, K., F. Concannon and J. M. Suflita (1991). "Relationship between hydrogen consumption, dehalogenation, and the reduction of sulfur oxyanions by Desulfomonile tiedjei." Applied and Environmental Microbiology **57**(7): 1929-1934.

Doherty, R. E. (2000). "A history of the production and use of carbon tetrachloride, tetrachloroethylene, trichloroethylene and 1, 1, 1-trichloroethane in the United States: part 1—historical background; carbon tetrachloride and tetrachloroethylene." Environmental forensics **1**(2): 69-81.

Dragun, J. (1998). The soil chemistry of hazardous materials, Amherst Scientific Publishers ^ eMassachusetts Massachusetts.

Duhamel, M., K. Mo and E. A. Edwards (2004). "Characterization of a highly enriched Dehalococcoides-containing culture that grows on vinyl chloride and trichloroethene." Applied and Environmental Microbiology **70**(9): 5538-5545.

EPA, U. (2017). Superfund Remedy Report 15th Edition. O. o. L. a. E. Management.

EPA, U. (2020) "Superfund Remedy Report 16th Edition."

EPA, U. (2023) "Superfund Remedy Report 17th Edition."

ESTCP (2009) "Emulsion Design Tool Kit."

Evans, P. J., D. Nguyen, R. W. Chappell, K. Whiting, J. Gillette, A. Bodour and J. T. Wilson (2014). "Factors controlling in situ biogeochemical transformation of trichloroethene: Column study." Groundwater Monitoring & Remediation **34**(3): 65-78.

Feenstra, S., J. Cherry and B. Parker (1996). "Conceptual models for the behavior of dense non-aqueous phase liquids (DNAPLs) in the subsurface." Dense chlorinated solvents and other DNAPLs in groundwater: history, behavior, and remediation: 53-88.

Freedman, D. L. and J. M. Gossett (1989). "Biological reductive dechlorination of tetrachloroethylene and trichloroethylene to ethylene under methanogenic conditions." applied and Environmental Microbiology **55**(9): 2144-2151.

Futagami, T., M. Goto and K. Furukawa (2008). "Biochemical and genetic bases of dehalorespiration." The chemical record **8**(1): 1-12.

GeoSyntec (2004). "Assessing the feasibility of DNAPL source zone remediation: Review of case studies."

Glover, K. C., J. Munakata-Marr and T. H. Illangasekare (2007). "Biologically enhanced mass transfer of tetrachloroethene from DNAPL in source zones: experimental evaluation and influence of pool morphology." Environmental Science & Technology **41**(4): 1384-1389.

Grisak, G. E. and J.-F. Pickens (1980). "Solute transport through fractured media: 1. The effect of matrix diffusion." Water resources research **16**(4): 719-730.

Guard, U. C. (1999). "Chemical Hazard Response Information System (CHRIS)-Hazardous Chemical Data." Commandant Instruction **16465**.

Guha, N., D. Loomis, Y. Grosse, B. Lauby-Secretan, F. El Ghissassi, V. Bouvard, L. Benbrahim-Tallaa, R. Baan, H. Mattock and K. Straif (2012). Carcinogenicity of trichloroethylene, tetrachloroethylene, some other chlorinated solvents, and their metabolites, Elsevier.

Haest, P. J., D. Springael, P. Seuntjens and E. Smolders (2012). "Self-inhibition can limit biologically enhanced TCE dissolution from a TCE DNAPL." Chemosphere **89**(11): 1369-1375.

Harkness, M. and A. Fisher (2013). "Use of emulsified vegetable oil to support bioremediation of TCE DNAPL in soil columns." Journal of contaminant hydrology **151**: 16-33.

Harkness, M. R., A. A. Bracco, M. J. Brennan, K. A. DeWeerd and J. L. Spivack (1999). "Use of bioaugmentation to stimulate complete reductive dechlorination of trichloroethene in Dover soil columns." Environmental Science & Technology **33**(7): 1100-1109.

He, J., K. M. Ritalahti, K.-L. Yang, S. S. Koenigsberg and F. E. Löffler (2003). "Detoxification of vinyl chloride to ethene coupled to growth of an anaerobic bacterium." Nature **424**(6944): 62-65.

Hendrickson, E. R., J. A. Payne, R. M. Young, M. G. Starr, M. P. Perry, S. Fahnestock, D. E. Ellis and R. C. Ebersole (2002). "Molecular analysis of Dehalococcoides 16S ribosomal DNA from chloroethene-contaminated sites throughout North America and Europe." Applied and Environmental Microbiology **68**(2): 485-495.

Hickman, J. (2000). "Tetrachloroethylene." Kirk-Othmer Encyclopedia of Chemical Technology.

Hnatko, J. P., L. Yang, K. D. Pennell, L. M. Abriola and N. L. Cápiro (2020). "Bioenhanced back diffusion and population dynamics of Dehalococcoides mccartyi strains in heterogeneous porous media." Chemosphere **254**: 126842.

Holliger, C., D. Hahn, H. Harmsen, W. Ludwig, W. Schumacher, B. Tindall, F. Vazquez, N. Weiss and A. J. Zehnder (1998). "Dehalobacter restrictus gen. nov. and sp. nov., a strictly anaerobic bacterium that reductively dechlorinates tetra-and trichloroethene in an anaerobic respiration." Archives of microbiology **169**(4): 313-321.

Holliger, C., G. Schraa, A. Stams and A. Zehnder (1993). "A highly purified enrichment culture couples the reductive dechlorination of tetrachloroethene to growth." Applied and environmental microbiology **59**(9): 2991-2997.

Hood, E., D. Major, J. Quinn, W. S. Yoon, A. Gavaskar and E. Edwards (2008). "Demonstration of enhanced bioremediation in a TCE source area at Launch Complex 34, Cape Canaveral Air Force Station." Groundwater Monitoring & Remediation **28**(2): 98-107.

Hopkins, G., L. Semprini and P. L. McCarty (1993). "Microcosm and in situ field studies of enhanced biotransformation of trichloroethylene by phenol-utilizing microorganisms." Applied and Environmental Microbiology **59**(7): 2277-2285.

Huang, B., C. Lei, C. Wei and G. Zeng (2014). "Chlorinated volatile organic compounds (Cl-VOCs) in environment—sources, potential human health impacts, and current remediation technologies." Environment international **71**: 118-138.

Huling, S. G., R. R. Ross and K. Meeker Prestbo (2017). "In situ chemical oxidation: Permanganate oxidant volume design considerations." Groundwater Monitoring & Remediation **37**(2): 78-86.

Jin, B., M. Rolle, T. Li and S. B. Haderlein (2014). "Diffusive fractionation of BTEX and chlorinated ethenes in aqueous solution: quantification of spatial isotope gradients." Environmental science & technology **48**(11): 6141-6150.

Joksimovich, V. and S. Koenigsberg (2002). "Application of time release electron donors and electron acceptors for accelerated bioremediation."

Joo, J. C., C. D. Shackelford and K. F. Reardon (2008). "Association of humic acid with metal (hydr) oxide-coated sands at solid–water interfaces." Journal of colloid and interface science **317**(2): 424-433.

Knauss, K. G., M. J. Dibley, R. N. Leif, D. A. Mew and R. D. Aines (2000). "The aqueous solubility of trichloroethene (TCE) and tetrachloroethene (PCE) as a function of temperature." Applied Geochemistry **15**(4): 501-512.

Krajmalnik-Brown, R., T. Hölscher, I. N. Thomson, F. M. Saunders, K. M. Ritalahti and F. E. Löffler (2004). "Genetic identification of a putative vinyl chloride reductase in Dehalococcoides sp. strain BAV1." Applied and Environmental Microbiology **70**(10): 6347-6351.

Kranzioch, I., S. Ganz and A. Tiehm (2015). "Chloroethene degradation and expression of Dehalococcoides dehalogenase genes in cultures originating from Yangtze sediments." Environmental Science and Pollution Research **22**(4): 3138-3148.

Kueper, B. H., H. F. Stroo, C. M. Vogel and C. H. Ward (2014). Chlorinated solvent source zone remediation, Springer.

Lendvay, J., F. E. Löffler, M. Dollhopf, M. Aiello, G. Daniels, B. Fathepure, M. Gebhard, R. Heine, R. Helton and J. Shi (2003). "Bioreactive barriers: a comparison of bioaugmentation and biostimulation for chlorinated solvent remediation." Environmental Science & Technology **37**(7): 1422-1431.

Liang, X., O. Molenda, S. Tang and E. A. Edwards (2015). "Identity and substrate specificity of reductive dehalogenases expressed in dehalococcoides-containing enrichment cultures

maintained on different chlorinated ethenes." Applied and environmental microbiology **81**(14): 4626-4633.

Löffler, F. E. and E. A. Edwards (2006). "Harnessing microbial activities for environmental cleanup." Current Opinion in Biotechnology **17**(3): 274-284.

Löffler, F. E., K. M. Ritalahti and S. H. Zinder (2013). Dehalococcoides and reductive dechlorination of chlorinated solvents. Bioaugmentation for groundwater remediation, Springer**:** 39-88.

Loffler, F. E., R. A. Sanford and J. M. Tiedje (1996). "Initial characterization of a reductive dehalogenase from Desulfitobacterium chlororespirans Co23." Applied and environmental microbiology **62**(10): 3809-3813.

Löffler, F. E., J. Yan, K. M. Ritalahti, L. Adrian, E. A. Edwards, K. T. Konstantinidis, J. A. Müller, H. Fullerton, S. H. Zinder and A. M. Spormann (2013). "Dehalococcoides mccartyi gen. nov., sp. nov., obligately organohalide-respiring anaerobic bacteria relevant to halogen cycling and bioremediation, belong to a novel bacterial class, Dehalococcoidia classis nov., order Dehalococcoidales ord. nov. and family Dehalococcoidaceae fam. nov., within the phylum Chloroflexi." International journal of systematic and evolutionary microbiology **63**(Pt_2): 625-635.

Mackay, D. M. and J. A. Cherry (1989). "Groundwater contamination: Pump-and-treat remediation." Environmental Science & Technology **23**(6): 630-636.

Mackay, D. M., P. V. Roberts and J. A. Cherry (1985). "Transport of organic contaminants in groundwater." Environmental science & technology **19**(5): 384-392.

Magnuson, J. K., M. F. Romine, D. R. Burris and M. T. Kingsley (2000). "Trichloroethene reductive dehalogenase from Dehalococcoides ethenogenes: sequence of tceA and substrate range characterization." Applied and Environmental Microbiology **66**(12): 5141-5147.

Major, D. W., M. L. McMaster, E. E. Cox, E. A. Edwards, S. M. Dworatzek, E. R. Hendrickson, M. G. Starr, J. A. Payne and L. W. Buonamici (2002). "Field demonstration of successful bioaugmentation to achieve dechlorination of tetrachloroethene to ethene." Environmental Science & Technology **36**(23): 5106-5116.

Marcet, T. (2014). Secondary impacts of in situ chlorinated solvent remediation due to metal sulfide precipitation and thermal treatment, Tufts University.

Marcet, T. F., N. L. Cápiro, L. A. Morris, S. M. Hassan, Y. Yang, F. E. Löffler and K. D. Pennell (2018). "Release of Electron Donors during Thermal Treatment of Soils." Environmental Science & Technology **52**(6): 3642-3651.

Maymó-Gatell, X., I. Nijenhuis and S. H. Zinder (2001). "Reductive dechlorination of cis-1, 2-dichloroethene and vinyl chloride by “Dehalococcoides ethenogenes”." Environmental science & technology **35**(3): 516-521.

McGuire, T. M., D. T. Adamson, M. S. Burcham, P. B. Bedient and C. J. Newell (2016). "Evaluation of Long-Term Performance and Sustained Treatment at Enhanced Anaerobic Bioremediation Sites." Groundwater Monitoring & Remediation **36**(2): 32-44.

McGuire, T. M., J. M. McDade and C. J. Newell (2006). "Performance of DNAPL source depletion technologies at 59 chlorinated solvent-impacted sites." Groundwater Monitoring & Remediation **26**(1): 73-84.

Mercer, J. W. and R. M. Cohen (1990). "A review of immiscible fluids in the subsurface: Properties, models, characterization and remediation." Journal of contaminant hydrology **6**(2): 107-163.

Mirza, B. S., D. L. Sorensen, R. R. Dupont and J. E. McLean (2016). "Dehalococcoides abundance and alternate electron acceptor effects on large, flow-through trichloroethene dechlorinating columns." Applied microbiology and biotechnology **100**(5): 2367-2379.

Molenda, O., S. Tang, L. Lomheim and E. A. Edwards (2018). "Eight new genomes of organohalide-respiring Dehalococcoides mccartyi reveal evolutionary trends in reductive dehalogenase enzymes." bioRxiv: 345173.

Moran, M. J., J. S. Zogorski and P. J. Squillace (2007). "Chlorinated solvents in groundwater of the United States." Environmental Science & Technology **41**(1): 74-81.

Müller, J. A., B. M. Rosner, G. Von Abendroth, G. Meshulam-Simon, P. L. McCarty and A. M. Spormann (2004). "Molecular identification of the catabolic vinyl chloride reductase from Dehalococcoides sp. strain VS and its environmental distribution." Applied and Environmental Microbiology **70**(8): 4880-4888.

NRC (2000). Natural attenuation for groundwater remediation.

NRC (2013). Alternatives for managing the nation's complex contaminated groundwater sites, National Academies Press.

NRC (2014). "Best Practices for Risk-Informed Decision Making Regarding Contaminated Sites: Summary of a Workshop Series."

Pankow, J. F., W. Luo, L. M. Isabelle, K. M. Hart and D. F. Hagen (1996). "Gas-solid retention volumes of organic compounds on styrene-divinylbenzene and ethylvinylbenzene-divinylbenzene co-polymer sorbent beads." Journal of Chromatography A **732**(2): 317-326.

Parker, B. L., S. W. Chapman and M. A. Guilbeault (2008). "Plume persistence caused by back diffusion from thin clay layers in a sand aquifer following TCE source-zone hydraulic isolation." Journal of contaminant hydrology **102**(1-2): 86-104.

Patil, S. S., E. M. Adetutu and A. S. Ball (2014). "Microbiology of chloroethene degradation in groundwater." Microbiology Australia **35**(4): 211-214.

Philips, J., R. Van Muylder, D. Springael and E. Smolders (2013). "Electron donor limitations reduce microbial enhanced trichloroethene DNAPL dissolution: a flux-based analysis using diffusion-cells." Chemosphere **91**(1): 7-13.

Puigserver, D., J. Herrero, X. Nogueras, A. Cortés, B. L. Parker, E. Playà and J. M. Carmona (2022). "Biotic and abiotic reductive dechlorination of chloroethenes in aquitards." Science of The Total Environment **816**: 151532.

Richardson, R. (2012). Systems Biology of Dehalococcoides: Using Network Inference Modeling to Integrate Omics Datasets Under Varied Conditions, CORNELL UNIV ITHACA NY OFFICE OF SPONSORED PROGRAMS.

Ritalahti, K. M., B. K. Amos, Y. Sung, Q. Wu, S. S. Koenigsberg and F. E. Löffler (2006). "Quantitative PCR targeting 16S rRNA and reductive dehalogenase genes simultaneously monitors multiple Dehalococcoides strains." Applied and environmental microbiology **72**(4): 2765-2774.

Rossi, M. M., B. Matturro, N. Amanat, S. Rossetti and M. Petrangeli Papini (2022). "Coupled adsorption and biodegradation of trichloroethylene on biochar from pine wood wastes: A combined approach for a sustainable bioremediation strategy." Microorganisms **10**(1): 101.

Roth, M. J. and L. F. Caslake (2019). Reducing soil permeability using in situ biofilm-forming bacteria: overcoming testing apparatus challenges. Geo-Congress 2019: Soil Improvement, American Society of Civil Engineers Reston, VA.

Russell, H. H., J. Matthews and G. Sewell (1992). TCE removal from contaminated soil and ground water. Ground-water issue, Environmental Protection Agency, Washington, DC (United States). Office of ….

Russell, H. H., J. E. Matthews and G. W. Sewell (2019). TCE Removal from Contaminated Soil and Ground Water 1. EPA environmental engineering sourcebook, CRC Press**:** 87-99.

Rusyn, I., W. A. Chiu, L. H. Lash, H. Kromhout, J. Hansen and K. Z. Guyton (2014). "Trichloroethylene: Mechanistic, epidemiologic and other supporting evidence of carcinogenic hazard." Pharmacology & therapeutics **141**(1): 55-68.

Sale, T., B. Parker, C. Newell and J. Devlin (2013). "State-of-the-science review: Management of contaminants stored in low permeability zones. SERDP Project ER-1740." Washington, DC.

Sandmeyer, E. (1981). Aliphatic hydrocarbons. Patty's Industrial Hygeine and Toxicology, John Wiley New York**:** 3175-3220.

Scheutz, C., M. M. Broholm, N. D. Durant, E. B. Weeth, T. H. Jørgensen, P. Dennis, C. S. Jacobsen, E. E. Cox, J. C. Chambon and P. L. Bjerg (2010). "Field evaluation of biological enhanced reductive dechlorination of chloroethenes in clayey till." Environmental science & technology **44**(13): 5134-5141.

Sims, J., J. Suflita and H. Russell (1992). In-situ bioremediation of contaminated ground water, Environmental Protection Agency, Washington, DC (United States). Office of ….

Sivadon, P., C. Barnier, L. Urios and R. Grimaud (2019). "Biofilm formation as a microbial strategy to assimilate particulate substrates." Environmental microbiology reports **11**(6): 749-764.

Sleep, B. E., D. J. Seepersad, K. Mo, C. M. Heidorn, L. Hrapovic, P. L. Morrill, M. L. McMaster, E. D. Hood, C. LeBron and B. Sherwood Lollar (2006). "Biological enhancement of tetrachloroethene dissolution and associated microbial community changes." Environmental science & technology **40**(11): 3623-3633.

Sonawane, J. M., A. K. Rai, M. Sharma, M. Tripathi and R. Prasad (2022). "Microbial biofilms: Recent advances and progress in environmental bioremediation." Science of The Total Environment: 153843.

Stroo, H. F., A. Leeson, J. A. Marqusee, P. C. Johnson, C. H. Ward, M. C. Kavanaugh, T. C. Sale, C. J. Newell, K. D. Pennell and C. A. Lebrón (2012). Chlorinated ethene source remediation: lessons learned, ACS Publications.

Suchomel, E. J., C. A. Ramsburg and K. D. Pennell (2007). "Evaluation of trichloroethene recovery processes in heterogeneous aquifer cells flushed with biodegradable surfactants." Journal of contaminant hydrology **94**(3-4): 195-214.

Sung, Y., K. M. Ritalahti, R. P. Apkarian and F. E. Loffler (2006). "Quantitative PCR confirms purity of strain GT, a novel trichloroethene-to-ethene-respiring Dehalococcoides isolate." Applied and Environmental Microbiology **72**(3): 1980-1987.

Sung, Y., K. M. Ritalahti, R. A. Sanford, J. W. Urbance, S. J. Flynn, J. M. Tiedje and F. E. Löffler (2003). "Characterization of two tetrachloroethene-reducing, acetate-oxidizing anaerobic bacteria and their description as Desulfuromonas michiganensis sp. nov." Applied and environmental microbiology **69**(5): 2964-2974.

Tobiszewski, M. and J. Namieśnik (2012). "Abiotic degradation of chlorinated ethanes and ethenes in water." Environmental Science and Pollution Research **19**(6): 1994-2006.

USDA Official Soil Series Descriptions.

USEPA (2009). National Primary Drinking Water Regulations. **1:** 7.

van der Zaan, B., F. Hannes, N. Hoekstra, H. Rijnaarts, W. M. de Vos, H. Smidt and J. Gerritse (2010). "Correlation of Dehalococcoides 16S rRNA and chloroethene-reductive dehalogenase genes with geochemical conditions in chloroethene-contaminated groundwater." Applied and environmental microbiology **76**(3): 843-850.

Verce, M. F., V. M. Madrid, S. D. Gregory, Z. Demir, M. J. Singleton, E. P. Salazar, P. J. Jackson, R. U. Halden and A. Verce (2015). "A long-term field study of in situ bioremediation in a fractured conglomerate trichloroethene source zone." Bioremediation Journal **19**(1): 18-31.

Wanner, P., B. L. Parker, S. W. Chapman, G. Lima, A. Gilmore, E. E. Mack and R. Aravena (2018). "Identification of degradation pathways of chlorohydrocarbons in saturated low-permeability sediments using compound-specific isotope analysis." Environmental science & technology **52**(13): 7296-7306.

Wartenberg, D., D. Reyner and C. S. Scott (2000). "Trichloroethylene and cancer: epidemiologic evidence." Environmental health perspectives **108**(suppl 2): 161-176.

Yan, J., K. M. Ritalahti, D. D. Wagner and F. E. Löffler (2012). "Unexpected specificity of interspecies cobamide transfer from Geobacter spp. to organohalide-respiring Dehalococcoides mccartyi strains." Applied and environmental microbiology **78**(18): 6630-6636.

Yang, M., M. D. Annable and J. W. Jawitz (2015). "Back diffusion from thin low permeability zones." Environmental science & technology **49**(1): 415-422.

Yang, Y., S. A. Higgins, J. Yan, B. Şimşir, K. Chourey, R. Iyer, R. L. Hettich, B. Baldwin, D. M. Ogles and F. E. Löffler (2017). "Grape pomace compost harbors organohalide-respiring Dehalogenimonas species with novel reductive dehalogenase genes." The ISME journal **11**(12): 2767-2780.

Yu, S. and L. Semprini (2002). "Comparison of trichloroethylene reductive dehalogenation by microbial communities stimulated on silicon-based organic compounds as slow-release anaerobic substrates." Water Research **36**(20): 4985-4996.

Yu, S. and L. Semprini (2009). "Enhanced reductive dechlorination of PCE DNAPL with TBOS as a slow-release electron donor." Journal of hazardous materials **167**(1-3): 97-104.